UNIVERSITAT POLITÈCNICA DE CATALUNYA BARCELONATECH

Optimization strategies for efficient dosage of H_2O_2 in Fenton and photo-Fenton processes

Xiangwei Yu

Optimization strategies for efficient dosage of H_2O_2 in Fenton and photo-Fenton processes

Xiangwei Yu

Doctoral Thesis

Directed by

Prof. Dr. Moisès Graells Sobré

Prof. Dr. Montserrat Pérez Moya

Universitat Politècnica de Catalunya

PhD Program in Chemical Engineering

2021

This thesis has contributed new and deeper insight into the nature and practical aspects of the dosage of hydrogen peroxide in photo-Fenton processes aimed at increasing their efficiency. The partial works in chapters 4, 5 and 6 have led to the following journal articles:

- Xiangwei, Y., Somoza-Tornos, A., Graells, M., Pérez-Moya, M., 2020. An experimental approach to the optimization of the dosage of hydrogen peroxide for Fenton and photo-Fenton processes. *Science of the Total Environment*, 743. https://doi.org/10.1016/j.scitotenv.2020.140402

- Xiangwei, Y., Graells, M., Miralles-Cuevas, S., Cabrera-Reina, A., Pérez-Moya, M., 2021. An improved hybrid strategy for online dosage of hydrogen peroxide in photo-Fenton processes. *Journal of Environmental Chemical Engineering*, 9. https://doi.org/10.1016/j.jece.2021.105235

- Xiangwei, Y., Cabrera-Reina, A., Graells, M., Miralles-Cuevas, S., Pérez-Moya, M. Towards an efficient generalization of the online dosage of hydrogen peroxide in photo-Fenton process to treat industrial wastewater **Submitted to Journal of Environmental Chemical Engineering**

The author of this thesis particularly acknowledges the State Scholarship Fund of China Scholarship Council (No. 201706950041).

The researches described in this thesis were financially supported by the project: Ministerio de Economía, Industria y Competitividad (MINECO) and the European Regional Development Fund, both funding the research Project AIMS (DPI2017-87435-R).

Acknowledgements

Looking back over the last four years, I really thank everyone who helped me in my research and life. It was hardly possible for me to finish my doctoral work without their participation and precious support.

First of all, I would like to extend my sincere gratitude to my supervisors, Prof. Montserrat Pérez Moya and Prof. Moisès Graells, for their instructive advice and useful suggestions on my training process, academic studies and my thesis. During these years, I am deeply grateful of their help and accompanies. I would like to express my heartfelt gratitude to Prof. Antonio Espuña for whom provides me the opportunity to do the research in CEPIMA group.

Secondly, I express my gratitude to all CEPIMA members. They have provided great companies during all those years in Barcelona. Especially, I must mention the valuable support that I received from Francesca Audino who helped me how to use all the apparatus and explained to me how to start my research. Special thanks to Ana Somoza and Shabnam Morakabatchiankar, with their constant encouragement.

I also want to thank my friends, Congcong Xing (IREC), for sharing my joy and sadness. Xiao Yang (CSIC), for being my daily support and my advisor.

Last but also most importantly, my thanks would go to my family, for their continuous support and encouragement. They really give me the great confidence and respect for every decision of me.

Abstract

This Thesis work addresses the challenge of designing hydrogen peroxide (H_2O_2) dosage strategies for improving Fenton and photo-Fenton applications. The determination of the H_2O_2 dosage scheme that minimizes hydrogen peroxide consumption while meeting the specified treatment outcome is crucial for the practicality of Fenton and photo-Fenton processes, as well as for further understanding the effect of the dosage.

A first part of the research addresses this challenge by providing a problem formulation, identifying and discussing objectives and constraints, and the nature of the optimal solution. From this point, the Thesis presents a novel dosage model and a consequent methodology aimed at experimentally optimizing the dosage profile along a discretized time horizon following recipe optimization concepts. The approach is parallel to the numerical solution of the model-based optimization problem posed by H_2O_2. The methodology is validated in the remediation of a Paracetamol (PCT) solution, and the obtained results are assessed and discussed in regard of the evolution of the concentration of hydrogen peroxide, the contaminant (PCT), and Total Organic Carbon (TOC). The concentration of dissolved oxygen (DO), which is also monitored, allows providing a more comprehensive explanation of the nature of the process.

A second part focuses on the practical limitations of this scheme by adopting a hybrid methodology between open and closed loop approaches and it is based on three different stages: (i) one-shot initial H_2O_2 addition (ii) continuous H_2O_2 dosage until reaching a specific dissolved oxygen (DO) level and (iii) on-off control of H_2O_2 dosage using DO slope as control variable. The proposed strategy is validated in the remediation of a Paracetamol solution (100 mg L^{-1}) and the results are assessed using H_2O_2 consumption and mineralization rate and level as performance criteria. The final tuning of the proposed strategy consists of: (i) only 40% of the stoichiometric H_2O_2 concentration, (ii) continuous feeding of H_2O_2 until a 4 mg L^{-1} DO concentration is attained, and (iii) on-off control dosage selecting DO slope set-points in 0.1 and 0.2 mg L^{-1} min^{-1}. The dosage scheme and settings developed in this second part show an improvement of the process performance by ~ 15% with respect to the same H_2O_2 amount in a single-addition.

Finally, the third part generalizes this strategy by expanding its application and exploring and assessing its performance on different water matrix (natural water and distilled water), different contaminant concentrations, and different contaminants (paracetamol and sulfamethazine) and mixtures. Towards this end, a set of assays were planned and executed involving Paracetamol and Sulfamethazine. In particular, assays performed on sulfamethazine presented higher efficiency (mg of TOC removed per mg of H_2O_2 consumed), which increased 25-35% with respect to the results obtained with only one-shot initial addition.

Furthermore, a deeper analysis of the results allowed detecting and assessing the option of a redesign of the dosage scheme by removing the idea of a specific DO set point and directly addressing the control of the DO slope. Hence, this thesis also opens new research lines in regard to increasing the simplicity and robustness of this efficient control strategy of the photo-Fenton process.

Resumen

Aquest treball de tesi aborda el repte de dissenyar estratègies de dosificació de peròxid d'hidrogen (H_2O_2) per millorar les aplicacions dels processos Fenton i foto-Fenton. La determinació d'una estratègia de dosificació d' H_2O_2 que en minimitzi el consum mentre s'assoleixen els objectius del tractament especificat és crucial per a l'aplicació pràctica dels processos de Fenton i foto-Fenton, així com per a la millor comprensió de l'efecte de la dosificació.

Una primera part de la investigació aborda aquest repte proporcionant una formulació del problema, identificant i discutint objectius i restriccions, i la naturalesa de la solució òptima. A partir d'aquest punt, la tesi presenta un nou model de dosificació i una metodologia derivada que pretén optimitzar experimentalment el perfil de dosificació al llarg d'un horitzó temporal convenientment discretitzat seguint conceptes d'optimització de receptes. L'enfocament és paral·lel a la solució numèrica del problema d'optimització basat en models i la metodologia que se'n deriva es valida en el tractament d'una solució de paracetamol (PCT). Els resultats obtinguts s'avaluen i es discuteixen en relació amb l'evolució de la concentració de peròxid d'hidrogen, el contaminant (PCT) i el carboni orgànic total (TOC). La concentració d'oxigen dissolt (DO), que també es controla, permet donar una explicació més completa de la naturalesa del procés.

Una segona part se centra en les limitacions pràctiques d'aquest esquema mitjançant l'adopció d'una metodologia híbrida entre el control en llaç obert i el control en llaç tancat. La metodologia es basa en tres etapes diferents: (i) addició inicial H_2O_2 inicial (ii) dosificació contínua d' H_2O_2 fins a arribar a un determinat nivell d'oxigen dissolt (DO) i (iii) control on-off de la dosi d' H_2O_2 utilitzant el pendent de DO com a variable de control. L'estratègia proposada es valida en el tractament d'una solució de paracetamol (100 mg L^{-1}) i els resultats s'avaluen utilitzant el consum de H_2O_2 i la taxa i el nivell de mineralització com a criteris de rendiment. L'ajust final de l'estratègia proposada es concreta de la següent manera: (i) només el 40% de la concentració estequiomètrica de H_2O_2, (ii) alimentació contínua de H2O2 fins a l'assoliment d'una concentració de 4 mg de L-1 DO i (iii) dosificació sota un control on-off seleccionant els valors de pendent de DO entre 0,1 i 0,2 mg L^{-1} min^{-1}. L'esquema de dosificació i la configuració desenvolupats en aquesta

segona part mostren una millora del rendiment del procés d'un 15% respecte al que s'obté amb mateixa quantitat de H_2O_2 en una única addició.

Finalment, la tercera part generalitza aquesta estratègia ampliant la seva aplicació, explorant i avaluant el seu rendiment en diferents matrius d'aigua (aigua natural i aigua destil·lada), diferents concentracions de contaminants, diferents contaminants (paracetamol i sulfametazina) i mescles. Amb aquesta finalitat, es van planificar i executar un conjunt d'assajos que van incloure paracetamol i sulfametazina. En particular, els assajos realitzats amb sulfametazina van presentar una eficiència més elevada (mg de TOC eliminats per mg d' H_2O_2 consumit), que va augmentar entre un 25 i un 35% respecte als resultats obtinguts amb només una única incorporació inicial.

A més, una anàlisi més profunda dels resultats va permetre detectar i avaluar l'opció d'un redisseny de l'esquema de dosificació eliminant la idea d'un punt de referència específic de DO i abordant directament el control del pendent de DO. Per tant, aquesta tesi també obre noves línies de recerca per augmentar la simplicitat i robustesa d'aquesta estratègia de control eficient del procés de foto-Fenton.

Resum

Este trabajo de tesis aborda el reto de diseñar estrategias de dosificación de peróxido de hidrógeno (H_2O_2) para mejorar las aplicaciones de los procesos Fenton y foto-Fenton. La determinación de una estrategia de dosificación de H_2O_2 que minimice el consumo mientras se alcanzan los objetivos del tratamiento especificado es crucial para la aplicación práctica de los procesos Fenton y foto-Fenton, así como para la mejor comprensión del efecto de la dosificación.

Una primera parte de la investigación aborda este reto proporcionando una formulación del problema, identificando y discutiendo objetivos y restricciones, así como la naturaleza de la solución óptima. A partir de este punto, la tesis presenta un nuevo modelo de dosificación y una metodología derivada que pretende optimizar experimentalmente el perfil de dosificación a lo largo de un horizonte temporal convenientemente discretizado siguiendo conceptos de optimización de recetas. El enfoque es paralelo a la solución numérica del problema de optimización basado en modelos y la metodología que se deriva se valida en el tratamiento de una solución de paracetamol (PCT). Los resultados obtenidos se evalúan y se discuten en relación con la evolución de la concentración de peróxido de hidrógeno, el contaminante (PCT) y el carbono orgánico total (TOC). La concentración de oxígeno disuelto (DO), que también se controla, permite dar una explicación más completa de la naturaleza del proceso.

Una segunda parte se centra en las limitaciones prácticas de este esquema mediante la adopción de una metodología híbrida entre el control en lazo abierto y el control en lazo cerrado. La metodología se basa en tres etapas diferentes: (i) adición inicial H_2O_2 inicial (ii) dosificación continua de H_2O_2 hasta llegar a un determinado nivel de oxígeno disuelto (DO) y (iii) control on-off de la dosis de H_2O_2 utilizando la pendiente de DO como variable de control. La estrategia propuesta se valida en el tratamiento de una solución de paracetamol (100 mg L^{-1}) y los resultados se evalúan utilizando el consumo de H_2O_2 y la tasa y el nivel de mineralización como criterios de rendimiento. El ajuste final de la estrategia propuesta se concreta de la siguiente manera: (i) sólo el 40% de la concentración estequiométrica de H_2O_2, (ii) alimentación continua de H_2O_2 hasta el logro de una concentración de 4 mg de L^{-1} DO y (iii) dosificación bajo un control on-off seleccionando los valores de pendiente de

DO entre 0,1 y 0,2 mg L^{-1} min^{-1}. El esquema de dosificación y la configuración desarrollados en esta segunda parte muestran una mejora del rendimiento del proceso de un 15% respecto al que se obtiene con misma cantidad de H_2O_2 en una única adición.

Finalmente, la tercera parte generaliza esta estrategia ampliando su aplicación, explorando y evaluando su rendimiento en diferentes matrices de agua (agua natural y agua destilada), diferentes concentraciones de contaminantes, diferentes contaminantes (paracetamol y sulfametazina) y mezclas. Con esta finalidad, se planificaron y ejecutar un conjunto de ensayos que incluyeron paracetamol y sulfametazina. En particular, los ensayos realizados con sulfametazina presentaron una eficiencia más elevada (mg de TOC eliminados por mg de H_2O_2 consumido), que aumentó entre un 25 y un 35% respecto a los resultados obtenidos con sólo una única adición inicial.

Además, un análisis más profundo de los resultados permitió detectar y evaluar la opción de un rediseño del esquema de dosificación eliminando la idea de un punto de referencia específico de DO y abordando directamente el control de la pendiente de DO. Por lo tanto, esta tesis también abre nuevas líneas de investigación para aumentar la simplicidad y robustez de esta estrategia de control eficiente del proceso de foto-Fenton.

Table of Contents

1. Introduction and thesis outline

1.1 Water pollution problem

1.1.1 Water problem in the world

The growth of the world's population and the rapid development of industry have made environmental issues become more and more prominent, of which water scarcity is especially significant. Water is a limited resource, freshwater on the earth makes up only 2.5% of all water. Global warming significantly increased the intensity of drought, the severity of drought induces water scarcity situation (European Commission, 2012) According to statistics, there is worse to follow, 2 billion tons of human waste discharges in water ecosystems every day, 80% of global wastewater discharges into water bodies without being disposed (WWAP, 2017). The critical fact is that half of the world's population will be living in water-stressed regions by 2025.

1.1.2 Freshwater pollution

We need freshwater for drinking, bathing, recreation, growing food, industry and sustaining biodiversity. However, the increasing pollution of freshwater impact human health. The pollution can be grouped into several types: organic matter, pathogens, chemical pollution, salinity and plastic pollution. Emerging contaminants as pharmaceuticals appear in natural water ecosystem from pharmaceuticals discharges (Organization, 2018) can trigger hazardous problems for human, but we largely unknown about the extent and impacts of residual pharmaceuticals in freshwater.

Four thousand children die every day due to diseases caused by the contaminated water and the lack of adequate sanitation. In addition, polluted water has a significant reverse effect on the wildlife habitat: agrochemicals and runoff of fertilizer lead to nutrient pollution, which poses a severe threat to fish and other aquatic organisms.

In Latin America, Africa and Asia, the UN Environment Programme finds that serious organic pollution exists in one-seventh of all rivers. Asia, South and Central America, and sub-Saharan Africa suffer from severe nutrient pollution. Even for European countries, the nitrate level is detected in drinking water is higher than the European Union limit value (50 mg L^{-1}). Once water is

contaminated with eutrophication, fish and other animals can peg out from lack of oxygen because of algal blooms.

Above all, the 10th World Congress of Chemical Engineering, 1–5 October 2017, reported how to efficiently manage, treat, reclaim and distribute the needed water is an unquestionable Grand Challenge for chemical engineering (Negro et al., 2018). Moreover, the report "Beyond the Molecular Frontier: Challenges in Chemistry and Chemical Engineering in the 21st Century" was produced by National Research Council, which stated clearly that social and economic issues are the specific challenges to process systems engineering (Grossmann, 2004). For example, hazard reduction and protection of health and the environment remain significant concerns for the process industries. The primary goals for process systems engineering are developing novel methods and technologies that allow chemical engineers to meet the societal and environmental challenges. The challenges will necessitate using safe solvents and catalysts, producing nontoxic intermediates and benign products. However, the development and implementation of techniques demand computationally efficient aid for all aspects of designing, operating, controlling, monitoring and optimizing chemical process systems.

1.2 Water treatment technologies

1.2.1 Advanced oxidation process

The increasing concern for environmental issues related to public health problems caused many countries to amend water recycling guidelines. Used wastewater produced by normal anthropogenic activities can be effectively removed by flocculation-sedimentation process, filtration, antiseptic, and conventional biodegradable treatment (Legrini et al., 1993). Conventional treatment methods can hardly treat many low biodegradable chemical matters, however, the Drinking Water Directive 98/83/EC (Meeting of the Drinking Water Committee Draft text of Annex III," 2013) requires that any microorganisms, parasite or potentially hazardous substance must be absent from drinking water when it is supplied to consumers.

Industrial activities affect the environment significantly. The main contributors to wastewater emissions can be categorized as the Chemical industry,

Agriculture, waste management, production and processing of metals, and mineral industry. The majority of Chemicals have persistent nature that undermines the efficiency of conventional treatments. This characteristic makes these types of compounds were detected in increasing concentrations in wastewaters and water resources. Meanwhile, tighter regulation of wastewater emission has been implemented according to Directive 2010/75/EU, the effluents produced by most industries would be hard to comply with the water discharge criterion. The negative influence of chemical contaminants has long been regarded as inferior to microbial contaminants, however chemical matters continuous exposure in drinking water damage humans' health. To overcome this issue, many efforts have been invested in developing effective techniques by chemical engineers such as biodegradation, coagulation-sedimentation and advanced oxidation processes (AOPs) (Gar Alalm et al., 2015; Kakavandi et al., 2016), the advanced wastewater treatments are supporting proper disposal to reduce the risk of wastewater to the environment.

The advanced oxidation method is a strong oxidation method that involves potent oxidizing agents, like hydroxyl radicals ($HO^{\bullet}$) (Rodríguez-Chueca et al., 2016), which are produced through a series of chemical reactions. $HO^{\bullet}$ can be used in-situ to degrade pollutants and convert the refractory organic compounds into harmless end products like CO_2, H_2O, and minerals (Labiadh et al., 2015). **Table 1.1** lists the most common classes of AOPs. The report of WHO (Thompson et al., 2007) proposed that fluoride and arsenic are the most essential and significant chemical pollutants in water supplies, both chemicals have induced hazardous effects on human health on a global scale. Searching database, AOPs have been applied to the treatment of wastewater containing fluoride and arsenic (Hug and Leupin, 2003; Moreira et al., 2012; Sorlini et al., 2014). AOPs have revealed to be used to remove color and odour, sludge treatment, and reduce chemical organic contaminants in wastewater (Gar Alalm et al., 2015; Yamal-Turbay et al., 2013), even prevent possible accumulation of toxicity from waters soon after, AOPs develop into application methods for water disinfection (Giannakis et al., 2016). The last decade has witnessed the application of AOPs have been identified in various areas of wastewater treatment. The application of AOPs to treat high-strength organic wastewaters individual or combination with other techniques is flexible. Several studies have been successfully reported the application of AOPs before or after the biological process for water disinfection and destructing pharmaceuticals residues in municipal wastewater treatment plants (Perini et al., 2018; Ziylan and Ince, 2011).

Table 1.1 The classification of most common AOPs (Parsons, 2004)

Advanced Oxidation Process	
Non-photochemical Process	Photochemical Process
Ozonation (O_3)	UV photolysis
Fenton (Fe^{2+}/H_2O_2)	UV/hydrogen peroxide (UV/H_2O_2)
Ultrasound	UV/ozonation (UV/O_3)
Electrochemical oxidation	UV/hydrogen peroxide/ozonation ($UV/H_2O_2/O_3$)
Wet-air oxidation	UV/ultrasound
Supercritical water oxidation	Photo-Fenton ($Fe^{2+}/H_2O_2/UV$)
Pulsed plasma	Photocatalysis
Catalytic wet peroxide oxidation	Vacuum UV (VUV)
Radiolysis	

1.2.2 Fenton and photo-Fenton process

In the procedure of using advanced oxidation processes to treat wastewater, every kind of method has its advantages and disadvantages. The optimal technology with the essential characteristics, including safe discharge target ultimate mineralization of most hard-degraded compounds, and appropriate operation cost by means of minimizing required chemicals and complete reaction time.

The Traditional Fenton process (Neyens and Baeyens, 2003) was invented by Henry Fenton in the 1890s. The process is based on the reaction between homogeneous metal catalyst (Fe^{2+}) and H_2O_2, which effectively produces hydroxyl radicals ($HO^{\bullet}$). Fenton process can be conducted at ambient temperature and barometric pressure. The capacity of easily obtained Fenton reagent, flexible operations, short reaction time, harmless end product and extensive toxicity reduction prompt Fenton process as a promising technology in the wastewater treatment field. A wide range of actual applications with combination Fenton process has been reported, such as pre-oxidation of pharmaceutical wastewater (San Sebastián Martínez et al., 2003; Tekin et al., 2006) before biological process, pre-oxidation and coagulation of textile

wastewater (Kang et al., 2002), pretreatment of fiber manufacturing wastewater (Wei et al., 2013), treatment of landfill leachate (Deng and Englehardt, 2006) and pretreatment of fermentation brines from green olives (Rivas et al., 2003).

However, the traditional Fenton treatment leads to the production of a large amount of iron sludge, the production of iron oxide sludge improve the disposal cost and generate secondary pollution (Sheu and Weng, 2017). The regeneration rate of Fe^{2+} is significantly slow, which reduces efficiency in Fe^{2+} utilization. In order to ensure this process reacts continually, a great quantity of Fe^{2+} and H_2O_2 are needed.

Some scientific literatures have shown that introducing light (λ≤580nm) to the traditional Fenton reagent can greatly improve the oxidation efficiency and reduce the iron sludge (Plgnatello, 1992; Walling and Amarnath, 1982). Thus, the so-called photo-Fenton processes, which uses UV radiation as an external source of energy, can yield effective pollutant degradation.

Photo-Fenton process involves a series of parallel and successive reactions, the main reactions in photo-Fenton process consist of two steps, ferrous iron catalyze decomposition of hydrogen peroxide and photo-reduction of Fe(Ⅲ)-complex (***Eq. 2.1-2.2***):

$$Fe^{2+} + H_2O_2 \rightarrow Fe^{3+} + HO^{\cdot} + HO^{-} \qquad \textit{Eq. 2.1}$$

$$Fe(OH)^{2+} \xrightarrow{hv} Fe^{2+} + HO^{\cdot} \qquad \textit{Eq. 2.2}$$

Photo-Fenton process requires less iron addition but achieve higher degradation performance. In order to meet the regulation of European Community Directives, the limitation of iron emissions at 2 ppm, photo-Fenton process following the way of decreasing iron dose and reducing further management cost. Considering the application of reused water for irrigation, the food and agriculture Organization of the United Nations stipulate the limitation of Fe for long-term use is 5 mg L^{-1} (Oller and Malato, 2021).

1.2.3 H_2O_2 dosage is critical

The doses of H_2O_2 and Fe^{2+} are the direct effects on the degradation performance and operational cost in photo-Fenton process. The addition of most desirable concentrations for both reagents is the highly important parameter to determine optimal quantitative pollutants degradation and kinetic rates.

Usually, the increases in H_2O_2 and Fe^{2+} concentration contributes to higher degradation efficiency. However, both reagents have the addition limitation, the excessive H_2O_2 react with $HO^{\bullet}$ brings about the scavenging effect and increases the operational costs; the excessive Fe^{2+} not only scavenging of $HO^{\bullet}$ and reduction in color removal efficiency, but also enhances the quantity of iron sludge and management costs.

In light of avoiding the scavenging effect, development of addition strategy of Fenton reagents:

Successive addition of each Fenton reagents or both Fenton reagents.
Instead of absolute dosages, efforts in researching optimal ratio of Fenton reagents.

This thesis focus on developing continuous dosage scheme of H_2O_2, which attempts to minimize the reverse effect and maximize degradation performance. There are some previous studies on using the concept of continuous dosage of H_2O_2 in Fenton process:

- Continuous dosing H_2O_2 at a constant rate along the reaction time.
- Splitting the total amount of H_2O_2 into several portions and adding them at different set time.
- Using the variation of dissolved oxygen to regulate H_2O_2 supply.
- Pre-established H_2O_2 dosage protocol.
- Optimization of batch and fed-batch operations by model-based approaches, to determine the best H_2O_2 supply profile.

However, the above solutions still far from optimal, most proposals are partial and only useful in particular situations:

The first crucial issue is building a methodology to provide the optimal H_2O_2 dosage recipe and continuously adding H_2O_2 in a systematic way: previous researches use arbitrary time intervals to add arbitrary portions of additional H_2O_2, prevents the strategy to be reported as optimal.

Secondly, the lack of detailed dynamic models in Fenton and photo-Fenton processes, prevents exploiting model-based optimization methods to address dosage problem.

Thirdly, designed an optimal recipe but lack of operation flexibility.

Finally, addressed the dosage problem in an open-loop approach, not in a closed-loop. The output does not directly reflect the control action, lacking of an accurate and reliable dynamic model to describe the process response to the dosage input and guide the dosage.

1.3 Objectives

The general objective of this thesis is to develop efficient H_2O_2 dosage strategies to remove pharmaceuticals from wastewater via photo-Fenton process. In particular:

Objective 1: Develop and execute experimental methods and tools for measuring and assessing the performance of the photo-Fenton process. Expected outcomes are documented plant protocols and Standard operating procedures (SOP) for developing and reproducing the experimental work.

Objective 2: Develop and execute at pilot plant level dosage procedures for controlling the addition of H_2O_2 in photo-Fenton process, and better managing its performance along the reaction time. Expected outcomes are comparative studies of the enhanced degradation performance obtained in experimental runs following convenient dosage protocol.

Objective 3: Develop optimization methods for determining the best H_2O_2 dosage profile (optimal recipe) and experimentally validate the results at the pilot plant level. Expected outcomes are the optimal recipes that can be executed and compared with reference operational conditions:

First, to propose a practical methodology for experimentally addressing the optimization problem of H_2O_2 dosage using recipe optimization concepts and a convenient time discretization.
Second, to develop a systematic, reliable and generalized H_2O_2 dosage methodology to improve practical applications and to further understand the nature of the dosage.

1.4 Thesis outline

The main objective of this thesis is the proposal of a generalized H_2O_2 addition strategy that can be applied in photo-Fenton process to degrade pharmaceuticals efficiently.

To reach this objective, this work encompasses four parts to explain the reason why we focus on current research, how we investigate current research, what objectives that we want to achieve, and what conclusions that we draw.

The first part composes two chapters: ***introduction*** and ***state of the art*** chapters. ***Chapter 1*** provides a general motivation and background of this work, water pollution problem is the critical challenge to motivate the improvement of wastewater treatments. This thesis takes advantage of advanced oxidation process, particularly, photo-Fenton process, as the water treatment throughout whole research. ***Chapter 2*** gives a deeper understanding of photo-Fenton process, and the required methods and tools that employed in optimization strategies.

Chapter 3 is the second part to carry on the introduction to the experimental settings and analytical method.

The third part including three chapters. ***Chapter 4*** faces recipe optimization issue, a methodology was proposed aimed at optimizing the dosage profile along a discretized time horizon following recipe optimization concepts, systematically addressed the H_2O_2 dosage problem. In ***Chapter 5***, a hybrid approach between open and closed loop for addressing the challenge of design H_2O_2 dosage strategies. ***Chapter 6*** verifies the generalization of second proposed H_2O_2 dosage protocol, using different water matrix, different initial contaminant concentration, contaminant mixtures and different contaminant

to test, different strategies were also tested in order to simplify the proposed strategy.

The last ***Chapter 7*** concludes the overall results of the studies and opens a research line for the future work

1.5 References

Deng, Y., Englehardt, J.D., 2006. Treatment of landfill leachate by the Fenton process. Water Research 40, 3683–3694. https://doi.org/10.1016/j.watres.2006.08.009

Meeting of the Drinking Water Committee Draft text of Annex III, 2013.

European Commission, 2012. Water Scarcity & Droughts-2012 Policy Review-Building blocks Non-Paper Background.

Gar Alalm, M., Tawfik, A., Ookawara, S., 2015. Comparison of solar TiO2 photocatalysis and solar photo-Fenton for treatment of pesticides industry wastewater: Operational conditions, kinetics, and costs. Journal of Water Process Engineering 8, 55–63. https://doi.org/10.1016/j.jwpe.2015.09.007

Giannakis, S., Polo López, M.I., Spuhler, D., Sánchez Pérez, J.A., Fernández Ibáñez, P., Pulgarin, C., 2016. Solar disinfection is an augmentable, in situ-generated photo-Fenton reaction—Part 1: A review of the mechanisms and the fundamental aspects of the process. Applied Catalysis B: Environmental 199, 199–223. https://doi.org/10.1016/j.apcatb.2016.06.009

Grossmann, I.E., 2004. Challenges in the new millennium: Product discovery and design, enterprise and supply chain optimization, global life cycle assessment, in: Computers and Chemical Engineering. pp. 29–39. https://doi.org/10.1016/j.compchemeng.2004.07.016

Hug, S.J., Leupin, O., 2003. Iron-catalyzed oxidation of Arsenic(III) by oxygen and by hydrogen peroxide: pH-dependent formation of oxidants in the Fenton reaction. Environmental Science and Technology 37, 2734–2742. https://doi.org/10.1021/es026208x

Kakavandi, B., Takdastan, A., Jaafarzadeh, N., Azizi, M., Mirzaei, A., Azari, A., 2016. Application of Fe3O4@C catalyzing heterogeneous UV-Fenton system for tetracycline removal with a focus on optimization by a response surface method. Journal of Photochemistry and Photobiology A: Chemistry 314, 178–188. https://doi.org/10.1016/j.jphotochem.2015.08.008

Kang, S.F., Liao, C.H., Chen, M.C., 2002. Pre-oxidation and coagulation of textile wastewater by the Fenton process. Chemosphere 46, 923–928. https://doi.org/10.1016/S0045-6535(01)00159-X

Labiadh, L., Oturan, M.A., Panizza, M., Hamadi, N. ben, Ammar, S., 2015. Complete removal of AHPS synthetic dye from water using new electro-fenton oxidation catalyzed by natural pyrite as heterogeneous catalyst. Journal of Hazardous Materials 297, 34–41. https://doi.org/10.1016/j.jhazmat.2015.04.062

Legrini, O., Oliveros, E., Braun, A.M., 1993. Photochemical Processes for Water Treatment. Chemical Reviews 93, 671–698. https://doi.org/10.1021/cr00018a003

Moreira, F.C., Vilar, V.J.P., Ferreira, A.C.C., dos Santos, F.R.A., Dezotti, M., Sousa, M.A., Gonçalves, C., Boaventura, R.A.R., Alpendurada, M.F., 2012. Treatment of a pesticide-containing wastewater using combined biological and solar-driven AOPs at pilot scale. Chemical Engineering Journal 209, 429–441. https://doi.org/10.1016/j.cej.2012.08.009

Negro, C., Garcia-Ochoa, F., Tanguy, P., Ferreira, G., Thibaulte, J., Yamamoto, S., Gani, R., 2018. Barcelona Declaration – 10th World Congress of Chemical Engineering, 1–5 October 2017. Chemical Engineering Research and Design 129, A1–A2. https://doi.org/https://doi.org/10.1016/j.cherd.2017.12.035

Neyens, E., Baeyens, J., 2003. A review of classic Fenton's peroxidation as an advanced oxidation technique. Journal of Hazardous Materials 98, 33–50.

Oller, I., Malato, S., 2021. Photo-Fenton applied to the removal of pharmaceutical and other pollutants of emerging concern. Current Opinion in Green and Sustainable Chemistry 29. https://doi.org/10.1016/j.cogsc.2021.100458

Organization, W.H., 2018. Developing drinking-water quality regulations and standards: general guidance with a special focus on countries with limited resources. World Health Organization.

Parsons, S., 2004. Advanced oxidation processes for water and wastewater treatment. IWA publishing.

Perini, J.A.L., Tonetti, A.L., Vidal, C., Montagner, C.C., Nogueira, R.F.P., 2018. Simultaneous degradation of ciprofloxacin, amoxicillin, sulfathiazole and sulfamethazine, and disinfection of hospital effluent after biological treatment via photo-Fenton process under ultraviolet germicidal irradiation. Applied

Catalysis B: Environmental 224, 761–771. https://doi.org/10.1016/j.apcatb.2017.11.021

Plgnatello, J.J., 1992. Dark and Photoassisted Fe3+-Catalyzed Degradation of Chlorophenoxy Herbicides by Hydrogen Peroxide. Environmental Science and Technology 26, 944–951. https://doi.org/10.1021/es00029a012

Rivas, F.J., Beltrán, F.J., Gimeno, O., Alvarez, P., 2003. Optimisation of Fenton's reagent usage as a pre-treatment for fermentation brines. Journal of Hazardous Materials 96, 277–290.

Rodríguez-Chueca, J., Mediano, A., Pueyo, N., García-Suescun, I., Mosteo, R., Ormad, M.P., 2016. Degradation of chloroform by Fenton-like treatment induced by electromagnetic fields: A case of study. Chemical Engineering Science 156, 89–96. https://doi.org/10.1016/j.ces.2016.09.016

San Sebastián Martínez, N., Fernández, J.F., Segura, X.F., Ferrer, A.S., 2003. Pre-oxidation of an extremely polluted industrial wastewater by the Fenton's reagent. Journal of Hazardous Materials 101, 315–322. https://doi.org/10.1016/S0304-3894(03)00207-3

Sheu, S.-H., Weng, H.-S., 2017. TREATMENT OF OLEFIN PLANT SPENT CAUSTIC BY COMBINATION OF NEUTRALIZATION AND FENTON REACTION. Wat. Res 35.

Sorlini, S., Gialdini, F., Stefan, M., 2014. UV/H2O2 oxidation of arsenic and terbuthylazine in drinking water. Environmental Monitoring and Assessment 186, 1311–1316. https://doi.org/10.1007/s10661-013-3481-z

Tekin, H., Bilkay, O., Ataberk, S.S., Balta, T.H., Ceribasi, I.H., Sanin, F.D., Dilek, F.B., Yetis, U., 2006. Use of Fenton oxidation to improve the biodegradability of a pharmaceutical wastewater. Journal of Hazardous Materials 136, 258–265. https://doi.org/10.1016/j.jhazmat.2005.12.012

Walling, C., Amarnath, K., 1982. Oxidation of mandelic acid by Fenton's reagent. Journal of the American Chemical Society 104, 1185–1189. https://doi.org/10.1021/ja00369a005

Wei, J., Song, Y., Tu, X., Zhao, L., Zhi, E., 2013. Pretreatment of dry-spun acrylic fiber manufacturing wastewater by Fenton process: Optimization, kinetics and mechanisms. Chemical Engineering Journal 218, 319–326. https://doi.org/10.1016/j.cej.2012.12.060

WWAP, U.N.W.W.A.P., 2017. The United Nations World Water Development Report 2017. Wastewater: The Untapped Resource. Paris, UNESCO, The United

Nations World Water Development Report 2017. Wastewater: The Untapped Resource. Paris, UNESCO.

Yamal-Turbay, E., Jaén, E., Graells, M., Pérez-Moya, M., 2013. Enhanced photo-fenton process for tetracycline degradation using efficient hydrogen peroxide dosage. Journal of Photochemistry and Photobiology A: Chemistry 267, 11–16. https://doi.org/10.1016/j.jphotochem.2013.05.008

Ziylan, A., Ince, N.H., 2011. The occurrence and fate of anti-inflammatory and analgesic pharmaceuticals in sewage and fresh water: Treatability by conventional and non-conventional processes. Journal of Hazardous Materials 187, 24–36. https://doi.org/10.1016/j.jhazmat.2011.01.057

2. State-of-the-Art

2.1 The influencing parameters of photo-Fenton process

2.1.1 pH

The pH dependency is the main disadvantage for homogeneous Fenton process to optimize process performance. Photo-Fenton process is usually conducted in acidic medium around pH 2-4 **(Table 2.1)** for degradation of organic pollutants. The pH lower or higher than optimal pH range induce reversed affect. The optimal pH value usually slightly below 3, normally at 2.8 (**Table 2.2**) by following the suggestion of Pignatello et al. (2006).

When pH lower than optimal value, abundant H^+ inhibits the shift formation of Fe^{2+} from Fe^{3+}. Hence, strong acidic media reduce the production of $HO^{\bullet}$.

$$Fe^{3+} + H_2O_2 \xrightarrow{hv} Fe^{2+} + HO_2^{\cdot} + H^+ \qquad \textit{Eq. 2.3}$$

In lower pH condition, H_2O_2 tend to be stable and generate the stability modality $H_3O_2^+$, which severely reduces $HO^{\bullet}$ formation, decreasing Fenton reagents accordingly. On the contrary, a higher pH value presents the decomposition of H_2O_2 to produce $HO^{\bullet}$ and accelerate auto-decomposition of H_2O_2 to water and oxygen (Badawy et al., 2006). pH value higher than 4, free Fe^{3+} and Fe^{2+} in solution tend to precipitation, induced to decrease Fenton reagents.

In the way of adding chemical additive (Romero et al., 2016a) or change catalyst type could extend the working pH range.

In order to overcome the drawback of limited pH range and reduce iron sludge, change catalyst type through replaced catalyst Fe^{2+} by solid catalyst, using various support to stabilize iron species, its heterogeneous Fenton process. However, heterogeneous Fenton process is hard to industrialization and not practically efficient in highly polluted wastewater (Ganiyu et al., 2018; Navalon et al., 2010).

Table 2.1 Optimal performance in a pH range

Contaminant	Process System & Experimental Setup and condition	Studied pH range	Optimal pH value & Remarks	References
Industrial Dyeing Effluent (IDE)	0.4 L IDE in photo-Fenton reactor Solar light and 350 nm artificial UV [COD] = 1636 ± 47 mg L^{-1} [H_2O_2] = 6 g/L [Fe^{2+}] = 0.05 g/L	pH 2, 3, 4, 5, 6, 7, 8, 11	120 min reaction time: The highest COD removal in the pH range of 2-3. pH value increased, IDE removal efficiency followed a decreased tendency.	(Módenes et al., 2012)
2,4-dichlorophenol (2,4DCP)	Fenton and photo-Fenton 3250 mL capacity of photoreactor [2,4 DCP] = 0.15 mM [H_2O_2] = 10 mM [Fe^{2+}] = 0.2 mM UV = 253.7 nm, 40W	pH 3, 4, 5	2, 4 DCP removal rate kept in a same value at pH 3, 4 and 5 ($k_{2,4\ DCP}$ = 0.65 min^{-1}). Higher mineralization rate was achieved at pH 3 (k_{TOC} = 0.10 min^{-1}), compared to the results at pH 4 (k_{TOC} = 0.058 min^{-1}) and 5(k_{TOC} = 0.76 min^{-1}).	(Karci et al., 2012)
Phenol	Fenton and Fenton-like reactions	pH 1-7	Phenol degradation and H_2O_2 decomposition	(Jiang et al., 2010)

	1000 mL glass reactor $[H_2O_2]$ = 0-5 mM $[Fe^{2+}]$ = 0-1 mM $[Fe^{3+}]$ = 0-1 mM T = 25 ± 2°C		Fenton process: optimum pH 2.5-6.0. Fenton-like process: optimum pH 2.8-3.8.	
Chlorobenzene	Fenton oxidation 500 mL reactor H_2O_2 and Fe^{2+} addition at a rate of 5 mL/h [Chlorobenzene] = 3.8mM $[H_2O_2]$ = 2.7 mM $[Fe^{2+}]$ = 5 mM T = 25°C	pH 2-7	120 min reaction time: The highest yield of product formed per mole of H_2O_2 consumed was observed at pH 2-3	(Sedlak and Andren, 1991)

Table 2.2 Application of optimal pH value 2.8/3 in references

Contaminant	Process System & Experimental Setup and condition	Studied pH range	Optimal pH value & Remarks	References
Phenol	Fenton: 500 mL solution in magnetic device Solar Fenton: 1L borosilicate beakers UV Fenton: 500 mL capacity in an immersion type photo-reactor; 150W; 254 nm [phenol] = 2.12 mM $[H_2O_2]$ = 30 mM $[Fe^{2+}]$ = 0.8 mM		All experiments were conducted at pH = 3.0 ± 0.2	(Kavitha and Palanivelu, 2004)
Cotton-textile dyeing wastewater	1L wastewater in lab-scale photoreactor prototype [DOC] = 152 mg C/L $[H_2O_2]$ = maintained between 100 - 500 mg L^{-1} $[Fe^{2+}]$ = 60 mg L^{-1} I = 44 W	pH 2.4, 2.8, 3.2, 3.6, 4.5	Optimal pH = 2.8. Compared pH 2.8 and 3.2, although both pH have very similar amount of dissolved iron during the experiments, initial pH 2.8 showed a faster kinetic rate, and best DOC abatement.	(Soares et al., 2014)

	T = 30°C			
Amoxicillin, Ampicillin, Diclofenac, Paracetamol	Solar photo-Fenton 4L solution in compound parabolic collectors 100 mg L^{-1} of each pharmaceuticals $[H_2O_2]$ = 1500 mg L^{-1} $[Fe^{2+}]$ = 500 mg L^{-1}	pH 3, 5, 7, 10	Optimal pH = 3. 120 min reaction time Amoxicillin completely removed at pH 3; pH increased from 5 to 10, degradation decreased from 97% to 62%. Same trend was observed with ampicillin, diclofenac, paracetamol	(Alalm et al., 2015)
Acid Orange 3 (AO3)	Fenton and photo-Fenton [AO3] = 50 mg L^{-1} $[H_2O_2]$ = 5 mM $[Fe^{2+}]$ = 2 mM T = 30°C 365 nm	pH 2, 3, 4, 5, 6, 7, 8	Optimal pH = 3. 60 min reaction time For both processes, the maximum AO3 removal and decolorization were achieved at pH 3. Fenton: increased pH from 3 to 8, AO3 removal decreased from 97% to 65%. Photo-Fenton: increased pH from 3 to 8, AO3 removal decreased from 98% to 50%.	(Naseem et al., 2019)
Thiabendazole (TBZ)	Photo-Fenton process	pH 2.8, 5	Optimal pH = 2.8.	(Caram et al., 2018)

	250 mL solution in a cylindrical Pyrex vessel 550W Xenon lamp with glass filter [TBZ] = 62.5 mg L^{-1} [H_2O_2] = 272 mg L^{-1} [Fe(III)] = 5 mg L^{-1}		60 min reaction time With or without soluble bioorganic substances, compared the ability of photo-Fenton to remove TBZ, pH 2.8 always faster than pH 5.	

2.1.2 Fenton reagents

One of the most significant steps in the photo-Fenton process is optimizing the concentration of H_2O_2 and iron catalyst. Both reagents play an equally important role in affecting degradation performance and operational cost. The efficiency of photo-Fenton is declined when the presence of excess H_2O_2 and Fe^{2+} in the system. The excessive Fenton reagents act as the H_2O_2 scavenger (**Eq. 2.4-2.5**) and undermine the quantity of $HO^{\bullet}$. Thus, the higher dose of H_2O_2 and Fe^{2+} may bring about the opposite effect on the degradation rate. In addition, treatment in an overdosage enhances the operational cost, and the unused quantity of iron sludge in sewage will be increased due to the excess iron salts (Babuponnusami and Muthukumar, 2014).

$$HO^{\cdot} + H_2O_2 \rightarrow HO_2^{\cdot} + H_2O \qquad \textit{Eq. 2.4}$$

$$Fe^{2+} + HO^{\cdot} \rightarrow Fe^{3+} + HO^{-} \qquad \textit{Eq. 2.5}$$

2.1.2.1 The optimization process of H_2O_2 or iron catalyst concentration

For example, 4-chlorophenol removal increased when the concentration of H_2O_2 increased from 3.1 mmol/L to 6.6 mmol/L, but the removal efficiency decreased with the H_2O_2 concentration increased to 30.7 mmol/L, and the efficiency follows a trend of decline as the H_2O_2 concentration continues to increase in the study conducted by Duan et al. (2014)

The influence of iron concentration on removal of different pharmaceuticals during photo-Fenton process was investigated by Alalm et al. (2015). After 60 min of irradiation, kept H_2O_2 dose at 1500 mg L^{-1}, increased Fe^{2+} from 100 mg $L^{-1}$to 500 mg L^{-1}, the degradation efficiency of amoxicillin increased from 33% to 97%; ampicillin removal from 40% to 88%; diclofenac from 35% reached to 94%, and degradation of paracetamol increased from 46% to 100%. Nonetheless, kept increasing Fe^{2+} dosage to 750 mg L^{-1}, limitation of improvement was observed in the degradation process.

2.1.2.2 The optimization process of H_2O_2/Fe^{2+} ratio

The similar results obtained by Gulkaya et al. (2006) for a carpet dyeing wastewater degradation. The H_2O_2 concentration changed between 19.3 and 577.5 g/L, the other parameters such as $FeSO_4$ dose, pH and temperature kept at a constant value. The results showed that the COD removal increased in the wake of H_2O_2 concentration increased from 19.3 to 385 g/L. However, no further COD removal was reached when H_2O_2 concentration higher than 385 g/l. On the other hand, the effect of $FeSO_4$ load was researched by increasing addition from 1.1 to 10.9 g/L. The growth in the COD removal efficiencies from 40 to 90% following iron dose from 1.1 to 5.5 g/L, whereas the further COD removal remained within 94-95% at higher iron dose. Presumably, the extent of oxidation performance increase reaches a margin at the certain reagent concentration. In this study, optimum ratio of H_2O_2/Fe^{2+} was investigated to obtain maximum COD removal. This concept (Pérez-Moya et al., 2010; Yamal-Turbay et al., 2015) superior than set the absolute dosages of Fenton reagents because its avoid one of them in the counteractive concentration. According to the reported outcomes, provided the H_2O_2/Fe^{2+} ratio is required remain unchanged, acquisition of the same treatment efficiency regardless of the certain concentration for H_2O_2 and iron salt. The optimal ratio 192 was chosen to remove dye efficiently and economically.

2.1.2.3 The optimization process of Fenton reagent-dosing strategy

Similarly, some contributions have been devoted to avoiding the scavenging effect by using different strategies to provoke the best oxidation efficiency. The strategy of successive addition of Fenton reagents during Photo-Fenton process was investigated and the decontamination capacity was compared with unique addition at the beginning of the process.

- Continuous dosage of H_2O_2 and addition of iron at the beginning (**Table 2.3**)

For one situation, successive addition of H_2O_2 during reaction time. Chu et al. (2007) successfully improved the performance of degrading atrazine by dosing the H_2O_2 at different times. Zazo et al. (2009) continuously feed H_2O_2 upon Fenton oxidation process of phenol, a higher conversion of phenol was reached.

To address dosage operation in a systematic way, a significant amount of work has been conducted in highly engineered systems that are the AOPs combine with process system engineering. A pre-established H_2O_2 dosage protocol was proposed to improve the dosage profile of photo-Fenton successfully (Yamal-Turbay et al., 2012). The protocol was influenced by the initial addition and the initial dosing time, the best performance was obtained with the operation condition of 20% total amount of H_2O_2 and initial dosage time at 36.1 min, which was 25% higher than the conversion results that produced without dosage scheme.

In order to control H_2O_2 addition automatically, some researchers aimed to develop an optimal recipe and strategy depend on the dissolved oxygen (DO) evolution, using the indicator of on-line measurement. The on-line measurements favour to control H_2O_2 concentration throughout the process, for the sake of maintaining the optimal concentration during the degradation process. Santos-Juanes et al. (2011) reported that an increase in oxygen concentration during the photo-Fenton process is a signal of H_2O_2 decomposition, this kind of H_2O_2 consumption is inefficient instead of reacting with organic matter. Thus, this research proposed that monitoring DO concentration as a promising tool for correcting continuous dosing H_2O_2. Some successful applications (Ortega-Gómez et al., 2012; Prieto-Rodríguez et al., 2011) used the indicator of DO concentration to regulate H_2O_2 addition.

— Continuous dosage of iron and addition of H_2O_2 at the beginning

Similar assumptions were tested by using addition of H_2O_2 at start time and continuous dosage of Fe^{2+} accompany experiment time. I. Carra et al. (2013) reported the strategy of iron additions permitted Photo-Fenton removed pesticides at neutral pH, the results of conducting Photo-Fenton at neutral pH resemble the reaction rate and mineralization values of Photo-Fenton at pH 2.8. The sequential iron dosage also be used to evaluate the influence on disinfection process (Ortega-G Omez et al., 2014). Compared with the test of adding 20 mg L^{-1} iron at the beginning (time=0 min), the successive iron dosage (at time = 0, 5, 10 min) slowed down the disinfection rate and increased the consumption of H_2O_2.

A recent study applied the sequential iron dosage strategy in the application of solar photo-Fenton at neutral pH. The removal efficiency of micropollutant and toxicity was higher than 99%. The strategy was carried out with an initial

dose of 30 mg $L^{-1}H_2O_2$ and fed four iron additions every 5 min to municipal wastewater. Fe-EDDS was used to conquer the problem of iron solubility and achieved similar effects in endocrine removal, as well as phytotoxicity and cytotoxicity (Rivas Ibáñez et al., 2017).

— Continuous dosage of H_2O_2 and iron during the treatment process **(Table 2.4)**

In contrast to the previous strategies, where only H_2O_2 or iron source was supplied step-wise, in some studies Fenton reagents were added simultaneously in order to reduce the adverse reactions. Prato-Garcia and Buitrón, 2012 used three reagent-dosing strategies to assess their influence on toxicity and biodegradability of a mixture of three azo dyes (acid blue 113, acid orange 7 and acid red 151). The first strategy (E1) dosed Fenton reagent (1000 mg H_2O_2 and 50 mg Fe^{2+}) at the initial time. The second strategy (E2) administrated the reagents continuously at a flow rate of 16.66 mg H_2O_2/min and 0.83 mg Fe^{2+}/min, five injection time was set to evaluate varied concentration effect of reagents. The E3 strategy added Fenton reagents during 60 min experiment time at a constant rate with different concentration of reagents. E3 strategy was the best condition allowed a lower chemical consumption and improved the quality of the effluent.

Table 2.3 Continuous dosage of H_2O_2 during the treatment process

Contaminant	Process System & Experimental Setup and condition	Addition approach	Objective function & Results	References
Indanthrene blue dye	UV/H_2O_2 A 0.5L thermostatic photochemical reactor $[dye]_0$ = 60 mg L^{-1} pH = 5	Single addition: 1500 mg L^{-1} H_2O_2 at the beginning. Continuous addition: 1500 mg L^{-1} H_2O_2 was fractionated into four parts (4*375 mg L^{-1}), which were injected at 0 min, 20 min, 40 min, 60 min.	OF: TOC removal, COD reduction at 60 min, 96.3% COD reduction with single aliquot 98.6% COD reduction, 92% TOC reduction with aliquots of 375 mg L^{-1}.	Almeida et al., 2015
Sawmill wastewater	Fenton process 200 mL raw wastewater in a batch stainless stell pressurized reactor $[COD]_0$ = 3 g/L pH = 3 Fe^{3+} = 25 mg L^{-1} T = 120°C	Single addition: 100 and 200% of the theoretical stoichiometric amount relative to COD (2.125 g H_2O_2 g^{-1} COD) was added at the beginning. H_2O_2 dose was distributed in 3 steps. A first addition was 50% of the total amount that initially added, the rest was divided as 25% each and	OF: TOC reduction 150 min reaction time Single 100% amount, 6400 mg L^{-1} H_2O_2: 52% TOC reduction. Continuous addition: 73% TOC reduction.	Macarena Munoz, 2014

		injected when the measured H_2O_2 was negligible after first addition.	Single 200% amount, 12800 mg L^{-1} H_2O_2: 62% TOC reduction. Continuous addition: 82% TOC reduction.	
phenol	Catalytic wet peroxide oxidation 1 g/L phenol solution 250 mL thermostated batch reactor 25 g/L CuO/alumina catalyst Initial pH value 7	Single addition, at 323 K or 343 K, 3.3 mL or 9.9 mL H_2O_2 added at the beginning. H_2O_2 was added in 3 steps (one-third each of total amount), after first addition, additional H_2O_2 was added when monitored H_2O_2 concentration was negligible.	OF: Phenol removal, TOC conversion At 180 min, For 323 K, single 3.3 mL H_2O_2: 71% phenol removal and 48% TOC conversion. Continuous addition: 87% phenol removal and 60% TOC conversion. Single 9.9 mL: 90% TOC conversion. Continuous addition: 86% TOC conversion. For 343 K, single 3.3 mL H_2O_2: 76% TOC conversion. Continuous	N. Inchaurrondo, 2012

			addition: 90% TOC conversion. Single 9.9 mL: 94% TOC conversion. Continuous addition: 91% TOC conversion. Conclusion: compared with single addition of high amount of H_2O_2, no benefit in multiple addition of H_2O_2.	
Reactive Blue 4 (RB4)	Solar photo-Fenton 35 L solution in Solar Compound Parabolic Collector (CPC) UV-A (300–400 nm). $[RB4]_0$ = 20 ppm Fe^{2+} = 4 ppm $(COOH)_2$ = 19 ppm pH 2 no air injection	Single addition: 250 ppm H_2O_2 at the beginning. Initial $[H_2O_2]$ = 50 ppm, prior to continuous addition of H_2O_2, continuous H_2O_2 was added through a needle at a flow rate = 0.29 mL/min.	OF: TOC removal 61% TOC removal with single addition. 82% TOC removal with continuous addition H_2O_2.	Monteagudo, J. M., et al., 2010

A synthetic phenolic mixture (protocatechuic, syringic, veratric, vanillic, 4-hydroxybenzoic, 3,4,5-trimethoxybenzoic acids)	Fenton process 300 mL of the mixture in a glass reactor $[TOC]_0$ = 370 mgC/L pH = 3 Fe^{2+} = 271 mg	Single addition: 488 mM H_2O_2 was added totally at the beginning. Total H_2O_2 was divided in 6 aliquots and injected each hour (6 h reaction time, 6 injections). Total H_2O_2 was divided in 12 aliquots and injected each 30 min.	OF: TOC removal 6 h reaction time Single addition: 55.7% TOC removal. 6 injections: 61.4% TOC removal. 12 injections: 67% TOC removal.	Rui C. Martins, 2010
Azo dye Orange II (OII)	Solar photo-Fenton 35 L solution in Solar Compound Parabolic Collector (CPC) UV-A (315-400 nm). $[OII]_0$ = 20 ppm Fe^{2+} = 2 ppm	75 ppm H_2O_2 added at the beginning, continuous H_2O_2 was added through a syringe pump at a constant flow rate along reaction	OF: TOC removal 95% TOC removal with continuous addition H_2O_2 80% TOC removal with single addition.	Monteagudo, J. M., et al. 2009

Atrazine (ATZ)	Fenton $[ATZ]_0$ = 0.01 mM Fe^{2+} = 0.1 mM pH = 3 Room temperature	Single addition: 0.1 mM H_2O_2 dosed at the beginning. Split 0.1 mM H_2O_2 in an even-dose way: 0.05 mM H_2O_2 at 0 min, 0.05 mM dosed at 1.5, 2.5, 4.0, 5.0, 7.5, 10.0, 12.5, and 15.0 min. Split 0.1 mM H_2O_2 in an uneven-dose way: the first dose H_1= 0.03, 0.04, 0.05, 0.06 and 0.07 mM at 0 min. The second dose H_2=0.1-H_1 mM was added at 5 min.	OF: ATZ removal At 25 min, Compared with one-shot 0.1 mM H_2O_2 addition, ATZ removal improved 10% with 0.05 mM H_2O_2 at 0 min and 0.05 mM H_2O_2 at 5 min. Compared with one-shot 0.1 mM H_2O_2 addition, ATZ removal improved 11% with 0.06 mM H_2O_2 at 0 min and 0.04 mM H_2O_2 at 5 min.	Chu et al., 2007

Acid Black 1 (AB1)	Photo-Fenton-like process 1 L volume solution 8W UVC 0.1 mM AB1 6.4 mM H_2O_2 0.5 g/L Cu/acid-activated bentonite clay pH = 3 T = 30°C	100% H_2O_2 added at 0 min. 80% H_2O_2 added at 0 min, 20% added at 0 min 100% H_2O_2 added at 0 min, 20% added at 60 min	OF: TOC removal At 120 min Single addition: 20% TOC was left over at 120 min. Splitting the required dosage into an 8:2 ratio, TOC removal was notably increased at 15 min. 94% TOC removal was recorded at 120 min. Excess 20% H_2O_2 added at 60min, similar TOC removal was achieved at 120 min to the second method.	Alex Chi-Kin Yip, 2005
Municipal wastewater effluent (SMWWE)	Photo-Fenton 60 L Compound Parabolic Collector (CPC) solar reactor UVA = 5.3(±1.2) W/m^2 pH = 3 Fe^{2+} = 5 and 10 mg L^{-1}	5 mg L^{-1} Fe^{2+} and 10 mg $L^{-1}H_2O_2$ were added at initial, 10 mg L^{-1} H_2O_2 dose was added every 30 min. 10 Fe^{2+} and 20 mg L^{-1} H_2O_2 were added at initial, 20 mg L^{-1} H_2O_2 dose was added every 30 min.	OF: DOC reduction, fungi spore inactivation In 5 h, spore inactivation and DOC reduction were enhanced with continuous addition of H_2O_2	M.I. Polo-López, et al., 2014

Table 2.4 Comparison of different feeding modes

Contaminant	Process System & Experimental Setup and condition	Addition approach	Objective function & Results	References
Landfill leachate	Fenton 1-L double jacket spherical plastic reactor pH = 2.5 T = 25°C	Strategy 1: 0.05 M Fe^{2+} was added at 0 min, 0.075 M H_2O_2 was added at 0 min or in two steps (at 0 and 30 min). Strategy 2: 0.05 M Fe^{2+} and 0.075 M H_2O_2 were added simultaneously in one feeding at 0 min; two feedings at 0 and 30 min; three feedings at 0, 15, 30 min; five feedings at 0, 7.5, 15, 22.5, and 30 min.	OF: TOC removal, COD removal At 60 min: With strategy 1: Initial COD = 1000 mg L^{-1}, COD removal increased from 57.4% (single addition) to 63.6% (two steps). Initial COD = 2000 mg L^{-1}, COD removal increased from 42% (single addition) to 49.7% (two steps). With strategy 2: Initial COD = 1000 mg L^{-1}, COD removal increased from 57.4% (single addition) to 65.9% (multiple feeding).	Hui Zhang, et. al, 2005

			Initial COD = 2000 mg L^{-1}, COD removal increased from 42% (single addition) to 53.4% (multiple feeding). Conclusion: Strategy 2 achieved a little higher COD removal than strategy 1.	
The mixture of acid blue 113, acid orange 7 and acid red 151	Solar photo-Fenton 2.5L compound parabolic concentrator $[mixture]_0$ = 300 mg L^{-1} pH = 2.8 - 3	First strategy (E_1): add Fenton reagent at the beginning, Fe^{2+} = 20 mg L^{-1}, H_2O_2 = 400 mg L^{-1}. (*E_2 and E_3, H_2O_2 and Fe^{2+} were supplied simultaneously*) E_2 strategy: the reactants were dosed continuously (16.66 mg H_2O_2/min and 0.83 mg Fe^{2+}/min), the duration of the injection time at five injection times (12, 24, 36, 48 and 60 min). After 12 min, 16.66 mg/min*12 min/2.5L= 69.97 mg L^{-1} H_2O_2, 20% of total H_2O_2; So at 24 min, 40% H_2O_2 was added; 36 min,	OF: Specific Ultraviolet Absorption index (SUVA) removal At 60 min: The lower reagent dose, 60% of the total reagent. For E_3, 10.4% SUVA removal. For E_1, 7.9%; for E_2, 7.7%. 100% reagent dose, E_3, 34.2% SUVA removal; for E_1, 29.6%; for E_2, 33.7%.	D. Prato-Garcia, Germán Buitrón, 2012

		60% H_2O_2; 48 min, 80%; 60 min, 100%. For Fe^{2+} strategy is the same as H_2O_2. E_3 strategy: the reactants were dosed during 60 min at a constant rate, but with different solution concentrations.	Conclusion: The best condition was the E_3	
Palm oil mill effluent (POME)	Fenton process Magnetic stirring at 500 rpm $[TOC]_0$ = 0.19 g/L $[COD]_0$ = 0.031 M $COD:H_2O_2:Fe^{2+}$ = 1:4:1 pH = 2-3 T = 25°C	Conventional: Total H_2O_2 and $FeSO_4$ were added at 0 min. Fractional H_2O_2: Total $FeSO_4$ was added at 0 min, H_2O_2 was divided into 5 similar portions and added at 0, 5, 10, 15 and 20 min. Fractional Fe^{2+}: Total H_2O_2 was added at 0 min, $FeSO_4$ was divided into 5 similar portions and added at 0, 5, 10, 15 and 20 min. Continuous H_2O_2: Total $FeSO_4$ was added at 0 min. H_2O_2 was dissolved in 60 mL ultrapure water, gradually pumped into the reactor at a constant flow rate (1 mL/min) for 60 min.	OF: TOC reduction, TN reduction At 120 min: Conventional: around 85% TOC reduction. Fractional H_2O_2: around 89% TOC reduction. Fractional Fe^{2+}: around 100% TOC reduction. Continuous H_2O_2: around 84% TOC reduction. Continuous Fe^{2+}:100% TOC reduction.	Disni Gamaralalage, et, al 2020

		Continuous Fe^{2+}: Total H_2O_2 was added at 0 min. FeSO4 was dissolved in 60 mL of ultrapure water, gradually pumped into the reactor at a constant flow rate (1 mL/min) for 60 min. Fractional H_2O_2 and Fe^{2+} (Simultaneous): both reagents were divided into 5 similar portions each and added together at 0, 5, 10, 15 and 20 min. Continuous H_2O_2 and Fe^{2+} (Simultaneous continuous): both reagents were dissolved in 60 mL ultrapure water each, pumped to solution for 60 min at identical flow rates (1 mL/min).	Fractional H_2O_2 and Fe^{2+}: around 89% TOC reduction. Continuous H_2O_2 and Fe^{2+}: around 89% TOC reduction. Conclusion: Except for 'Continuous H_2O_2' addition, when compared with single addition, fractional addition methods obtained higher organics degradation. 'Continuous Fe^{2+}'showed the highest TOC and TN reduction.	

2.1.3 Ultraviolet irradiation

It is well known that irradiation spectrum and intensity are key factors for photolytic degradation of toxic pollutants (Cruz González et al., 2018). The irradiation holds two roles: in some cases, direct photolysis of pollutants and improve the yield of oxidizing radicals. The light sensitive nature of various compounds may affect the procedure of photolysis, using different range of radiation wavelength can produce different mechanism.

Photo-Fenton process is dependent on different wavelengths of irradiation have been reported. A number of papers have studied the decontamination of water using monochromatic radiation at 254nm (Asaithambi et al., 2017; Cruz González et al., 2018; Velo-Gala et al., 2017) by low-pressure mercury vapor lamps. This kind of photo-Fenton process involves UVC and hydrogen peroxide (UVC/H_2O_2) process. During the UVC/H_2O_2 process, $HO^{\bullet}$ generated when H_2O_2 is photodecomposed by UVC irradiation. It means that three simultaneous reactions exist in this process:

- Direct photolysis
- Hydrogen peroxide photolysis

$$H_2O_2 + hv \rightarrow 2HO^{\cdot} \qquad \textit{Eq. 2.6}$$

- Fenton reaction

Most of the previous researches on investigating the treatment effect in UV-irradiation process. Polychromatic and monochromatic (UVA, UVB and UVC) radiation for treating detected contaminate show diverse behavior. UVC light had been proved as the most effective on degrading methylene blue (MB) (Joseph et al., 2016). The UVC light had the ability to direct photodecomposition of MB, in the present of TiO_2, the short wavelength of UVC greatly impede the electron-hole combination of photocatalyst to induce the higher photolysis. The degradation rate constant of MB increased associated with decreasing wavelength. In comparison of UVA, UVB and UVC radiation for changing cytotoxicity effect of photoproducts on Jurkat cells (Mutou et al., 2006), different UV radiated bisphenol A (BPA) and chlorinated BPAs (ClBPAs). UVB and UVC enhanced the cytotoxicities of BPA and ClBPAs at 100 J/m^2, but UVA had a negligible effect on their toxicities.

In a study by Romero et al. (2016b), the removal of Metoprolol (MET) at lab-scale experiment was investigated by Photo-Fenton in different photoreactors. Different radiation sources come from: black blue lamps (BCB) (the lamps emit radiation between 350 and 400 nm), compound parabolic collectors (CPC) (using solar irradiation), solarbox (SB) (Xenon lamp emit radiation very close to the solar irradiation) and UVC reactor (the lamps emit 254 nm radiation). Although the UVC is much absorbed by MET, and UVC covers the range of spectrums where Fe(III) complex absorbs (Herney-Ramirez et al., 2010), BCB and UVC reactors presented not significant differences on degradation of MET, and it means that both reactors showed close results on final efficiency. Regarding to the capital cost issue, SB at a much higher price than others. For the contrast on toxicity removal, the four photoreactors promoted toxicity reduction to nontoxic final treating fluid with similar efficacy.

It is generally accepted that with higher UV power, photodegradation increases accordingly (Muthukumari et al., 2009). A linear relationship between UV power and process efficiency.

Under the consideration of environmental issues, mercury-free lamps as the alternative irradiation source have been widely utilized in the field of water treatment. The viable options are pulsed UV lamps, excimer UV lamps(Murcia et al., 2020), microwave electrodeless discharge lamps and ultraviolet light emitting diodes (Vilhunen and Sillanpää, 2010). However, the commercialization of the novel light source still exist some obstacles, the high prices and inefficient radiance limit the new UV lamps competitive with typical UV sources, in light of this, the demand of environmental protection drive a search for improvements.

2.1.4 Temperature

Ambient temperature can be effectively applied in photo-Fenton process. Dependence of Arrhenius theory, linking the relationship of rate constants and temperature, higher temperature is expected to higher generation rate of $HO^{\bullet}$. However, when operational temperature higher than 50°C, thermal decomposition of H_2O_2 to oxygen and water leads to the reduction of removal rate. Naseem et al. (2019) researched the temperature effects on the decolorization efficiency of Acid Orange 3, used a range from 30°C to 70°C.

The percentage dye removal increased when the temperature increased form 30°C to 50°C. The removal efficiency decreased when the temperature continuously increased up to 70°C.

2.1.5 Water matrix and salinity of substrate

Photo-Fenton process has been addressed in different types of water matrix.

The most important different characteristics of those water are their content, traces of pesticides, and inert ingredients that comprise commercial products and their by-products.

The constituent of the treated water is greatly affect the oxidation performance of photo-Fenton process, including the existence of microorganism and the type of water (Rahim Pouran et al., 2015). The presence of inorganic ions such as carbonate (CO_3^{2-}), bicarbonate (HCO_3^-), fluoride (F^-), chloride (Cl^-), bromide (Br^-), sulfate (SO_4^{2-}) and phosphate (PO_4^{3-}), are the influence factors:

Reacting with H_2O_2 lead (Rahim Pouran et al., 2015) to higher H_2O_2 utilization ($Cl^-, Cl^{\cdot}, Cl_2^{\cdot-}$)
Scavenging $HO^{\bullet}$ and generating less reactive radicals
Generation of $Fe(III)$ compounds and suppression of the activity of iron species.

Maclel et al. (2004) carried out photo-Fenton treatment in moderately saline wastewater, the removal of phenol and total organic carbon (TOC) was improved, however, moderate TOC removal was attained in the highest NaCl concentration. Bacardit et al. (2007) explored the effect of salinity on the global TOC abatement by photo-Fenton process. The chloride did not influence the overall TOC removal, but reduced the rate of photo-Fenton process. The formation of photoactive iron-chloride complexes participated in the process under irradiation with a slower rate. In this literature, the investigators also reported that phosphate inhibited TOC removal severely in Fenton process. This is due to the fact that the addition of iron was precipitated with the generation of iron-phosphate complexes.

However, pH predominate the inhibitory effect of chloride ion in photo-Process. Chlorine radical anions ($Cl_2^{\cdot-}$) were produced by the photolysis of

Fe^{3+} complexes $(Fe(Cl)^{2+})$ when the pH is adjust equal to value 2 and below, competed with $HO^{\bullet}$ in degradation process in the presence of target contaminant. At the initial pH appropriate at 3, the inhibitory effect of chloride ion could be lightly moderate (Machulek et al., 2007).

The presence of dissolved organic matter (DOM) also affect mineralization efficacy. The concentration of DOM higher than contaminant causes decrement in degradation performance:

DOM reacts with $HO^{\bullet}$ and competes with micropollutants.
DOM prohibits light penetration during irradiation absorption period in the photo-Fenton process.

2.1.6 Dissolved oxygen

The extent of organic contaminant oxidation strongly depends on dissolved oxygen (DO), one thing needs to be noted that the effects of DO presence in the Fenton system rely on the characteristics of the various organic radicals. The role of DO plays in oxidation process during Fenton process is a controversial question reserves deeper investigation.

2.1.6.1 Dissolved oxygen favour oxidation process

DO usually promote the rate of mineralization in photo-Fenton process (Du et al., 2007; Kim and Vogelpohl, 1998; Utset et al., 2000). DO improvements in the following mechanisms:

Photo-labile Fe(III)-complexes are formed by the reaction of DO with intermediate organ radical, increased photo mineralization promotes total mineralization accordingly (Sun and Plgnatello, 1993).
According to Dorfman mechanism (Dorfman et al., 1962), DO is involved in the reaction with organic radicals to regenerate H_2O_2.

$$R^{\cdot} + O_2 \rightarrow RO_2^{\cdot} \xrightarrow{H_2O} ROH + HO_2^{\cdot} \qquad \textit{Eq. 2.7}$$

$$HO_2^{\cdot}+HO_2^{\cdot} \rightarrow H_2O_2 + O_2 \qquad \textit{Eq. 2.8}$$

Partially DO replace H_2O_2 as oxidant, replacement of H_2O_2 by O_2 in Fenton and photo-Fenton process extend the existence capability of H_2O_2.
DO could serve as $HO^{\bullet}$ to react with radical, so less consumption of $HO^{\bullet}$ in oxygenated system. Therefore, DO could enhance the degradation rate (Du et al., 2007). In addition, intermediates were produced in the absence of oxygen could promote the reduction process of Fe^{3+} to Fe^{2+}, the higher concentration of Fe^{2+} caused quicker consumption of H_2O_2.

2.1.6.2 Dissolved oxygen hamper oxidation process

Walling (Cheves Walling, 1975) reported that organic radicals influence the performance of Fenton process mainly through effect on iron redox cycle. In the presence of oxygen, some types of organic radicals are converted into oxidant species that effect on the chain cycle of the Fenton process. Under anoxic condition, only reducing agents are available to favour propagate Fenton process via reduction of Fe(III).

In contrast to most reported results, Duesterberg et al. (2005) proposed a reaction mechanism by investigating the degradation performance of formic acid (HCOOH) in the presence and absence of oxygen condition during Fenton process. The decomposition rate of HCOOH show more rapid in argon-saturated than in air-saturated conditions. $HO^{\bullet}$ attacks HCOOH to produce carboxyl radicals ($HCOO^{\bullet}$) which are the strong reducing species (**Eq. 2.9**). $HCOO^{\bullet}$ regenerate Fe(II) and prolong chain cycle. Oxygen act as scavenger to capture $HCOO^{\bullet}$ and yield superoxide radical ($HO_2^{\bullet}/O_2^{\bullet-}$)**.** Partly superoxide radical oxide Fe(II) to Fe(III) cause termination of Fenton chain cycle (**Eq. 2.9-2.13**), also superoxide radical react with $HO^{\bullet}$ pose competition with HCOOH (**Eq. 2.13**).

$$HO^{\cdot} + HCOOH \rightarrow HCOO^{\cdot} + H_2O \qquad \textit{Eq. 2.9}$$

$$HO^{\cdot} + HCOOH \rightarrow CO_2 + HO_2^{\cdot}/O_2^{\cdot-} \qquad \textit{Eq. 2.10}$$

$$HCOO^{\cdot} + O_2 \rightarrow CO_2 + HO_2^{\cdot}/O_2^{\cdot -} \qquad \textit{Eq. 2.11}$$

$$Fe(II) + HO_2^{\cdot}/O_2^{\cdot -} \rightarrow Fe(III) + H_2O_2 \qquad \textit{Eq. 2.12}$$

$$HO^{\cdot} + HO_2^{\cdot}/O_2^{\cdot -} \rightarrow H_2O + O_2 \qquad \textit{Eq. 2.13}$$

2.2 Process modelling and optimization

A mathematical process model is an abstract model that uses mathematical language to explain and predict the behavior of a system process. Process models are popular for describing system dynamics in many industries and apply to various environment. Additionally, the procedures of modeling and optimization are extremely important for the growth efficiency with minimizing costs in pollutants purification processes.

2.2.1 Kinetic and Process modeling

There are many different reasons to create the process models, reasons include:

- Express and increase scientific understanding of a system process
- Design and optimization of experimental plans
- Transfer knowledge generated from laboratory-sized experiments to a commercial scale operation
- Help to explain and evaluate obtained results from experiments
- Using a model can indicate the property measurement
- Control and optimize a process
- Models can be treated as a method of technology transfer and help the engineer to make good decision

There is a large component integrated into mathematical process modeling. Although mathematical models have the potential to model the majority of simple systems, the real world is too complicated to model because of the

messy interacting systems. Considering the specific reason and clear objectives before embarking on new model development. A multitude of decisions should be determined by much deliberation of the purpose when developing a model.

2.2.1.1 Mechanistic Kinetic Modelling

Kinetic modelling is considered as a useful approach, which gives ample information on mechanisms. Models are developed based on rigorous reactions scheme. There are more attempts on proposing kinetic models to assess the degradation performance of hazardous organic matters and optimal experimental operation condition (Saltmiras and Lemley, 2001). For the photo-Fenton, the system behavior depends largely on lamp type and geometry of the reactor. The influence of irradiation and photon absorbance on process efficiency in the reactor was also considered. Rossetti et al. (2004) developed a reactor model using mathematical expression to describe the evolution of formic acid in the Fenton and Photo-Fenton oxidation process. A reported mechanism scheme of formic acid was used to propose a kinetic model. The complete mass balance equations allowed for the irradiated and nonirradiated liquid volume. The local volumetric rate of photon absorption (VRPA) could be predicted, also the decay behavior of formic acid and H_2O_2, following a radiation field model. Based on this research, exception of VRPA, Cabrera-Reina et al. (2015) improved the dynamic modeling comprised the effect of irradiated volume to total volume ratio and liquid depth. The kinetic model proposed according to rigorous photo-Fenton reaction mechanism. Since the reaction mechanism took account into each principal components in the system, including Fe(II), Fe(III), H_2O_2, R, hydroxyl radical, dissolved oxygen (O_2) and three different types of organic matters. The model could give a well prediction of the evolution of dissolved oxygen, H_2O_2 and TOC.

Beyond that, temperature, pH value and iron type also the influencing factors for photo-Fenton. Farias considered the effects of temperature on changing kinetic parameters through adopting the Arrhenius equation. The Arrhenius equation, and the local volumetric rate of photon absorption as well, were accounted into the reaction rate expressions, the approach in favour of calculating all the parameters simultaneously. De Lima Perini proposed a semi-empirical model to evaluate the degradation performance of ciprofloxacin (CIP) at different iron catalyst type and pH value by Photo-Fenton process. Experimental data were used to fit the model obeyed least

squares criterion, the rate constant of mineralization and maximum TOC removal were obtained as the indicators to assess the process efficiency. PH became a leading factor when the production of organic ligands (the complexes of organic compound with citrate, oxalate and nitrate) existed in the system. The best CIP conversion presented with the experimental condition: H_2O_2/CIP ratio between 50 and 123, pH 4.5 and the iron citrate as the catalyst.

— Experimental design (ED) and response surface methodologies (RSM)

Experimental design as a powerful optimization tool can be applied to the system that comprise lumped cross-effects factors. Various types of experimental design (such as central composite design, factorial experimental design, D-optimality, Box–Behnken experimental design and Box–Hunter spherical experimental design) adapt to a wide range of problems. Photo-assisted Fenton process is an extremely complex reaction, the complexity of influenced factors involving effective and economic Fenton reagent dosage, photon absorbance efficiency, dissolved organic matters in water matrix and unknown detailed mechanism of degradation performance.

Experimental design methodology has been shown as an effective approach in the treatment of highly degradation-resistant wastewaters. Dopar et al. (2011) reported the application of Photo-Fenton for treating simulated industrial wastewater by using Box-Behnken experimental design (BBD). Thirteen experiments with three independent variables for determining optimal initial pH, iron catalyst and H_2O_2 concentration, were developed according to BBD, the experiments also set for comparing the influences on mineralization rate constant with different UV radiation. RSM was applied to estimate the interaction between the independent variables and process response by means of empirical techniques. The predicted mineralization rate constants were obtained following a quadratic model, compared with the results of fitting the “pseudo”-second order kinetics that take advantages of experimental data, highly significant was presented depend on the calculation results of analysis of variance (ANOVA). The study suggested an optimal UV-A/Fe/H_2O_2 process for the wastewater remediation.

2.2.1.2 Artificial neural network (ANN)

Since the system of Fenton treatment for wastewater is quite complex, modeling and simulation of multivariate systems are hindered due to such complexity. The application of ANN is commonly reported in wastewater remediation areas. The advantages of ANN models are describing the multifarious and interlaced relationship without requiring well understand the mechanisms.

ANN combine with experimental design can evaluate the optimum variables and optimize process operational, accordingly improve system efficiency. Durán et al. (2006) investigated the simulation of the degradation mechanism of reactive blue 4 by photo-Fenton with a combination approach of multivariate experimental design and ANNs. The factorial experimental design was applied to evaluate the influenced parameters. PH effect was predominant for RB4 degradation performance. ANNs were used to fit obtained data and the reproduced experimental data presented well confidence. The values of decoloration constant and mineralization constant were obtained based on ANNs fittings and degradation reaction of RB4. The combination approach has been applied to Sono-Photo-Fenton process by Expósito et al. (2017). The study adopted four-factor Central-Composite Experimental Design (CCD) Matrix to municipal wastewater degradation experiments. The mineralization constant value (k_{TOC}) was calculated from TOC result. ANN was used to predict mineralization constant by integrating pseudo-first-order kinetic and estimate the optimal experimental condition.

Kasiri et al. (2008) employed ANN and RSM to heterogeneous Photo-Fenton process for degradation of C.I. Acid Red 14 azo dye. ANN and RSM models extracted important information based on experimental data. The central composite design was adopted as the major tool for RSM in the experimental design part, the experimental data following a response surface regression procedure to estimate mainly influential variables (including the concentration of the catalyst, molar ratio of H_2O_2/dye, the initial concentration of dye and pH). These variables as the input parameters to feed ANN and the output variable was the degradation efficiency. Compared with the results obtained by RSM, the concentration of dye and initial pH as the more overwhelming parameters, the importance of both parameters on the experimental response show the good agreement with RSM. The ANN and RSM models are equally precision.

Artificial neural networks have been greatly implemented as predictive models in pollutant degradation process. Elmolla et al. (2010) applied ANN modeling to Fenton process to predict COD removal from mixture solution of antibiotic. For employing ANN models, a series of input and output variables were obtained from experimental performance. The principal component analysis (PCA) was employed for determining the critical input variables. The H_2O_2/Fe^{2+} molar ratio showed the strongest effect on COD removal among other variables (e.g., pH and H_2O_2/COD molar ratio). The predicted results generated by the optimized ANN model were consistent with experimental data (R^2 = 0.997).

2.2.2 Computational aid on automatic dosage of H_2O_2

To systematically and efficiently operate the dosage of H_2O_2, some researches concentrate on the development of systematic procedures and optimization of dosage strategies to deal with such problem.

— Model-based approach

Model-based approach is a kind of mathematical optimization. To apply the ideas from mathematical optimization is using the formulations to describe the problems. And then, using the algorithms to solve the problem.

To solve H_2O_2 dosage problems in photo-Fenton system, from the publish literatures, the first issue is developing a mathematical model to describe the degradation system. D. Sannino et al. (2013) used LaFeO3 heterogeneous structured catalyst supported on a monolithic structure in UV-C photo-Fenton process. A mathematical model was proposed based on acetic acid oxidation (using Eley-Rideal-type kinetics) and the photolysis of H_2O_2 (using the first order kinetics). Different H_2O_2 dosage strategies were used to validate the model, step dosage with 0.035 mol/L each hour and continuous dosage at a constant flow rate 0.038 mol/h. The model calculated data show the good agreement with experimental data, the results showed the continuous dosage presented the better results in minimizing the oxidant consumption and maximizing TOC removal with less irradiation time.

Audino et al. (2019) proposed a model that combined kinetic model and reactor model to consider the H_2O_2 dosage problem. This model showed the

available for solving multi-objective dynamic optimization problem. The optimal H_2O_2 could be determined under different operational, cost and environmental constraints.

The application of model-based approach allows to reduce the experimental work, however, the complicated system consists of enormous components and it hard to be represented accurately by a mathematical model. To address the problem of H_2O_2 dosage, the model is proposed by describing a degradation system in a certain reactor under a certain type of process, in other words, the model lack of generalization. For example, to apply a proposed model to a different reactor, preliminary work need to be done to validate some variables that allow the model can be used in a different type or different scale reactor.

— Optimal recipe design

In the study researched by Yamal-Turbay et al. (2012), a pre-established dosage protocol was proposed. This protocol is characterized by the fixed total amount of H_2O_2, the initial load fraction, the starting time of the dosage, and the continuous dosage duration. An improved model-based recipe was developed by M. Moreno-Benito, et al. (2013). A kinetic model was adapted to model the kinetic behavior of lumped variables, so the performance criterion subject to process model and defined constraints. Based on the dosage protocol from Yamal-Turbay et al. (2012), a piecewise constant profile was used to consider more dosage intervals. The cost had been reduced 5.1% compared with no dosage.

— On-line measurement control-dissolved oxygen concentration

Considering control H_2O_2 concentration depends on monitoring dissolved oxygen (DO) variation, Ortega-Gómez et al. (2012) proposed a process model that can be applied to designing automatic controllers. It was used for correcting H_2O_2 concentration throughout the process to keep optimized concentration, and automatically dosing H_2O_2. For this purpose, a linear dynamic model was experimentally obtained to relate the DO concentration and H_2O_2 consumption. Based on this model, a control system, a proportional and integral controller with anti-windup mechanism, was developed. Compared with non-assisted addition methods, an economic saving lead to 50% decrease in H_2O_2 consumption, and obtained higher process efficiency.

In view of the objective of optimizing H_2O_2 dosage, this concept can be used to reduce process costs in the degradation system. Carra et al. (2013) also exploit the controller to control H_2O_2 addition in solar photo-Fenton process. An on/off model using a given DO value as a set point. A dose of H_2O_2 pulsing added at the beginning. After that, the pump dosed varying amounts of H_2O_2 at different times, depends on the DO concentration and H_2O_2 concentration was corrected by Proportional Integral system controller. Controller dosage would be a better choice for higher mineralization requirements.

2.3 References

Alalm, M.G., Tawfik, A., Ookawara, S., 2015. Degradation of four pharmaceuticals by solar photo-Fenton process: Kinetics and costs estimation. Journal of Environmental Chemical Engineering 3, 46–51. https://doi.org/10.1016/j.jece.2014.12.009

Almeida, C.V.D.S., Macedo, M.S., Eguiluz, K.I.B., Salazar-Banda, G.R., Queissada, D.D., 2015. Indanthrene blue dye degradation by UV/H2O2 process: H2O2 as a single or fractioned aliquot? Environmental Engineering Science 32, 930–937. https://doi.org/10.1089/ees.2015.0171

Asaithambi, P., Alemayehu, E., Sajjadi, B., Aziz, A.R.A., 2017. Electrical energy per order determination for the removal pollutant from industrial wastewater using UV/Fe2+/H2O2 process: Optimization by response surface methodology. Water Resources and Industry 18, 17–32. https://doi.org/10.1016/j.wri.2017.06.002

Audino, F., Campanyà, G., Pérez-Moya, M., Espuña, A., Graells, M., 2019. Systematic optimization approach for the efficient management of the photo-Fenton treatment process. Science of the Total Environment 646, 902–913. https://doi.org/10.1016/j.scitotenv.2018.07.057

Babuponnusami, A., Muthukumar, K., 2014. A review on Fenton and improvements to the Fenton process for wastewater treatment. Journal of Environmental Chemical Engineering 2, 557–572. https://doi.org/10.1016/j.jece.2013.10.011

Bacardit, J., Stötzner, J., Chamarro, E., Esplugas, S., 2007. Effect of salinity on the photo-fenton process. Industrial and Engineering Chemistry Research 46, 7615–7619. https://doi.org/10.1021/ie070154o

Badawy, M.I., Ghaly, M.Y., Gad-Allah, T.A., 2006. Advanced oxidation processes for the removal of organophosphorus pesticides from wastewater. Desalination 194, 166–175. https://doi.org/10.1016/j.desal.2005.09.027

Cabrera Reina, A., Santos-Juanes, L., García Sánchez, J.L., Casas López, J.L., Maldonado Rubio, M.I., Li Puma, G., Sánchez Pérez, J.A., 2015. Modelling the photo-Fenton oxidation of the pharmaceutical paracetamol in water including the effect of photon absorption (VRPA). Applied Catalysis B: Environmental 166–167, 295–301. https://doi.org/10.1016/j.apcatb.2014.11.023

Caram, B., García-Ballesteros, S., Santos-Juanes, L., Arques, A., García-Einschlag, F.S., 2018. Humic like substances for the treatment of scarcely soluble pollutants by mild photo-Fenton process. Chemosphere 198, 139–146. https://doi.org/10.1016/j.chemosphere.2018.01.074

Carra, I., Casas López, J.L., Santos-Juanes, L., Malato, S., Sánchez Pérez, J.A., 2013. Iron dosage as a strategy to operate the photo-Fenton process at initial neutral pH. Chemical Engineering Journal 224, 67–74. https://doi.org/10.1016/j.cej.2012.09.065

Carra, Irene, Ortega-Gómez, E., Santos-Juanes, L., Casas López, J.L., Sánchez Pérez, J.A., 2013. Cost analysis of different hydrogen peroxide supply strategies in the solar: Photo-Fenton process. Chemical Engineering Journal 224, 75–81. https://doi.org/10.1016/j.cej.2012.09.067

Cheves Walling, 1975. Fenton's reagent revisited. Accounts of chemical research 8, 125–131.

Chu, W., Chan, K.H., Kwan, C.Y., Choi, K.Y., 2007. Degradation of atrazine by modified stepwise-Fenton's processes. Chemosphere 67, 755–761. https://doi.org/10.1016/j.chemosphere.2006.10.039

Cruz González, G., Julcour, C., Chaumat, H., Jáuregui-Haza, U., Delmas, H., 2018. Degradation of 2,4-dichlorophenoxyacetic acid by photolysis and photo-Fenton oxidation. Journal of Environmental Chemical Engineering 6, 874–882. https://doi.org/10.1016/j.jece.2017.12.049

de Lima Perini, J.A., Perez-Moya, M., Nogueira, R.F.P., 2013. Photo-Fenton degradation kinetics of low ciprofloxacin concentration using different iron sources and pH. Journal of Photochemistry and Photobiology A: Chemistry 259, 53–58. https://doi.org/10.1016/j.jphotochem.2013.03.002

Dopar, M., Kusic, H., Koprivanac, N., 2011. Treatment of simulated industrial wastewater by photo-Fenton process. Part I: The optimization of process parameters using design of experiments (DOE). Chemical Engineering Journal 173, 267–279. https://doi.org/10.1016/j.cej.2010.09.070

Dorfman, L.M., Taub, I.A., Bühler, R.E., 1962. Pulse radiolysis studies. I. Transient spectra and reaction-rate constants in irradiated aqueous solutions of benzene. The Journal of Chemical Physics 36, 3051–3061. https://doi.org/10.1063/1.1732425

Duan, F., Yang, Y., Li, Y., Cao, H., Wang, Y., Zhang, Y., 2014. Heterogeneous Fenton-like degradation of 4-chlorophenol using iron/ordered mesoporous carbon catalyst. Journal of Environmental Sciences (China) 26, 1171–1179. https://doi.org/10.1016/S1001-0742(13)60532-X

Duesterberg, C.K., Cooper, W.J., Waite, T.D., 2005. Fenton-mediated oxidation in the presence and absence of oxygen. Environmental Science and Technology 39, 5052–5058. https://doi.org/10.1021/es048378a

Durán, A., Monteagudo, J.M., Mohedano, M., 2006. Neural networks simulation of photo-Fenton degradation of Reactive Blue 4. Applied Catalysis B: Environmental 65, 127–134. https://doi.org/10.1016/j.apcatb.2006.01.004

Du, Y., Zhou, M., Lei, L., 2007. The role of oxygen in the degradation of p-chlorophenol by Fenton system. Journal of Hazardous Materials 139, 108–115. https://doi.org/10.1016/j.jhazmat.2006.06.002

Elmolla, E.S., Chaudhuri, M., Eltoukhy, M.M., 2010. The use of artificial neural network (ANN) for modeling of COD removal from antibiotic aqueous solution by the Fenton process. Journal of Hazardous Materials 179, 127–134. https://doi.org/10.1016/j.jhazmat.2010.02.068

Expósito, A.J., Monteagudo, J.M., Durán, A., Fernández, A., 2017. Dynamic behavior of hydroxyl radical in sono-photo-Fenton mineralization of synthetic municipal wastewater effluent containing antipyrine. Ultrasonics Sonochemistry 35, 185–195. https://doi.org/10.1016/j.ultsonch.2016.09.017

Gamaralalage, D., Sawai, O., Nunoura, T., 2020. Effect of reagents addition method in Fenton oxidation on the destruction of organics in palm oil mill effluent. Journal of Environmental Chemical Engineering 8. https://doi.org/10.1016/j.jece.2020.103974

Ganiyu, S.O., Zhou, M., Martínez-Huitle, C.A., 2018. Heterogeneous electro-Fenton and photoelectro-Fenton processes: A critical review of fundamental principles and application for water/wastewater treatment. Applied Catalysis B: Environmental 235, 103–129. https://doi.org/10.1016/j.apcatb.2018.04.044

Gulkaya, I., Surucu, G.A., Dilek, F.B., 2006. Importance of H2O2/Fe2+ ratio in Fenton's treatment of a carpet dyeing wastewater. Journal of Hazardous Materials 136, 763–769. https://doi.org/10.1016/j.jhazmat.2006.01.006

Herney-Ramirez, J., Vicente, M.A., Madeira, L.M., 2010. Heterogeneous photo-Fenton oxidation with pillared clay-based catalysts for wastewater treatment: A review. Applied Catalysis B: Environmental 98, 10–26. https://doi.org/10.1016/j.apcatb.2010.05.004

Inchaurrondo, N., Cechini, J., Font, J., Haure, P., 2012. Strategies for enhanced CWPO of phenol solutions. Applied Catalysis B: Environmental 111–112, 641–648. https://doi.org/10.1016/j.apcatb.2011.11.019

Jiang, C., Pang, S., Ouyang, F., Ma, J., Jiang, J., 2010. A new insight into Fenton and Fenton-like processes for water treatment. Journal of Hazardous Materials 174, 813–817. https://doi.org/10.1016/j.jhazmat.2009.09.125

Joseph, C.G., Taufiq-Yap, Y.H., Li Puma, G., Sanmugam, K., Quek, K.S., 2016. Photocatalytic degradation of cationic dye simulated wastewater using four radiation sources, UVA, UVB, UVC and solar lamp of identical power output. Desalination and Water Treatment 57, 7976–7987. https://doi.org/10.1080/19443994.2015.1063463

Karci, A., Arslan-Alaton, I., Olmez-Hanci, T., Bekbölet, M., 2012. Transformation of 2,4-dichlorophenol by H 2O 2/UV-C, Fenton and photo-Fenton processes: Oxidation products and toxicity evolution. Journal of Photochemistry and Photobiology A: Chemistry 230, 65–73. https://doi.org/10.1016/j.jphotochem.2012.01.003

Kasiri, M.B., Aleboyeh, H., Aleboyeh, A., 2008. Modeling and optimization of heterogeneous photo-fenton process with response surface methodology and artificial neural networks. Environmental Science and Technology 42, 7970–7975. https://doi.org/10.1021/es801372q

Kavitha, V., Palanivelu, K., 2004. The role of ferrous ion in Fenton and photo-Fenton processes for the degradation of phenol. Chemosphere 55, 1235–1243. https://doi.org/10.1016/j.chemosphere.2003.12.022

Kim, S.-M., Vogelpohl, A., 1998. Degradation of Organic Pollutants by the Photo-Fenton-Process. Chemical Engineering & Technology 21, 187–191.

Machulek, A., Moraes, J.E.F., Vautier-Giongo, C., Silverio, C.A., Friedrich, L.C., Nascimento, C.A.O., Gonzalez, M.C., Quina, F.H., 2007. Abatement of the inhibitory effect of chloride anions on the photo-fenton process. Environmental Science and Technology 41, 8459–8463. https://doi.org/10.1021/es071884q

Martins, R.C., Rossi, A.F., Quinta-Ferreira, R.M., 2010. Fenton's oxidation process for phenolic wastewater remediation and biodegradability enhancement. Journal of Hazardous Materials 180, 716–721. https://doi.org/10.1016/j.jhazmat.2010.04.098

Módenes, A.N., Espinoza-Quiñones, F.R., Manenti, D.R., Borba, F.H., Palácio, S.M., Colombo, A., 2012. Performance evaluation of a photo-Fenton process applied to pollutant removal from textile effluents in a batch system. Journal of Environmental Management 104, 1–8. https://doi.org/10.1016/j.jenvman.2012.03.032

Monteagudo, J.M., Durán, A., Aguirre, M., Martín, I.S., 2010. Photodegradation of Reactive Blue 4 solutions under ferrioxalate-assisted UV/solar photo-Fenton system with continuous addition of H2O2 and air injection. Chemical Engineering Journal 162, 702–709. https://doi.org/10.1016/j.cej.2010.06.029

Monteagudo, J.M., Durán, A., San Martín, I., Aguirre, M., 2009. Effect of continuous addition of H2O2 and air injection on ferrioxalate-assisted solar photo-Fenton degradation of Orange II. Applied Catalysis B: Environmental 89, 510–518. https://doi.org/10.1016/j.apcatb.2009.01.008

Moreno-Benito, M., Yamal-Turbay, E., Espuña, A., Pérez-Moya, M., Graells, M., 2013. Optimal recipe design for Paracetamol degradation by advanced oxidation processes (AOPs) in a pilot plant. Computer Aided Chemical Engineering 32, 943–948. https://doi.org/10.1016/B978-0-444-63234-0.50158-5

Munoz, M., Pliego, G., de Pedro, Z.M., Casas, J.A., Rodriguez, J.J., 2014. Application of intensified Fenton oxidation to the treatment of sawmill wastewater. Chemosphere 109, 34–41. https://doi.org/10.1016/j.chemosphere.2014.02.062

Murcia, M.D., Gómez, M., Gómez, E., Gomez, J.L., Hidalgo, A.M., Murcia, S., Campos, D., 2020. Comparison of two excilamps and two reactor configurations in

the UV-H2O2 removal process of amaranth. Journal of Water Process Engineering 33. https://doi.org/10.1016/j.jwpe.2019.101051

Muthukumari, B., Selvam, K., Muthuvel, I., Swaminathan, M., 2009. Photoassisted hetero-Fenton mineralisation of azo dyes by Fe(II)-Al2O3 catalyst. Chemical Engineering Journal 153, 9–15. https://doi.org/10.1016/j.cej.2009.05.030

Mutou, Y., Ibuki, Y., Terao, Y., Kojima, S., Goto, R., 2006. Chemical change of chlorinated bisphenol A by ultraviolet irradiation and cytotoxicity of their products on Jurkat cells. Environmental Toxicology and Pharmacology 21, 283–289. https://doi.org/10.1016/j.etap.2005.09.005

Naseem, Z., Bhatti, H.N., Iqbal, M., Noreen, S., Zahid, M., 2019. Fenton and photo-fenton oxidation for the remediation of textile effluents: An experimental study, in: Textiles and Clothing: Environmental Concerns and Solutions. pp. 235–251. https://doi.org/10.1002/9781119526599.ch9

Navalon, S., Alvaro, M., Garcia, H., 2010. Heterogeneous Fenton catalysts based on clays, silicas and zeolites. Applied Catalysis B: Environmental 99, 1–26. https://doi.org/10.1016/j.apcatb.2010.07.006

Ortega-G Omez, E., García, B.E., Ballesteros Martín, M.M., Ferná Ndez Ibá ~ Nez, P., Sá Nchez P Erez, J.A., 2014. Inactivation of natural enteric bacteria in real municipal wastewater by solar photo-Fenton at neutral pH. Water Research 63, 316–324. https://doi.org/10.1016/j.watres.2014.05.034

Ortega-Gómez, E., Moreno úbeda, J.C., Álvarez Hervás, J.D., Casas López, J.L., Santos-Juanes Jordá, L., Sánchez Pérez, J.A., 2012. Automatic dosage of hydrogen peroxide in solar photo-Fenton plants: Development of a control strategy for efficiency enhancement. Journal of Hazardous Materials 237–238, 223–230. https://doi.org/10.1016/j.jhazmat.2012.08.031

Pérez-Moya, M., Graells, M., Castells, G., Amigó, J., Ortega, E., Buhigas, G., Pérez, L.M., Mansilla, H.D., 2010. Characterization of the degradation performance of the sulfamethazine antibiotic by photo-Fenton process. Water Research 44, 2533–2540. https://doi.org/10.1016/j.watres.2010.01.032

Pignatello, J.J., Oliveros, E., MacKay, A., 2006. Advanced oxidation processes for organic contaminant destruction based on the fenton reaction and related chemistry. Critical Reviews in Environmental Science and Technology 36, 1–84. https://doi.org/10.1080/10643380500326564

Polo-López, M.I., Castro-Alférez, M., Oller, I., Fernández-Ibáñez, P., 2014. Assessment of solar photo-Fenton, photocatalysis, and H2O2 for removal of

phytopathogen fungi spores in synthetic and real effluents of urban wastewater. Chemical Engineering Journal 257, 122–130. https://doi.org/10.1016/j.cej.2014.07.016

Prato-Garcia, D., Buitrón, G., 2012. Evaluation of three reagent dosing strategies in a photo-Fenton process for the decolorization of azo dye mixtures. Journal of Hazardous Materials 217–218, 293–300. https://doi.org/10.1016/j.jhazmat.2012.03.036

Prieto-Rodríguez, L., Oller, I., Zapata, A., Agüera, A., Malato, S., 2011. Hydrogen peroxide automatic dosing based on dissolved oxygen concentration during solar photo-Fenton. Catalysis Today 161, 247–254. https://doi.org/10.1016/j.cattod.2010.11.017

Rahim Pouran, S., Abdul Aziz, A.R., Wan Daud, W.M.A., 2015. Review on the main advances in photo-Fenton oxidation system for recalcitrant wastewaters. Journal of Industrial and Engineering Chemistry 21, 53–69. https://doi.org/10.1016/j.jiec.2014.05.005

Rivas Ibáñez, G., Bittner, M., Toušová, Z., Campos-Mañas, M.C., Agüera, A., Casas López, J.L., Sánchez Pérez, J.A., Hilscherová, K., 2017. Does micropollutant removal by solar photo-Fenton reduce ecotoxicity in municipal wastewater? A comprehensive study at pilot scale open reactors. Journal of Chemical Technology and Biotechnology 92, 2114–2122. https://doi.org/10.1002/jctb.5212

Romero, V., Acevedo, S., Marco, P., Giménez, J., Esplugas, S., 2016a. Enhancement of Fenton and photo-Fenton processes at initial circumneutral pH for the degradation of the β-blocker metoprolol. Water Research 88, 449–457. https://doi.org/10.1016/j.watres.2015.10.035

Romero, V., González, O., Bayarri, B., Marco, P., Giménez, J., Esplugas, S., 2016b. Degradation of Metoprolol by photo-Fenton: Comparison of different photoreactors performance. Chemical Engineering Journal 283, 639–648. https://doi.org/10.1016/j.cej.2015.07.091

Rossetti, G.H., Albizzati, E.D., Alfano, O.M., 2004. Modeling of a flat-plate solar reactor. Degradation of formic acid by the photo-Fenton reaction. Solar Energy 77, 461–470. https://doi.org/10.1016/j.solener.2004.04.019

Saltmiras, D.A., Lemley, A.T., 2001. Anodic Fenton Treatment of Treflan MTF®. Journal of Environmental Science and Health - Part A Toxic/Hazardous

Substances and Environmental Engineering 36, 261–274. https://doi.org/10.1081/ESE-100102921

Sannino, D., Vaiano, V., Ciambelli, P., Isupova, L.A., 2013. Mathematical modelling of the heterogeneous photo-Fenton oxidation Of acetic acid on structured catalysts. Chemical Engineering Journal 224, 53–58. https://doi.org/10.1016/j.cej.2013.01.078

Santos-Juanes, L., Sánchez, J.L.G., López, J.L.C., Oller, I., Malato, S., Sánchez Pérez, J.A., 2011. Dissolved oxygen concentration: A key parameter in monitoring the photo-Fenton process. Applied Catalysis B: Environmental 104, 316–323. https://doi.org/10.1016/j.apcatb.2011.03.013

Sedlak, D.L., Andren, A.W., 1991. Oxidation of Chiorobenzene with Fenton's Reagent. Environmental Science and Technology 25, 777–782. https://doi.org/10.1021/es00016a024

Soares, P.A., Silva, T.F.C.V., Manenti, D.R., Souza, S.M.A.G.U., Boaventura, R.A.R., Vilar, V.J.P., 2014. Insights into real cotton-textile dyeing wastewater treatment using solar advanced oxidation processes. Environmental Science and Pollution Research 21, 932–945. https://doi.org/10.1007/s11356-013-1934-0

Sun, Y., Plgnatello, J.J., 1993. Photochemical Reactions Involved in the Total Mineralization of 2,4-D by Fe3+/H202/UV. Environ. Sci. Technoi 27, 304–310.

Utset, B., Garcia, J., Casado, J., Domènech, X., Peral, J., 2000. Replacement of H2O2 by O2 in Fenton and photo-Fenton reactions. Chemosphere 41, 1187–1192. https://doi.org/10.1016/S0045-6535(00)00011-4

Velo-Gala, I., Pirán-Montaño, J.A., Rivera-Utrilla, J., Sánchez-Polo, M., Mota, A.J., 2017. Advanced Oxidation Processes based on the use of UVC and simulated solar radiation to remove the antibiotic tinidazole from water. Chemical Engineering Journal 323, 605–617. https://doi.org/10.1016/j.cej.2017.04.102

Vilhunen, S., Sillanpää, M., 2010. Recent developments in photochemical and chemical AOPs in water treatment: A mini-review. Reviews in Environmental Science and Biotechnology 9, 323–330. https://doi.org/10.1007/s11157-010-9216-5

Yamal-Turbay, E., Graells, M., Pérez-Moya, M., 2012. Systematic assessment of the influence of hydrogen peroxide dosage on caffeine degradation by the

photo-Fenton process. Industrial & engineering chemistry research 51, 4770–4778.

Yamal-Turbay, E., Ortega, E., Conte, L.O., Graells, M., Mansilla, H.D., Alfano, O.M., Pérez-Moya, M., 2015. Photonic efficiency of the photodegradation of paracetamol in water by the photo-Fenton process. Environmental Science and Pollution Research 22, 938–945. https://doi.org/10.1007/s11356-014-2990-9

Yip, A.C.K., Lam, F.L.Y., Hu, X., 2005. Chemical-vapor-deposited copper on acid-activated bentonite clay as an applicable heterogeneous catalyst for the photo-fenton-like oxidation of textile organic pollutants. Industrial and Engineering Chemistry Research 44, 7983–7990. https://doi.org/10.1021/ie050647y

Zazo, J.A., Casas, J.A., Mohedano, A.F., Rodriguez, J.J., 2009. Semicontinuous Fenton oxidation of phenol in aqueous solution. A kinetic study. Water Research 43, 4063–4069. https://doi.org/10.1016/j.watres.2009.06.035

Zhang, H., Heung, J.C., Huang, C.P., 2005. Optimization of Fenton process for the treatment of landfill leachate. Journal of Hazardous Materials 125, 166–174. https://doi.org/10.1016/j.jhazmat.2005.05.025

3. Experimental settings and analytical methods

3.1 Pilot plant

The photo-Fenton experiments were performed in a batch-mode pilot plant, **Figure 3.1**, consisting of a 13.5 L glass reservoir tank, a 1.5 L glass tubular photo-reactor. The radiation source is a Philips Actinic BL TL 36 W/10 1SL lamp (UVA-UVB), **Figure 3.2**, the incident photon power, E= 3.36×10^{-4} Einstein min^{-1} (300 and 420 nm) was measured by Yamal-Turbay et al. (2015) through potassium ferrioxalate actinometry method (Murov et al., 1993).

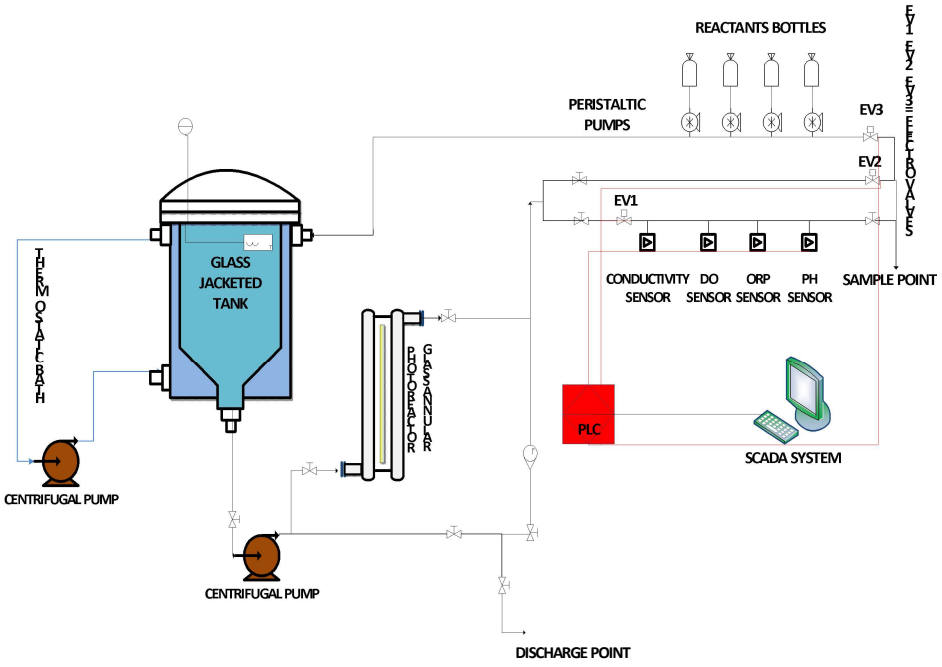

Figure 3.1. Pilot Plant schematic representation

Figure 3.2 is the observed spectrum of the lamp that considers a Pyrex envelope.

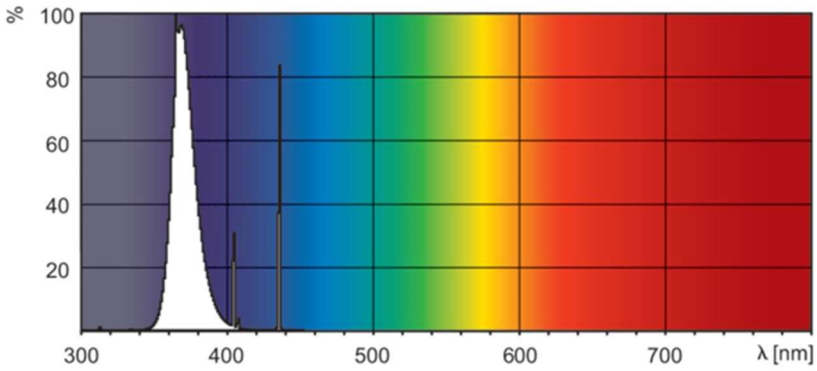

Figure 3.2. Spectrum of a Philips Actinic BL TL-DK 36 W/10 1sl lamp considering a Pyrex envelope.

The recirculation of the working solution depends on a centrifugal pump (Iwaki Magnet Pump, MD-30RZ-220, 1-16HP-220V) and the connecting tubing. On-line measurement sensors are equipped for pH (Hamilton Polilyte HTVP 120), temperature and dissolved oxygen (Hamilton Oxysens). Four peristaltic pumps (Watson Marlow, OEM 313 24V) are controlled by a PLC (Programmable Logic Controller) program (Siemens SIMATIC S7-1200) that manages and allows for collecting data by the plant SCADA (Supervisory Control And Data Acquisition) system (InTouchR® software), the pumps are installed for adding reagents into pilot plant automatically.

Sensors that connect with a PLC-SCADA system favors monitoring influential parameters during the photo-Fenton process, which support making the decision in a closed-loop system.

3.2 Analytical methods

3.2.1 Total organic carbon (TOC)

Total organic carbon is a comprehensive and convenient indicator for evaluating the degree of organic pollution in water, and is also one of the important variables in water monitoring. TOC is the value of the difference between Total carbon (TC) and Total inorganic carbon (TIC).

In this thesis, Total organic carbon concentration was measured by a TOC (TOC-VCSH/CSN Shimadzu; Kyoto, Japan) analyzer. The analysis of a sample is treated with 3M HCl acid to eliminate the existing inorganic carbon.

For TOC measurement, each sample takes 15 min. In order to study the degradation process during the early stage of photo-Fenton treatment, more samples were taken at each 5 min.

3.2.2 H_2O_2 concentration determination

The determination of H_2O_2 concentration constantly during degradation of organic contaminant via photo-Fenton process contributes to evaluating the efficiency of TOC mineralization. Tracking H_2O_2 concentration and cooperates with on-line measurements, especially dissolved oxygen concentration and dissolved oxygen slope value, could keep H_2O_2 concentration in a desired level during the degradation process. The desired level makes higher TOC mineralization with less H_2O_2 addition.

H_2O_2 concentration was determined by using the colorimetric method (Nogueira et al., 2005). In an acidic medium, H_2O_2 reacts with ammonium metavanadate to produce peroxovanadium cation VO_2^{3+} that allows being detected by spectrophotometric technique. The production absorption at 450 nm was detected via a Perkin Elmer Lambda 2 UV / VIS Spectrometer.

$$VO_3^- + 4H^+ + H_2O \rightarrow VO_2^{3+} + 3H_2O \qquad \textit{Eq. 3.1}$$

The H_2O_2 concentration was quantified through a standard calibration curve: 3, 6, 12, 30, 60, 120, 180 mg L^{-1}. The corresponding equation is $[H_2O_2]$ = 117.6*ABSORBANCE – 0.176, R^2= 1.

3.2.3 Model contaminant determination

Model contaminant is detected and quantified by High Performance Liquid Chromatography (HPLC).

In this study, an HPLC Agilent 1200 series with UV-DAD (Agilent Technologies, Santa Clara, CA, USA) is used for the detection measurements. The stationary phase is an Akady 5 µm C-18 150×4.6 mm column.

In order to understand the evolution of model contaminant during the photo-Fenton process, the sampling time was reduced. Based on the principle, the model contaminant is easily decomposed than the intermediates. The samples were kept with methanol to capture $HO^{\bullet}$ to stop the further reaction.

The chromatographic conditions for paracetamol (PCT) are presented in **Table 3.1.**

Table 3.1 chromatographic conditions for paracetamol

Contaminant	**Mobile phase**	**Temperature (℃)**	**Flow rate (mL min^{-1})**	**Λ (nm)**	**Retention time (min)**
PCT	Methanol 25% H_2O 75%	25	0.4	243	9.0

3.3 References

Murov, S.L., Carmichael, I., Hug, G.L., 1993. Handbook of photochemistry. CRC Press.

Nogueira, R.F.P., Oliveira, M.C., Paterlini, W.C., 2005. Simple and fast spectrophotometric determination of H2O 2 in photo-Fenton reactions using metavanadate. Talanta 66, 86–91. https://doi.org/10.1016/j.talanta.2004.10.001

Yamal-Turbay, E., Ortega, E., Conte, L.O., Graells, M., Mansilla, H.D., Alfano, O.M., Pérez-Moya, M., 2015. Photonic efficiency of the photodegradation of paracetamol in water by the photo-Fenton process. Environmental Science and Pollution Research 22, 938–945. https://doi.org/10.1007/s11356-014-2990-9

4. An experimental approach to the optimization of the dosage of hydrogen peroxide for Fenton and photo-Fenton processes

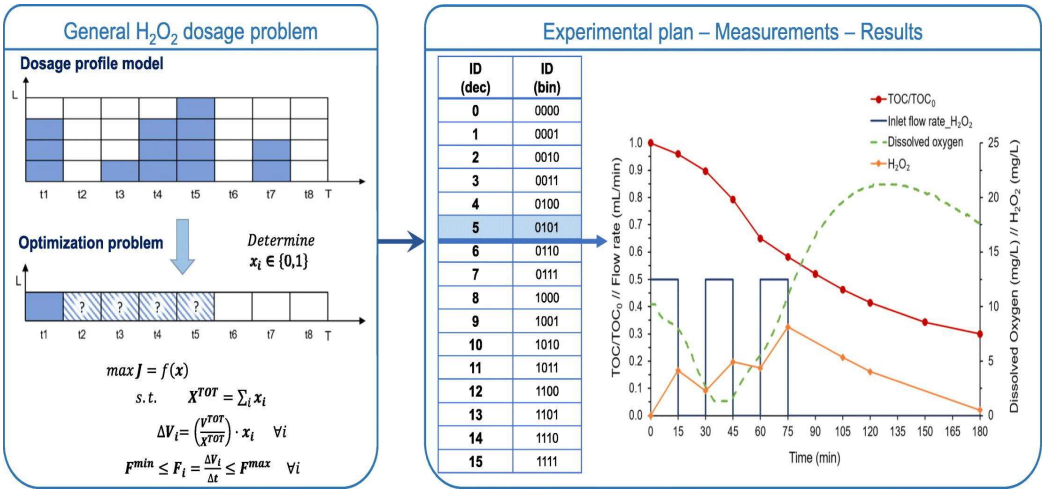

ID (dec)	ID (bin)
0	0000
1	0001
2	0010
3	0011
4	0100
5	0101
6	0110
7	0111
8	1000
9	1001
10	1010
11	1011
12	1100
13	1101
14	1110
15	1111

4.1 Introduction

The application of advanced oxidation processes (AOPs) to the degradation of recalcitrant organic matter has been extensively studied over the last decades. Among AOPs, the Fenton process, stemming from the work by Henry Fenton in the 1890s, has received increasing attention as it has proved to be highly efficient in the treatment of wastewaters containing non-biodegradable contaminants and producing extensive toxicity reduction. The advantages of the Fenton process are the need of a reagent easy to obtain, the flexibility of the operations, a short reaction time, and harmless by-products (Pignatello et al., 2006). In addition, the Fenton process takes place at ambient temperature and barometric pressure.

In the Fenton process, hydrogen peroxide (H_2O_2) and a Fe(II) catalyst produce highly reactive hydroxyl radicals ($HO^{\bullet}$), (**Eq. 4.1-4.2**), which unselectively react with organic matter, concomitantly with the oxidation of Fe (II) into Fe(III).

The presence of UV-vis light ($\lambda \leq 580nm$) allows reducing Fe(III) again into Fe (II), which in turn produces further $HO^{\bullet}$ radicals (**Eq. 4.3**) and results in a cycle continuously supplying $HO^{\bullet}$ until H_2O_2 is depleted. Shorter wavelengths ($\lambda \leq 310nm$) cause peroxide photolysis (**Eq. 4.4**) and the direct production of extra $HO^{\bullet}$. Therefore, the oxidation rate of photo-Fenton results much higher than that of the Fenton process.

$$Fe(II) + H_2O_2 \rightarrow Fe(III) + OH^- + HO^{\bullet} \qquad \textit{Eq. 4.1}$$

$$Fe(III) + H_2O_2 \rightarrow Fe(II) + H^+ + HO_2^{\bullet} \qquad \textit{Eq. 4.2}$$

$$Fe^{III}(OH)^{2+} + hv \rightarrow Fe^{2+} + HO^{\bullet} \qquad \textit{Eq. 4.3}$$

$$H_2O_2 + hv \rightarrow 2\,HO^{\bullet} \qquad \textit{Eq. 4.4}$$

Improved versions of the Fenton process are classified according to their hydroxyl radical production and include Photo-Fenton, electro-Fenton, sono-Fenton, photo-electro-Fenton, photo-sono-Fenton and sono-electro-Fenton.

This work focuses on the Photo-Fenton process, an effective method that takes place on the presence of Fenton reagents and UV radiation, including natural sunlight, which has been reported to reduce the operation cost.

The $HO^{\bullet}$ radical is the key species attacking organic molecules in an efficient but non-selective manner. However, an unnecessarily high concentration of $HO^{\bullet}$ (if H_2O_2 is added in excess) can cause unproductive reactions (**Eq. 4.5-4.6**) downgrading process performance (Tokumura et al., 2011):

$$HO^{\bullet} + HO^{\bullet} \rightarrow H_2O_2 \qquad \textit{Eq. 4.5}$$

$$H_2O_2 + HO^{\bullet} \rightarrow HO_2^{\bullet} + H_2O \qquad \textit{Eq. 4.6}$$

Using H_2O_2 is essential, but oversupplying is counterproductive. The supply of hydrogen peroxide, as a means to control the concentration of hydroxyl radicals, is the most important operational parameter for the photo-Fenton process affecting both reaction outcome and process cost (Ortega-Gomez et al., 2012). Accordingly, a number of works has been dedicated to determining conditions enhancing process performance through a sensible hydrogen peroxide supply. Despite the progress reported by recent works (Yamal-Turbay et al., 2012; Pouran et al., 2015; Wang et al., 2016; Esteves et al., 2018), solutions are still partial and far from optimal.

Most proposals are heuristic strategies that are useful in particular situations, although they that cannot provide the optimal solution. However, optimization is a systematic strategy leading not to an improved solution but to the solution for which is proved that no other better solution exists.

Initially, research sought for adequate concentration ratios of H_2O_2 to contaminant and iron (Pignatello et al., 2006) in an attempt to minimize the scavenging effect. However, constant ratios may suit steady operation, but time-varying batch processes (such as these addressed in this work and those usually reported in the literature –e.g. Pouran et al., 2015) require H_2O_2

supply to be continuously adapted to maximize the final operation performance. Thus, the real research challenge is the optimization of a continuous time-dependent H_2O_2 dosage profile.

Monteagudo et al. (2009) and Zazo et al. (2009) proved that continuously dosing H_2O_2 along the reaction time can increase oxidation efficiency beyond that obtained by administering a total dose of H_2O_2 at the beginning of the reaction (henceforth no dosage). H_2O_2 discretized dosage by splitting the total supply into several portions and adding them at different times has also been reported to produce improvements respect no dosage. However, the use of arbitrary time intervals prevents the solutions to be reported as optimal. Some researchers reported that sequential addition of discrete amounts of H_2O_2 leads to better results than adding a great initial dose (Chu et al., 2007; Almeida et al., 2015). Other previous works reported that adding H_2O_2 at a constant rate into the reactor along the reaction time increases the process efficiency (Monteagudo et al. 2009 Prato-Garcia et al., 2012). However, other researchers have drawn completely opposite conclusions (Chidambara and Quen, 2005; Zhou et al., 2016). Certainly, this divergence shows that dosage is still an open issue deserving attention, particularly with regard to a systematic approach and the standardized comparison of methods and results. Other works have addressed H_2O_2 dosage as a continuous control problem. Santos-Juanes et al. (2011) used the on-line monitoring of dissolved oxygen (DO) to regulate the dosage of H_2O_2 and greatly improve the operation performance. Despite the practical achievement, the strategy relies on the expert setting of an indirect factor (DO set-point) assumed to reveal the operation performance, and it cannot be proved optimal. A general systematic strategy based on an accurate statement of an optimization problem is still pending.

On the other hand, the optimization of similar problems has been successfully reported, such as the optimization of batch and fed-batch operations by model-based approaches (Biegler, 2018; Jang et al., 2016; Nie et al., 2014). The general dynamic optimization problem addressed consists on determining a control law (the recipe) that drives the process through a feasible trajectory on a continuous time interval and minimizes a given cost function at the end of the interval. The ordered set of decisions made along the given time horizon and the practical discrete approximation required by the numerical solution approach is in the basis of this work.

Nevertheless, for Fenton and photo-Fenton processes, the lack of suitable dynamic models hinders model-based optimization to a great extent (Qin and Badgwell, 2003; Jung et al., 2015), and the idea of model-based optimization to determine the best hydrogen peroxide supply profile along a batch run (the recipe) has been hardly addressed (Audino et al., 2019).

Since, the optimization of the operation of the photo-Fenton process, and particularly of the H_2O_2 dosage problem, is a continuous optimal control problem that should be formulated and addressed as such, this work uses recipe optimization concepts and a convenient time discretization to propose a practical methodology for experimentally addressing the optimization of hydrogen peroxide dosage profile. The adoption of this approach favors the convergence with the model-based optimization approach.

The proposed methodology is tested through its application to the remediation of a Paracetamol (PCT) solution. Furthermore, taking into account that several authors (Prieto-Rodríguez et al., 2011; Ortega-Gómez et al., 2012) have proposed using the variation of the concentration of dissolved oxygen (DO) for tactically adjusting hydrogen peroxide supply, this work also measures and discusses the response in DO concentration in order to provide deeper insight into the nature of the process.

4.2 Dosage modelling and problem formulation

Dosing hydrogen peroxide in batch Fenton and Photo-Fenton processes is a decision-making problem. Once admitted the existence of dosage alternatives, the problem consists in selecting a feasible alternative satisfying the given constraints and, eventually, the alternative producing the best outcome, the so-called optimal decision. Heuristic rules (tactical step moves based on local information) provide fast and practical decision-making support, but they do not drive to the optimal decision (the full set of moves for which the inexistence of any better alternatives for the complete problem can be proved), and they lean towards concealing misconceptions (mistaking the goal). Conversely, optimization techniques seek for the optimum at the expense of analyzing and quantitatively assessing all the alternatives (explicitly or implicitly, in the case of efficient search methods).

This work addresses the optimization of hydrogen peroxide dosage in batch Fenton and Photo-Fenton processes. Accordingly, this work undertakes a systematic problem analysis and formulation (including declared assumptions and simplifications) that contributes a methodological approach aimed at stirring discussion and further research. Next, this section sets system boundaries and operational constraints, offers the definition of an objective function quantitatively assessing the outcomes of the decisions, and proposes a search method. The search can be performed using a mathematical abstraction accurately representing the system under study, or experimentally (Box et al., 2005). Lacking convenient kinetic models, this work undertakes an experimental approach, which is more expensive but consistent with the model-based optimization approach used for solving similar dynamic optimization problems in industrial applications (Biegler, 2018; Jang et al., 2016; Nie et al., 2014).

A first assumption is batch operation. While continuous operation might be the choice for industrial solutions, most of the academic research focuses on batch assays (Pouran et al. 2015), probably because of the operational costs. Dosage in batch processing poses a dynamic optimization problem: determine the dosage level at each infinitesimal time interval (the trajectory of the control action) that minimizes (or maximizes) a given integral function at the end of a given finite interval.

The discrete approximation applied in the numerical solution of the model-based approach is for the experimental approach not only inevitable, but required of additional simplification.

4.2.1 Problem formulation

The proposed dosage model assumes a single objective J to be minimized by the operation of a Fenton or photo-Fenton reactor. J is the outcome of the operation after some reaction time T and after the addition of some total amount A of reactant (e.g. volume of H_2O_2 solution). As Fenton and photo-Fenton processes are mostly operated in batch, this outcome has to be a fix value that describes the performance of the process, such as an economic indicator or the final concentration of a given species. Likewise, the method could be applied to continuous processes by selecting a derivative (e.g. reaction rate) as an indicator.

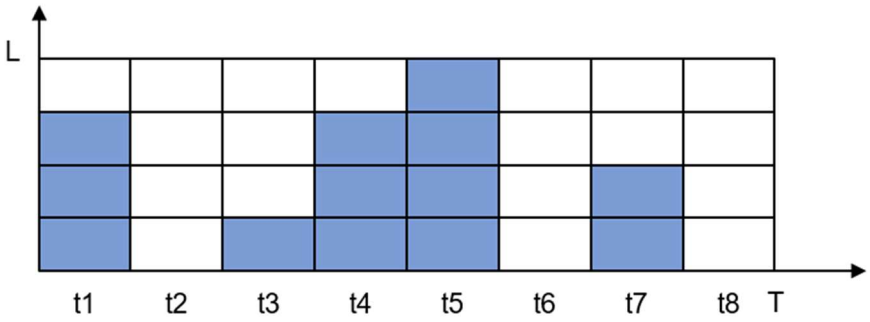

Fig 4.1. General discretization of the dosage profile. Theoretical framework.

A fraction f ($0 \leq f \leq 1$) of this total amount A can be dosed following different schemes during the time horizon, while the remaining fraction ($A_0 = (1-f) \cdot A$) is assumed to be added at once at the very beginning. Assume the reaction time T is discretized in $i = 1,2,3 \ldots N$ time slots, each of duration $\Delta t = T/N$, and $L \in N$ dosage levels as represented in **Figure 4.1** (in the limit, $N, L \to \infty$, this discretization allows considering time and supply as a continuous decision variables). Hence, for each time slot i the dosage level $x_i \in \{0,1,2 \ldots, L\}$ needs to be determined so that the balance and flow constraints on A are satisfied and the outcome $J = f(\boldsymbol{x}, f, A, T)$ is minimized (**Eq. 4.7**).

The formulation of the dosage model includes the integral of dosage bits (X, **Eq. 4.8**) that determines the incremental addition at each time interval (ΔA_i, **Eq. 4.9**). Hence, **Eq. 4.10** allows determining and bounding (e.g. pumping capacity) the corresponding dosage flows F_i for each time slot.

$$J = f(\boldsymbol{x}, f, A, T) \qquad \textit{Eq. 4.7}$$

s.t.

$$X = \sum_i x_i \qquad \textit{Eq. 4.8}$$

$$\Delta A_i = \left(\frac{f \cdot A}{X}\right) \cdot x_i \quad \forall i \qquad \textit{Eq. 4.9}$$

$$F^{min} \leq F_i = \frac{\Delta A_i}{\Delta t} \leq F^{max} \quad \forall i \qquad \textit{Eq. 4.10}$$

The outcome $J = f(\boldsymbol{x}, f, A, T)$ could be inexpensively determined through a convenient mathematical model f, if available, or experimentally. This work relies on the experimental measurement of the objective function J for exploring and assessing the alternatives and detecting the best one. The infinite solution space and the too expensive experimental search requires some further assumptions to positively address such identification.

In regard of decision variables, the following experimental work assumes a given time horizon T (thus, excluding the minimization of the reaction time) and disregards the consideration of any initial amount of reactant ($f = 1 \rightarrow A_0 = 0$). The total amount A will be also assumed fixed, but some assays will be presented providing insight and discussion concerning the stoichiometric amount. Thus, the general dosage problem presented is addressed in a reduced form consisting in determining the maximum distance we can drive on this road given this time and this amount of fuel; lacking a map of the road, the problem is addressed by methodically planning and executing a series of runs.

In regard of the modelling parameters N and Δt, this work proposes a first discretization aimed at achieving the practicality required by the evaluation of the methodology. Besides, the work also explores an alternative in order to offer data and discussion on the effect and sensitivity of such parameter values. Other implementations are deemed for future research and, in the same way that further problem extensions, may be envisaged stemming from the proposed formulation.

4.2.2 Design of Experiments

While this problem statement defines a comprehensive theoretical framework to address the dosage problem (consistent with the numerical solution of the optimization problem, if a reliable process model was

available), it also defines an unaffordable solution space of $(L+1)^N$ experimental assays. Thus, this work also analyses the practical ways to address the corresponding design of experiments by identifying and removing unrealistic solutions. Further simplifications are discussed in regard to the granularity adopted and the practicality of the solutions attained.

A first issue to decide is the objective function. As stated in the previous section, it has to be a final indicator of the performance of the process of a batch process. Among other complex alternatives (economic and/or environmental impacts), this work sets the outcome to be minimized as the Total Organic Carbon (TOC) concentration measured at the end of a given reaction time (i.e. $[TOC]_T$). The particular choice of TOC at the end of a time horizon, is commonly used by many authors, including those addressing hydrogen peroxide dosage (Herney-Ramirez et al., 2010; Pouran et al., 2015). TOC is a valuable index of water quality as it reveals the extent of mineralization of mother starting (pollutants plus the formed intermediates). The reagent to be dosed is Hydrogen peroxide, and its amount A is defined in terms of volume of water solution (reagent-grade, 33% w/v).

Moreover, the dosage level is simplified to a binary decision for each time slot i; thus, $x_i \in \{0,1\}$ (**Figure 4.2A**). Further considerations include setting $x_i = 1$ for the first slot (since no reaction is expected otherwise) and setting $x_i = 0$ for the last slots in the series (since the reaction is expected to continue for a while without further dosage) as represented in **Figure 4.2B**. These are practical assumptions (e.g., the first time slot could have no duration, in order to consider an initial immediate addition of reactant), and they can be revised later on depending on the results.

The time horizon T is set to 120 minutes. This reaction time is fixed according to the preliminary experiments using a single H_2O_2 addition. The monitoring of the H_2O_2 concentration (**Figure 4.3B**) shows that the stoichiometric amount of H_2O_2 is almost exhausted after 120 minutes. Thus, the slot size Δt is the last decision to be made. It is set to 15 min, which leads to $N = 8$ and $2^N = 256$ alternatives to be explored. Since there are four slots assumed to be determined beforehand (the first and the last three) the solution space is again reduced and only $2^{N-4} = 16$ assays are finally planned. For the sake of illustration, assume a finer partition given by a Δt value reduced to 5 min (only to one third). Hence, $N = 24$ and the alternatives to be explored would be $2^{N-4} = 1048576$, which is experimentally unaffordable (**Table 4.1**)

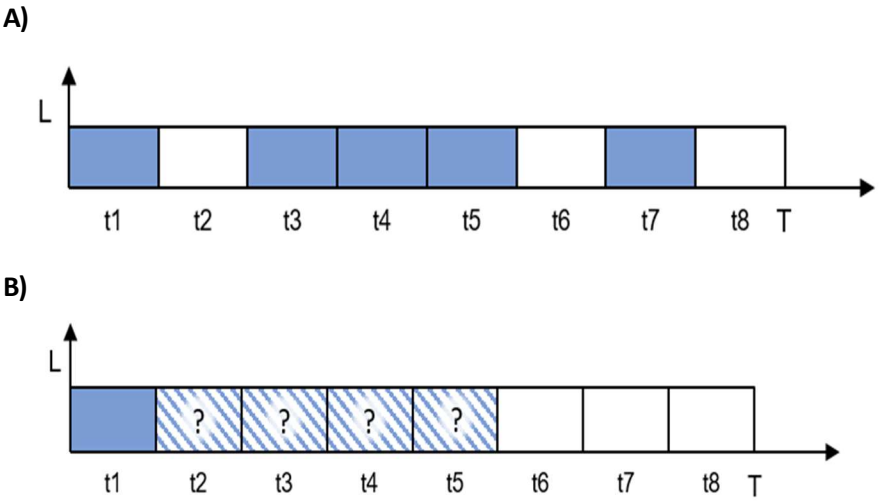

Fig 4.2. Discretization of the dosage profile (A) considering binary decisions and (B) fixing first and last time slots.

Table 4.1. Design of experiments. The dosage level (0, 1) is given for the eight time slots S1 to S8; the preset values for slots S1, S6, S7 and S8 are shadowed. The reactant fraction to be dosed at each active slot is also given.

ID (dec)	ID (bin)	S1	S2	S3	S4	S5	S6	S7	S8	Fraction per slot
0	0000	1	0	0	0	0	0	0	0	1
1	0001	1	0	0	0	1	0	0	0	1/2
2	0010	1	0	0	1	0	0	0	0	1/2
3	0011	1	0	0	1	1	0	0	0	1/3
4	0100	1	0	1	0	0	0	0	0	1/2
5	0101	1	0	1	0	1	0	0	0	1/3
6	0110	1	0	1	1	0	0	0	0	1/3
7	0111	1	0	1	1	1	0	0	0	1/4
8	1000	1	1	0	0	0	0	0	0	1/2
9	1001	1	1	0	0	1	0	0	0	1/3
10	1010	1	1	0	1	0	0	0	0	1/3
11	1011	1	1	0	1	1	0	0	0	1/4
12	1100	1	1	1	0	0	0	0	0	1/3
13	1101	1	1	1	0	1	0	0	0	1/4
14	1110	1	1	1	1	0	0	0	0	1/4
15	1111	1	1	1	1	1	0	0	0	1/5

4.3 Materials and methods

Paracetamol (98% purity) was purchased from Sigma-Aldrich. Hydrogen peroxide (reagent-grade, 33% w/v) was purchased from Panreac. Heptahydrate ferrous sulfate ($FeSO_4 \cdot 7H_2O$) used as the ferrous ion was acquired from Merck. Sulfuric acid (H_2SO_4 95%) from Fisher was used for pH adjustment. Ammonium metavanadate (NH_4VO_3 98.5%) was used for H_2O_2 measurement. HPLC gradient grade Methanol (MeOH) was acquired from J.T. Baker Inc. and ultra-pure solvents (Milli-Q® water) were prepared for HPLC mobile phase. Distilled water was used as water matrix for solution preparation.

The experimental setup is an automated photochemical pilot plant. The reaction system includes a 13.5 L glass jacked reservoir tank and a 1.5 L glass tubular photo-reactor (10% of the total volume) with an irradiated height of 130 mm). The radiation source is a Philips Actinic BL TL 36 W/10 1SL lamp (UVA-UVB), the incident photon power, $E = 3.36 \times 10^{-4}$ Einstein min^{-1} (300 and 420 nm) was measured using potassium ferrioxalate actinometry. The recirculation fluid is driving through the reservoir tank and the photo-reactor by a centrifugal pump (Iwaki Magnet Pump, MD-30RZ-220, 1-16HP-220V). Sensors are also equipped for measuring pH (Hamilton Polilyte HTVP 120), intensity of UV radiation on the external surface (Sglux UV_Surface_A_4-20mA_cable), temperature and dissolved oxygen (Hamilton Oxysens). H_2O_2 dosage is automatically performed through a peristaltic pump (Watson Marlow, OEM 313 24V) and a PLC (Siemens SIMATIC S7-1200) managed by the plant SCADA system (InTouchR® software).

4.3.1 Analytical methods

Total organic carbon (TOC) concentration was determined with a TOC (TOC-VCSH/CSN Shimadzu; Kyoto, Japan) analyzer. Samples were taken every 15 min and kept in the ice to slow down further oxidation.

PCT concentration was measured via HPLC Agilent 1200 series (Agilent Technologies) with UV-DAD array detector. The chromatographic column was a 5 µm 4.6 mm×150 mm Akady Ultrabase C-18. 20 µl samples, the detection wavelength was set to 243 nm and the temperature was fixed to

25 ˚C. The eluent was a mixture of methanol and water (25:75) with a flow rate of 0.4 mL min^{-1} (Yamal-Turbay et al., 2015), retention time was 7.3 min under these conditions. Samples were taken at different times and were previously treated with methanol (in proportion 50:50) in order to stop further degradation of PCT.

H_2O_2 concentration was measured by using the spectrophotometric method (Nogueira et al., 2005). The absorption at 450 nm was detected via a U-2001 UV–vis spectrophotometer (Hitachi, Tokyo, Japan).

4.3.2 Experimental procedure

The conditions of the photo-Fenton experiments were: pH adjusted to 2.8 ± 0.2 using H_2SO_4 and temperature 26-28 ˚C. The initial solution in the reactor was prepared with 15 L of distilled water and 0.6122 g of model pollutant PCT and 0.7468 g of $FeSO_4 \cdot 7H_2O$ (40 mg L^{-1} PCT and 10 mg L^{-1} Fe(II)). The total amount of hydrogen peroxide to be dosed, A, is set to be the stoichiometric concentration (considering H_2O_2 as the only oxidant in the media, **Eq. 4.11**), S, for the given amount of PCT: this is 9.545 g (8.5909 mL of solution 33% w/v), which corresponds to a concentration of 189 mg L^{-1} (S).

$$C_8H_9NO_2 + 21H_2O_2 \rightarrow 8CO_2 + 25H_2O + H^+ + NO_3^- \qquad \textit{Eq. 4.11}$$

The UV light was switched on as soon as $FeSO_4 \cdot 7H_2O$ and PCT were added in order to guarantee its stabilization. The execution of the dosage program started 10 min after to ensure perfect mixing. The dosage of the H_2O_2 solution followed the specific values set for experiment and shown in **Table 4.2**, and the specific dosage time intervals 0, 15, 30, 45, 60 min. All experiments were repeated twice, the average values were obtained to exhibit the TOC conversion, PCT degradation, and H_2O_2 evolution.

Table 4.2. List of assays carried out using 40 mg L^{-1} PCT and 189 mg L^{-1} of H_2O_2 (the corresponding to the stoichiometric amount, S).

ID (dec)	ID (bin)	S1 (mL)	S2 (mL)	S3 (mL)	S4 (mL)	S5 (mL)	S6 (mL)	S7 (mL)	S8 (mL)
0	0000	8.60	0	0	0	0	0	0	0
1	0001	4.30	0	0	0	4.30	0	0	0
2	0010	4.30	0	0	4.30	0	0	0	0
3	0011	2.87	0	0	2.87	2.87	0	0	0
4	0100	4.30	0	4.30	0	0	0	0	0
5	0101	2.87	0	2.87	0	2.87	0	0	0
6	0110	2.87	0	2.87	2.87	0	0	0	0
7	0111	2.15	0	2.15	2.15	2.15	0	0	0
8	1000	4.30	4.30	0	0	0	0	0	0
9	1001	2.87	2.87	0	0	2.87	0	0	0
10	1010	2.87	2.87	0	2.87	0	0	0	0
11	1011	2.15	2.15	0	2.15	2.15	0	0	0
12	1100	2.87	2.87	2.87	0	0	0	0	0
13	1101	2.15	2.15	2.15	0	2.15	0	0	0
14	1110	2.15	2.15	2.15	2.15	0	0	0	0
15	1111	1.72	1.72	1.72	1.72	1.72	0	0	0

4.4 Results and discussion

4.4.1 Preliminary results

Preliminary tests were performed to a 40 mg L^{-1} PCT sample to identify the contribution to the mineralization of PCT of factors such as reagent and irradiation. The tests (**Figure 4.3**) were performed at pH= 2.8 ± 0.2 and T = 26-28 °C, and the loads of the Fenton reagents were [Fe(II)] = 10 mg L^{-1} and [H_2O_2] = 189 mg L^{-1} (corresponding to the stoichiometric amount, S).

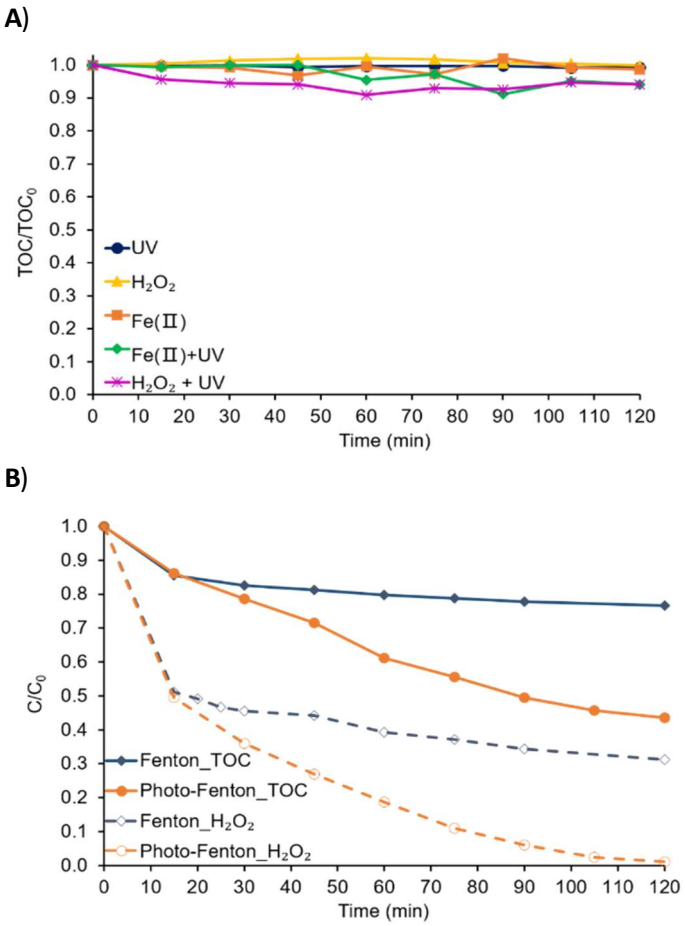

Fig 4.3. (A) Evolution of TOC concentrations upon blank assays. (B) Comparison of Fenton and photo-Fenton process: evolution of TOC and H_2O_2 concentrations

The results of these tests can be summarized as follows:

Negligible mineralization was attained in all the blank tests (**Figure 4.3A**), even in the assays with sole H_2O_2, sole irradiation, and the combination of both.

The comparison between the results of the Fenton and the photo-Fenton processes (**Figure 4.3B**) shows that UV irradiation significantly enhanced the

conversion attained. This is due to already mentioned role of UV-vis light, which increases the mineralization from 23.3 % to 57.15 %.

Once demonstrated the higher mineralization capacity of the photo-Fenton process, the next step is studying the effect of H_2O_2 dosage on the performance of photo-Fenton processes aimed at determining the best dosage scheme.

4.4.2 Base case

The 16 dosage schemes planned (**Table 4.2**) were first performed for 40 mg L^{-1} PCT and the stoichiometric amount of H_2O_2 (S, 189 mg L^{-1}) to be dosed along a time horizon of two hours (T= 120 min). Clearly, the stoichiometric amount cannot be expected to achieve total mineralization. However, it is useful for providing reference results for quantitative comparison.

Additional measurements were taken beyond this time horizon for TOC (up to 240 min, in order not to miss further reaction progress), while measurements for PCT were interrupted earlier, as they fell below the detection limits of the analytical techniques.

Table 4.2 presents the assays using the binary code, which clearly express the dosage profile. The label NO_DOSAGE refers to the assay for which the same total amount of H_2O_2 was supplied all at once at the beginning. All these assays were repeated twice and variability of TOC concentration was found to be low (below 4 %). Therefore, from here on, only the average of all these repeated measurements is presented.

All these assays show that PCT completely reacts within the first 45 min. However, the time required for PCT concentration to drop below the detection limits depends on the number and size of the dosing bits (the distribution of the H_2O_2 supply along the time). For a first assay, G1 = {0000}, no presence of PCT is detected after 15 min; for the group of assays G2 = {0001, 0010, 0100, 1000}, no presence of PCT is detected after 25 min; for the groups G3 = {0011, 0101, 0110, 1100, 1001, 1010}, G4 = {0111, 1011, 1101, 1110}, and G5 = {1111}, tending to continuous supply, the time spans from 25 to 45 min.

The higher the number of the dosing bits (the lower the H_2O_2 amount added in each time slot), the slower the PCT elimination. **Figure 4.4** shows the hydrogen peroxide present in the system for each group. NO_DOSAGE is the assay producing the PCT fastest elimination, while the rest G1 (0.573 mL/min at first dosing interval), G2 (0.286 mL/min at each dosing interval), G3 (0.286 mL/min), G4 (0.286 mL/min), and G5 (0.286 mL/min), result increasingly slower. Thus, these results allow concluding that, only in regard to PCT removal, the most concentrated reactants at the beginning, the best performance, which suggests that the scavenging effect should be expected later and involved with intermediate products.

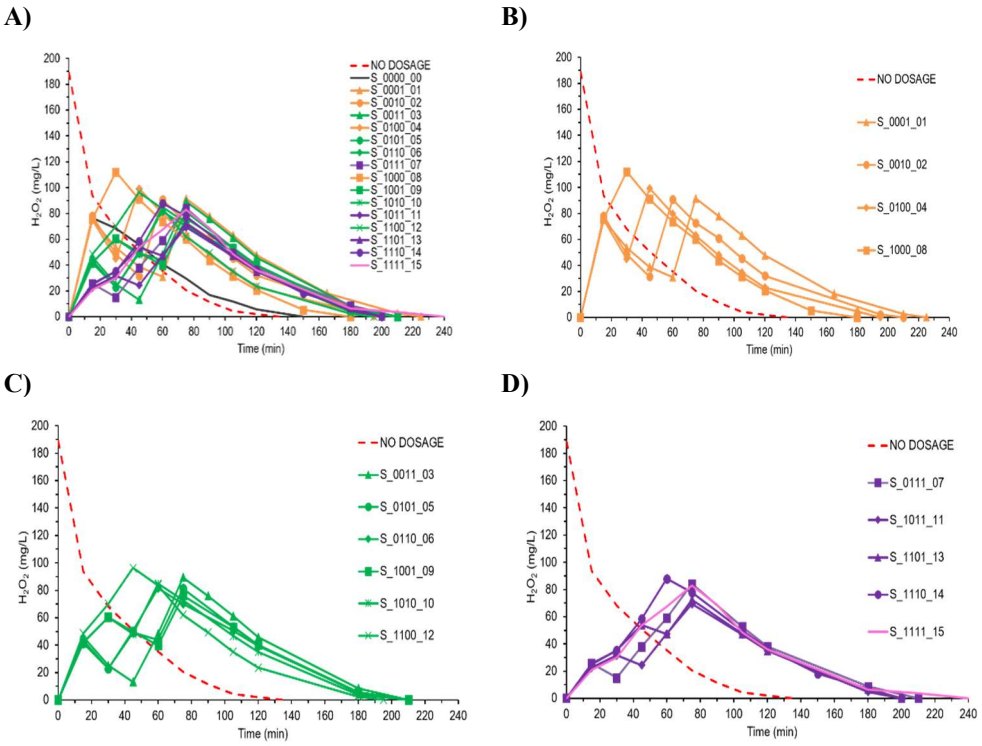

Fig 4.4. Hydrogen peroxide profiles (A) all assays (B) with two doses, G2 (C) with three doses, G3 (D) with four and five doses, G4 and G5.

The evolution of the concentration of H_2O_2 is studied and presented in the above set of figures (**Figure 4.4**). The dashed line plotting the evolution when H_2O_2 is added all at once at the beginning (NO_DOSAGE) reveals that the

same amount, S, of H_2O_2 is consumed much faster and exhausted by 135 min. On the other hand, other dosing schemes produce H_2O_2 profiles that span longer and may exhibit peaks and valleys (**Figures 4.4B** and **4.4C**), which may be interpreted as a gap between supply and demand. This seems not the case for the more continuous dosage given by G4 and G5 (**Figure 4.4D**), although this cannot be deemed as the most efficient.

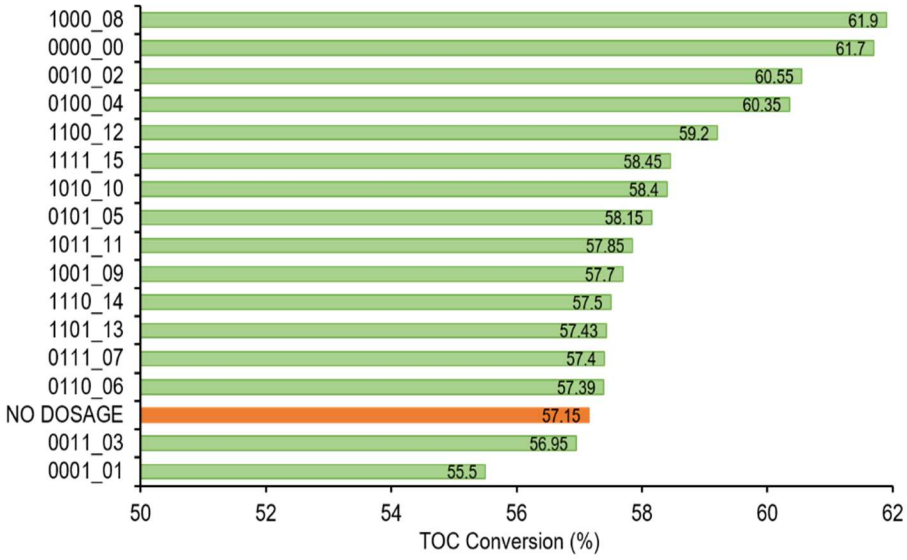

Fig 4.5. TOC conversion after 120 min under photo-Fenton treatment. The total amount of hydrogen peroxide added during 120 min is the stoichiometric quantity. Table 2 summarize the dosing strategies.

The identification of the best protocol is given by **Figure 4.5** (according to the objective function set to be minimized, $J = [TOC]_{120}$) and is revealed to be 1000 (61.90% conversion) and 0000 (61.70% conversion), which is an improvement of 4.75 percent points NO DOSAGE (57.15% conversion). This may seem a minor improvement, but it can be much more significant in regard of process economy. Despite this numerical value, the improvement is shown to be systematically determined by the dosage modelling proposed and the experimental design derived accordingly. On the other hand, 0011 and 0001 are revealed to have worse performance than NO_DOSAGE; indeed, this can be attributed to a demand of H_2O_2 that is attended too late

(although it can be expected to have an effect beyond $T = 120$ min). The comparative details of these extreme situations are given in **Figure 4.6**.

A)

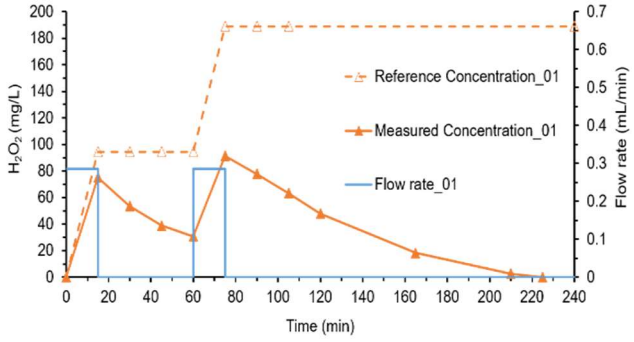

B)

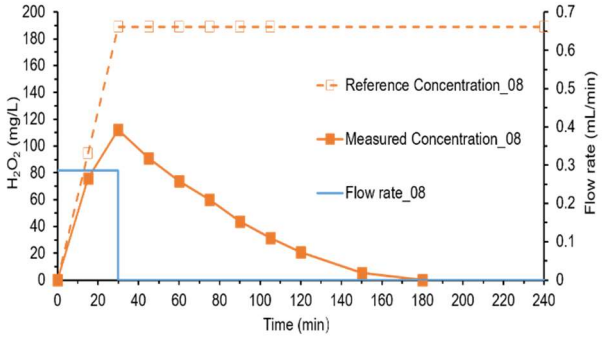

Fig 4.6. Hydrogen peroxide inlet flow, measured hydrogen peroxide concentration, and reference concentration (the one that would result from the addition to a non-reacting system): (A) 0001 (the worse scheme) (B) and 1000 (the best scheme)

Finally, the evolution of dissolved oxygen concentration (DO) is also monitored for tactical purposes and for a more complete interpretation of the underlying nature of the process (**Figure 4.7**). DO level has been interpreted as a practical indicator of process efficiency (Santos-Juanes et al., 2011). Thus, while low DO levels might indicate the need for more H_2O_2, the

rising of DO might indicate an unproductive decomposition of hydrogen peroxide that should be avoided.

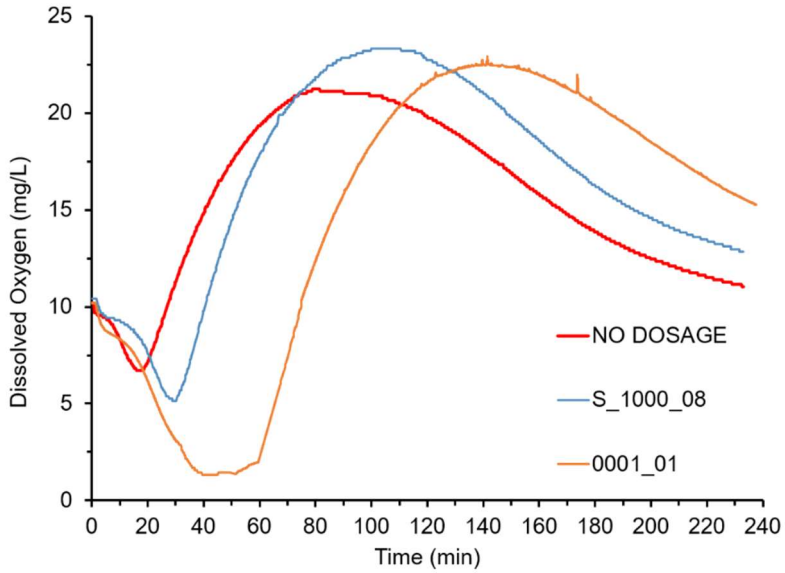

Fig 4.7. Evolution of DO level for assays NO_DOSAGE, 1000 and 0001.

Accordingly, **Figure 4.7** might suggest that NO_DOSAGE, providing more moderate peaks and valleys, should produce the best performance, which is obtained by 1000. Conversely, both assays 1000 and 0001, experience a smoother start. This shows that, although DO is a practical indicator, the relationship between this indicator and the performance (minimizing TOC, or cost, or any other objective function that may be proposed) is not direct and deserves attention beyond this first experimental design proposed to illustrate the methodology.

On one hand, the aggregate and indirect information provided by the DO level at time $t < T$ cannot anticipate the outcome of the process at time T, and it cannot drive decisions to an optimal outcome. On the other hand, the change in the DO level (its derivative at time $t < T$) may provide local information that could eventually drive tactical decisions (adding H_2O_2). In this regard, the change of the DO level is a robust measurement, since it is relative and insensitive to offsets and interferences caused by side reactions and intermediate products. However, developing an accurate correlation of

the level of dissolved oxygen with these factors, including delays due to the diffusion of the dissolved oxygen, is complex challenge out of the scope of this paper.

4.4.3 Extended cases

This section investigates some of the implicit assumptions accepted up to this point.

The proposed dosage model assumes a general single objective J that for the base case was TOC concentration after 120 min: $J = [TOC]_{120}$. In addition to this objective function, the total amount of hydrogen peroxide to be added was set to be the stoichiometric ($A = S$) and the initial amount was set to be zero ($A_0 = 0$). Finally yet importantly, the intervals were arbitrarily fixed to 15 min. Such decisions are not inherent to the methodology and they could be controlled to achieve better performance.

4.4.3.1 Objective function

A first extension in the objective function consists in changing the reaction time. Thus, a new set of assays was performed for a time horizon of four hours (T= 240 min), and the conversions obtained for $J = [TOC]_{240}$ were ranked and compared with those in the previous section. For this extended reaction span, the best conversion was 6% higher than that obtained without dosage.

A new objective function can also be proposed by considering the reverse approach: the earliest time to achieve a specified conversion. Given the same conversions, such a time is obtained by the linear interpolation of the measured values. For instance, the time required for reaching 70% conversion show that while 240 min are required if no dosage is applied, only 167 min (73 min less) are required for the most efficient dosage protocol (1000).

4.4.3.2 Hydrogen peroxide amount

The first set of assays were planned with a total amount of hydrogen peroxide, A, equal to the stoichiometric amount. This is an assumption based on the idea that an ideal dosage protocol should exist that would cause no hydrogen peroxide dissipation in any unproductive reaction. However, more than the stoichiometric amount could achieve better performance. Therefore, this sub-section explores the effect of different amounts of hydrogen peroxide. Certainly, the idea of A as decision variable instead of a fixed parameter is implicit in the problem formulation (Eq.7), but attempting such an extended optimization problem is out of the scope of this work.

In **Figure 4.8** and from this point on, experiments are codified using the same ID (bin) from **Table 4.2**, plus the amount of hydrogen peroxide referred to the stoichiometric amount, S, specifically S (189 mg L^{-1}), 1.2S (226.8 mg L^{-1}), and 2S (378 mg L^{-1}).

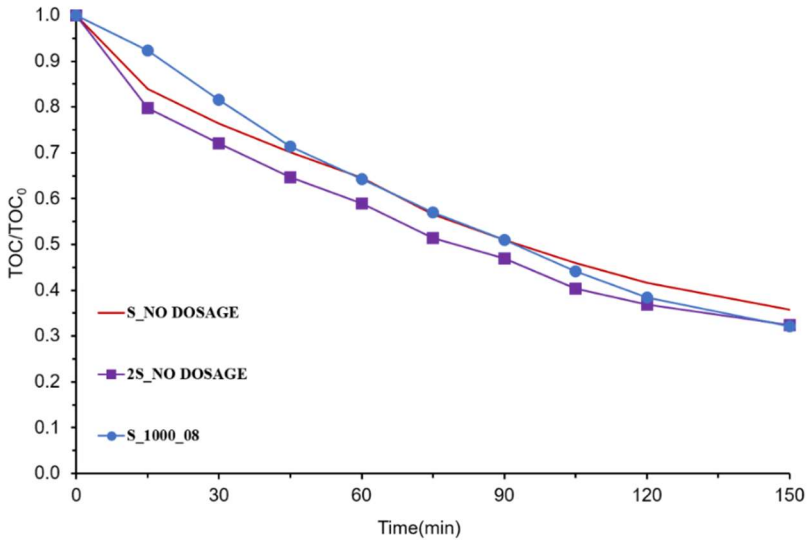

Fig 4.8. Evolution of the TOC concentration (normalized) for the assays S_NO DOSAGE, 2S_NO DOSAGE and S_1000_08.

Figure 4.8 shows how the best dosage protocol (S_1000_08) reaches similar mineralization value (68 %, 150 min) than NO_DOSAGE assay with double

hydrogen peroxide amount (2S_No Dosage). The methodology allows to save half of the hydrogen peroxide amount.

4.4.3.3 Hydrogen peroxide initial amount (A_0)

DO performance allows analyzing the appropriate initial amount of hydrogen peroxide in order to avoid the marked decrease in oxygen consumption general produced in dosage assays at early stages of the oxidation process. Towards this end, a new set of experiments were performed to obtain a new set of outcomes at 120 min for different initial amounts of hydrogen peroxide (**Table 4.3**).

Table 4.3. TOC conversions obtained at 120 min with different hydrogen peroxide amounts (A) and initial amounts (A_0) and the conversion obtained. The stoichiometric amount (S) is 189 mg·L^{-1}.

A	A_0	Assay	TOC_{120min} (%)
189.0	189.0	S_No dosage	58
189.0	0.0	S_1000	62
226.8	226.8	1.2S_No dosage	62
226.8	0.0	1.2S_1000	63
226.8	37.8	0.2S+S_1000	65
378.0	378	2S_No dosage	63
378.0	0.0	2S_1000	59
378.0	189.0	S+S_1000	64

Figure 4.9 presents the corresponding DO profiles. For this particular case (the dynamics of the photo-Fenton process are strongly dependent on the nature of the organic matter to be degraded), 0.2S obtain flatter DO performance at the first time reactions.

It is worth noting that DO levels attain levels far beyond saturation. As commented previously, DO absolute values usually depend on many factors (pressure, temperature, salinity…) in addition to those specifically provided by the Photo-Fenton reacting environment (intermediates, radicals…). Other works monitoring DO in Photo-Fenton processes also report similar values noticeably exceeding DO saturation (Santos-Juanes et al. 2011, Ortega-

Gómez et al. 2012). This works also propose the reactions producing O_2. Another important factor to observe is process dynamics, and the accumulation caused by O_2 production rates larger than the oxygen diffusion rate. This effect is included in the model introduced by Cabrera-Reina et al. (2012).

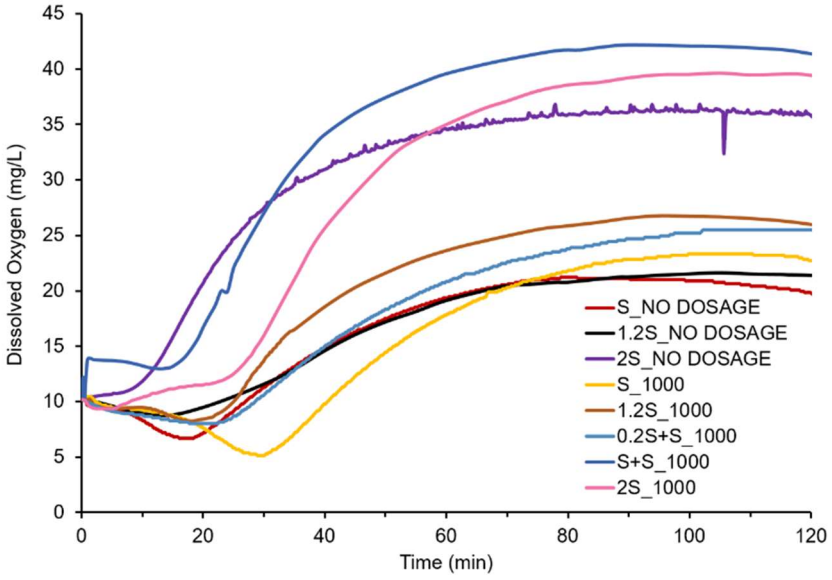

Fig 4.9. Evolution of the DO concentration for the assays given in Table 3.

4.4.3.4 Time discretization

Finally, time discretization is addressed in this last experiment. Related to the interval time slots only two options were tested (from 15 to 5 min) the results (**Figure 4.10**) evidence a clear effect of this parameter. Further studies are required in order to optimize it.

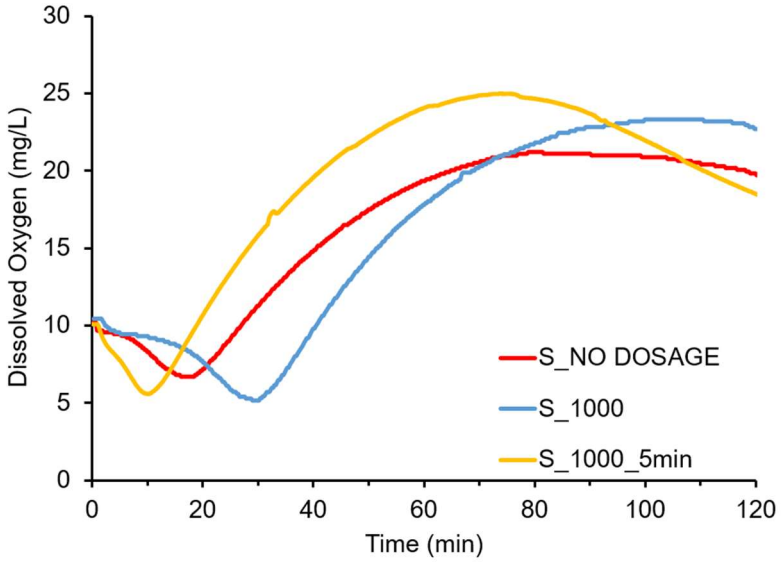

Fig 4.10. Evolution of the DO concentration for the assays with different time discretization.

All these results are exploring different variations of the initial experimental design open promising research lines. The development of a methodology for determining the best dosage protocol for the photo-Fenton process deserves the attention of future work.

4.5 Conclusions

This work presents a comprehensive theoretical framework to address the problem of hydrogen peroxide dosage for Fenton and photo-Fenton processes in a systematic way. The work proposes a problem formulation that provides a new insight into the nature of the decision-making problem, and allows further discussion of tactical and strategic solution approaches. The framework is based on the underlying dynamic optimization essence of the problem. A natural discretization scheme is adopted to develop a new dosage model for which advantages and limitations are discussed. With the aim to overcome the current lack of models that provide model-based

solution approaches, this work is expected to shed new light to the dosage problem by addressing it from an experimental approach.

A practical experimental design is proposed and assumptions are made to reduce the dosage level to a set of binary decisions, as well as fixing reaction time and the total amount of hydrogen peroxide. This experimental approach is consistent with the model-based optimization approach and sets a framework to further develop and validate a mathematical model for the dosage. Accordingly, a complete set of dosage schemes were implemented and assessed for the study of paracetamol (PCT) degradation.

The quantitative results obtained allow sorting out the alternatives and identifying the best dosage profile, which increases TOC conversion by 4.75 percent points (after 120 minute). Additionally, complementary measurements allowed to further discuss the complex nature of the different interconnected processes causing such an outcome. All the treatments under study attained the total elimination of initial PCT within a minimum time of 7 min and maximum time of 45 min (over a time horizon of 120 min). The measurement of the corresponding DO concentration allowed concluding that no simple relation seems to exist between the observed DO values and the final outcome of the process at the end of the time horizon (e.g. $[TOC]_T$). However, the study of DO profiles in parallel to the corresponding dosage profiles might provide meaningful and practical correlations for tactical purposes.

Other objectives and configurations were studied to envisage new aspects to be explored. Thus, decisions not inherent to the methodology (the total amount of hydrogen peroxide to be added, the initial amount of hydrogen peroxide, the intervals time slots) were modified and tested to achieve better system performance. When the goal was to minimize TOC concentration after 240 min ($J = [TOC]_{240}$), the mineralization was further improved (by to 6 percent points) with the same amount of hydrogen peroxide.

Conversely, attending the inverse objective (the earliest time required to meet a certain TOC value) led to determining that the same mineralization was achieved within 167 min or 240 min, depending on the dosage protocol. The effect of an initial amount of hydrogen peroxide was also addressed and studied. When the monitoring of the DO levels was included, the marked decrease in oxygen consumption produced at early stages of the oxidation

process was shown to be moderated. Finally, changing time discretization (from 15 to 5 min) revealed that this is a very influencing aspect deserving further studies and that future work should continue progressing towards a model-based optimal control of photo-Fenton processes.

Notation

Table 4.4. Notation for the mathematical model.

Symbol	Description
i	Time slot
T	Total reaction time
L	Dosage levels
ΔA_i	Amount of H_2O_2 for each time slot i
A	Total amount of H_2O_2 to be added
A_0	Initial amount of H_2O_2 to be added
X	Total number of dosage bits
F_i	Flow of H_2O_2 at each time slot i
F_{min}	Minimum flow of H_2O_2
F_{max}	Maximum flow of H_2O_2

4.6 References

Almeida, C. V. D. S., Macedo, M. S., Eguiluz, K. I. B., Salazar-Banda, G. R., Queissada, D. D., 2015. Indanthrene Blue Dye Degradation by UV/H_2O_2 Process: H_2O_2 as a Single or Fractioned Aliquot? Environ. Eng. Sci. 32, 930-937. doi:10.1089/ees.2015.0171.

Audino, F., Campanyà, G., Pérez-Moya, M., Espuña, A., Graells, M., 2019. Systematic optimization approach for the efficient management of the photo-Fenton treatment process. Sci. Total Environ. 646, 902-913. doi:10.1016/j.scitotenv.2018.07.057.

Biegler, L.T., 2018. Advanced optimization strategies for integrated dynamic process operations. Comp. Chem. Engng. 114, 9, 3-13. doi:10.1016/j.compchemeng.2017.10.016.

Box, G. E. P., Hunter, J.S., Hunter, W.G., 2005. Statistics for Experimenters: Design Innovation and Discovery, USA, NY, New York:Wiley-Interscience.

Cabrera-Reina, A., Santos-Juanes, L., García, J.L., Casas, J.L., Sánchez, J.S., 2012. Modelling photo-Fenton process for organic matter mineralization, hydrogen peroxide consumption and dissolved oxygen evolution. Appl. Catal. B Environ., 119-120,132–138. doi:10.1016/j.apcatb.2012.02.021

Chu, W., Chan, K. H., Kwan, C. Y., Choi, K. Y., 2007. Degradation of atrazine by modified stepwise-Fenton's processes. Chemosphere 67, 755-761. doi:10.1016/j.chemosphere.2006.10.039.

Chidambara Raj, C. B., Quen, H. L., 2005. Advanced oxidation processes for wastewater treatment: Optimization of UV/H_2O_2 process through a statistical technique. Chem. Eng. Sci. 60, 5305-5311. doi:10.1016/j.ces.2005.03.065.

Esteves, B. M., Rodrigues, C. S., Madeira, L. M., 2018. Synthetic olive mill wastewater treatment by Fenton's process in batch and continuous reactors operation. Environ. Sci. Pollut. Res. 25, 34826–34838. doi:10.1007/s11356-017-0532-y.

Herney-Ramirez J., Vicente M. A., Madeira, L. M.,2010. Heterogeneous photo-Fenton oxidation with pillared clay-based catalysts for wastewater treatment: A review, Appl. Catal. B: Environ., 98, 10-26. doi:10.1016/j.apcatb.2010.05.004

Jang H., Lee J.H., Biegler L.T., 2016. A robust NMPC scheme for semi-batch polymerization reactors. IFAC-PapersOnLine 49, 37-42. doi:10.1016/j.ifacol.2016.07.213.

Jung, T. Y., Nie, Y., Lee, J. H., Biegler, L. T., 2015. Model-based on-Line optimization framework for semi-batch polymerization reactors. IFAC-PapersOnLine. 48, 164-169. doi:10.1016/j.ifacol.2015.08.175.

Monteagudo, J. M., Durán, A., San Martín, I., Aguirre, M., 2009. Effect of continuous addition of H_2O_2 and air injection on ferrioxalate-assisted solar photo-Fenton degradation of Orange II. Appl. Catal. B 89, 510-518. doi:10.1016/j.apcatb.2009.01.008.

Nie, Y., Biegler, L. T., Villa, C. M., Wassick, J. M., 2014. Discrete time formulation for the integration of scheduling and dynamic optimization. Ind. Eng. Chem. Res. 54, 4303-4315. doi:10.1021/ie502960p.

Nogueira, R. F. P., Oliveira, M. C., Paterlini, W. C., 2005. Simple and fast spectrophotometric determination of H_2O_2 in photo-Fenton reactions using metavanadate. Talanta. 66, 86-91. doi::10.1016/j.talanta.2004.10.001.

Ortega-Gómez, E., Úbeda, J. M., Hervás, J. Á., López, J. C., Jordá, L. S. J., Pérez, J. S., 2012. Automatic dosage of hydrogen peroxide in solar photo-Fenton plants: development of a control strategy for efficiency enhancement. J. Hazard. Mater. 237, 223-230. doi:10.1016/j.jhazmat.2012.08.031.

Pignatello, J. J., Oliveros, E., MacKay, A., 2006. Advanced oxidation processes for organic contaminant destruction based on the Fenton reaction and related chemistry. Crit Rev Environ Sci Technol 36, 1-84. doi:10.1080/10643380500326564

Pouran, S. R., Aziz, A. A., Daud, W. M. A. W., 2015. Review on the main advances in photo-Fenton oxidation system for recalcitrant wastewaters. J Ind Eng Chem 21, 53-69. doi:10.1016/j.jiec.2014.05.005.

Prato-García, D., Buitrón, G., 2012. Evaluation of three reagent dosing strategies in a photo-Fenton process for the decolorization of azo dye mixtures. J. Hazard. Mater., 217–218, 293-300. doi:10.1016/j.jhazmat.2012.03.036

Prieto-Rodríguez, L., Oller, I., Zapata, A., Agüera, A., Malato, S., 2011. Hydrogen peroxide automatic dosing based on dissolved oxygen concentration during solar photo-Fenton. Catal. Today 161, 247-254. doi:10.1016/j.cattod.2010.11.017.

Qin, S. J., Badgwell, T. A., 2003. A survey of industrial model predictive control technology. Control. Eng. Pract. 11, 733-764. doi:10.1016/s0967-0661(02)00186-7.

Santos-Juanes, L., Sánchez, J. G., López, J. C., Oller, I., Malato, S., Pérez, J. S., 2011. Dissolved oxygen concentration: A key parameter in monitoring the photo-Fenton process. Appl. Catal. B 104, 316-323. doi:10.1016/j.apcatb.2011.03.013.

Tokumura, M., Morito, R., Hatayama, R., Kawase, Y., 2011. Iron redox cycling in hydroxyl radical generation during the photo-Fenton oxidative degradation: Dynamic change of hydroxyl radical concentration. Appl. Catal. B 106, 565-576. doi:10.1016/j.apcatb.2011.06.017.

Wang, N., Zheng, T., Zhang, G., Wang, P., 2016. A review on Fenton-like processes for organic wastewater treatment. J. Environ. Chem. Eng. 4, 762-787. doi:10.1016/j.jece.2015.12.016.

Yamal-Turbay, E., Graells, M., Pérez-Moya, M., 2012. Systematic assessment of the influence of hydrogen peroxide dosage on caffeine degradation by the photo-Fenton process. Ind. Eng. Chem. Res. 51, 4770-4778. doi:10.1021/ie202256k.

Yamal-Turbay, E., Ortega, E., Conte, L. O., Graells, M., Mansilla, H. D., Alfano, O. M., Pérez-Moya, M., 2015. Photonic efficiency of the photodegradation of paracetamol in water by the photo-Fenton process. Environ. Sci. Pollut. Res. 22, 938-945. doi:10.1007/s11356-014-2990-9.

Zazo, J. A., Casas, J. A., Mohedano, A. F., Rodriguez, J. J., 2009. Semicontinuous Fenton oxidation of phenol in aqueous solution. A kinetic study. Water Res. 43, 4063-4069. doi:10.1016/j.watres.2009.06.035.

Zhou, W., Zhao, H., Gao, J., Meng, X., Wu, S., Qin, Y., 2016. Influence of a reagents addition strategy on the Fenton oxidation of rhodamine B: control of the competitive reaction of ·OH. RSC Adv. 6, 108791-108800. doi: 10.1039/C6RA20242J.

5. An improved hybrid strategy for online dosage of hydrogen peroxide in photo-Fenton processes

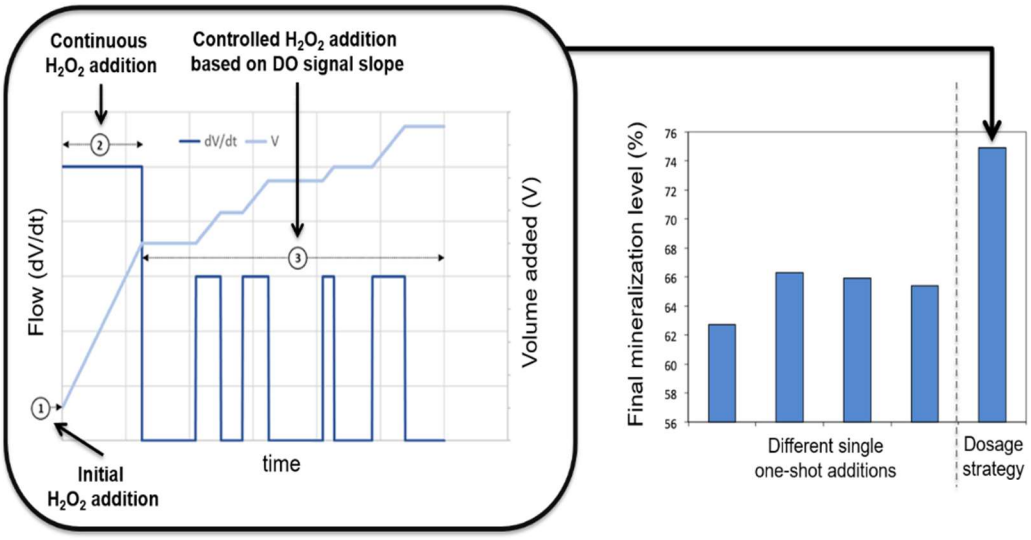

5.1 Introduction

Hydrogen peroxide (H_2O_2) supply is inherent to Fenton and photo-Fenton processes, since it is the source of the highly oxidant hydroxyl radicals. However, an excess of H_2O_2 favours reactions consuming such radicals, which is an adverse effect, (**Eq. 5.1-5.2**) and is downgrading process performance (Tokumura et al., 2011)

$$HO^{\bullet} + HO^{\bullet} \rightarrow H_2O_2 \qquad \textit{Eq. 5.1}$$

$$H_2O_2 + HO^{\bullet} \rightarrow HO_2^{\bullet} + H_2O \qquad \textit{Eq. 5.2}$$

Thus, the determination of the H_2O_2 dosage scheme minimizing such scavenging reactions and maximizing process efficiency is a crucial issue to be addressed. This is the reason why some authors (Ortega-Gómez et al., 2012) claim that the supply of H_2O_2, as a means to set the concentration of hydroxyl radicals, is the most significant operational parameter for the photo-Fenton process affecting both reaction outcome and process cost.

A considerable number of works has been devoted to empirically determine operational conditions supplying H_2O_2 in convenient portions along the reaction time to improve process performance. While many proposed approaches have shown to be valuable in particular experimental setups, determining a general strategy is still pending (Esteves et al., 2018; Wang et al., 2016).

Splitting the total supply of H_2O_2 into several portions and adding them at different times has been reported to produce improvements respect no dosage. However, the use of arbitrary amounts and time intervals prevents the solutions to be reported as optimal. Some researchers reported that sequential addition of discrete amounts of H_2O_2 leads to better results than adding a great initial dose (Almeida et al., 2015; Chu et al., 2007). Other previous works reported that adding H_2O_2 at a constant rate into the reactor along the reaction time increases the process efficiency (Monteagudo et al., 2009; Prato-Garcia and Buitrón, 2012, Sannino et al. 2013).

To address dosage in a more systematic way, a pre-established H_2O_2 dosage protocol was proposed to improve the performance of the photo-Fenton process (Yamal-Turbay et al., 2012). Although such dosage protocol can be successfully adjusted, it is limited to an initial addition and an initial dosing time, and only two degrees of freedom cannot accurately represent the operation flexibility.

Determining convenient schemes for adding finite amounts of reactant at prefixed time intervals has been a natural preliminary approach to the dosage problem. Yet, this neglects the continuous nature of the problem. In this regard, Yu et al., (2020) have recently addressed the open-loop continuous dosage of H_2O_2 as a dynamic optimization problem, which consist on determining a control law (the recipe) that drives the process through a feasible trajectory on a continuous time interval and minimizes a given cost function at the end of the interval. However, lacking of an accurate and reliable dynamic model describing the process response to the dosage, the practical solution of such dynamic optimization problem was achieved through a coarse discretization and the experimental evaluation of a reduced set of dosage schemes.

Furthermore, all these works address the problem in an open-loop approach. No feedback is contemplated and the output does not affect the control action, the dosage, which is pre-set. However, a robust on-line approach should consider closed-loop strategies adjusting the dosage in response to disturbances and deviations of the desired output (this would further set another problem: i.e. the agreement of a quantitative assessment of the desired output at each time t, or at the end of a given time horizon). Towards this end, on-line measurements are needed and a practical reliable observable should be adopted to guide the control action.

Oxidation reduction potential (ORP) and dissolved oxygen concentration (DO) are parameters that can easily be measured on-line. As these variables show significant changes during the photo-Fenton process, they can be envisaged as practical means to infer the process evolution (Prieto-Rodríguez et al., 2011; Santos-Juanes et al., 2011; Tokumura et al., 2011). Certainly, without a model explaining the correlation, the inference is purely empirical, but it could lead to practical results. For instance, Martínez, (2007) proposed an extremum-seeking control cascade for automating Advanced Oxidation Processes (AOPs) and successfully implemented it for a photo-Fenton

process, although no justification was provided for targeting at constantly driving ORP readings to its achievable maximum.

A practical alternative to ORP is dissolved oxygen (noted as DO when referred to the on-line signal). Since a product of the scavenging reactions is oxygen (O_2), **Eq. 5.3**, DO concentration is a sensible and promising measure that can be used as an indirect estimation of the extent of this effect. Prieto-Rodríguez et al., (2011) reported that excess H_2O_2 decomposes to generate O_2 is directly suggesting the inefficient consumption of H_2O_2. Thus, the adaptive addition of H_2O_2 depending on the monitored DO has also been investigated, and practical improvements have been reported (Ortega-Gómez et al., 2012). However, since a convenient fixed DO set-point is adopted, the approach cannot be considered general and further improvement could be attained (optimality is not guaranteed).

$$2HO_2^{\bullet} \rightarrow H_2O_2 + O_2 \qquad \textit{Eq. 5.3}$$

Again, the lack of an accurate and reliable dynamic model prevents a rigorous approach towards the optimal dosage scheme. Thus, practical dosage strategies still need to be developed to improve practical applications and to further understanding the nature of the dosage. Since both open and closed loop approaches provide partial advantages, a hybrid approach is presented.

Considering the strategies reported in literature as starting point, this work focuses on the development of a systematic, reliable and generalized H_2O_2 dosage methodology for the treatment of a highly concentrated aqueous paracetamol solution by photo-Fenton process. The approach conceived consists in dividing the reaction span and consequently H_2O_2 dosage in three stages and addressing them separately, assuming their different qualitative effects in the reaction outcome: (1) initial H_2O_2 addition aimed at increasing initial mineralization rate, which is mainly influenced by thermal Fenton reaction, (2) continuous H_2O_2 addition aimed at reaching a suitable H_2O_2 concentration in the reaction bulk for the photo-Fenton process and (3) automatic H_2O_2 dosage based on a control system aimed at keeping the H_2O_2 concentration constant at such concentration. In order to validate and assess the performance of this dosage strategy, highly concentrated acetaminophen (paracetamol commercial name) aqueous solution was

generated as model pollutant, using mineralization rate, mineralization level and H_2O_2 consumption as performance criterion.

Assuming the concentration of the H_2O_2 solution given (33% w/v as usual) the dosage scheme has five degrees of freedom. While there is only one degree of freedom in the first stage, flexibility increases up to three degrees of freedom for the last stage. **Table 5.1** presents the decision variables considered, along with the nomenclature used, and **Figure 5.1** shows a qualitative image of the dosage scheme.

Table 5.1. Dosage decision variables.

	Initial addition (1)	Constant flow (2)	On-off control (3)
Decision variables	• Initial added volume (V_0)	• Flow ($F_1 = dV/dt$) • DO set point (SP_1)	• Flow ($F_2 = dV/dt$) • Upper control limit ($\overline{SP_2}$) • Lower control limit ($\underline{SP_2}$)

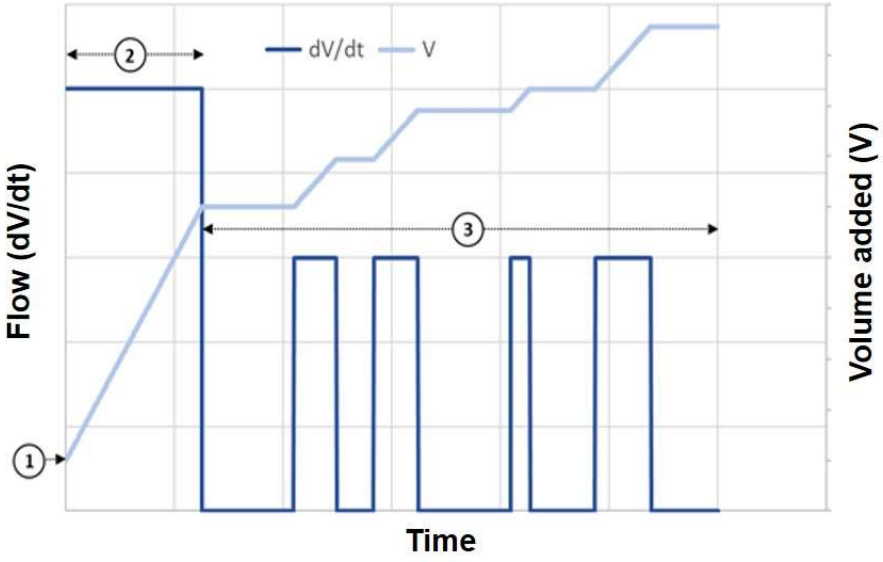

Figure 5.1. Qualitative illustration of the H_2O_2 dosage scheme: (1) Initial addition (2) Constant flow and (3) On-Off control.

5.2 Materials and methods

5.2.1 Reagents

Paracetamol (98% purity) was supplied by Sigma-Aldrich. Hydrogen peroxide (reagent-grade, 33% w/v) was provided by Panreac. Heptahydrate ferrous sulphate ($FeSO_4 \cdot 7H_2O$) used as ferrous ion source was purchased from Merck. Sulfuric acid (H_2SO_4 95%) was acquired from Fisher.

5.2.2 Pilot plant

The photo-Fenton experiments were performed in a batch-mode pilot plant **Figure 3.1**, consisting of a 13.5 L glass reservoir tank, a 1.5 L glass tubular photo-reactor, a centrifugal pump (Iwaki Magnet Pump, MD-30RZ-220, 1-16HP-220V) and connecting tubing. Total reaction volume was 15 L for all experiments in this research. The radiation source is a Philips Actinic BL TL 36 W/10 1SL lamp (UVA-UVB), the incident photon power, $E = 3.36 \times 10^{-4}$ Einstein min^{-1} (300 and 420 nm) was measured using potassium ferrioxalate actinometry. On-line measurement sensors are equipped for pH (Hamilton Polilyte HTVP 120), temperature and DO (Hamilton Oxysens) monitoring. H_2O_2 is automatically dosed through a peristaltic pump (Watson Marlow, OEM 313 24V) and a PLC program (Siemens SIMATIC S7-1200) managed by the plant SCADA system (InTouchR® software).

5.2.3 Analytical methods

Total organic carbon (TOC) concentration was measured by a TOC (TOC-VCSH/CSN Shimadzu; Kyoto, Japan) analyser. H_2O_2 concentration was determined by means of the spectrophotometric method developed by Nogueira et al., (2005). The absorption at 450 nm was detected via a U-2001 UV–vis spectrophotometer (Hitachi, Tokyo, Japan). Iron concentration in the reaction bulk was measured in filtered samples using the 1,10-phenantroline method according to ISO 6332.

5.2.4 Experimental procedure

The conditions of all the photo-Fenton experiments were listed as follows: the pilot plant was filled with 15 L of distilled water including 100 mg L^{-1} of dissolved Paracetamol, which is equivalent to 63 mg L^{-1} of TOC. Afterwards, the pH was adjusted to optimum acidic conditions (2.8) with H_2SO_4 and, then, 20 mg L^{-1} pre-dissolved $FeSO_4 \cdot 7H_2O$ were added. After 10 min of homogenization, the first sample was taken for initial iron and TOC measurements. Finally, H_2O_2 was added and the UV lamp switched on immediately after to trigger the photo-Fenton process. Duplicate TOC and iron measurements were always performed.

Experiments with hybrid H_2O_2 dosing strategies were performed following the three-stage procedure described next:

1. **Initial stage (open-loop):** Single one-shot addition at the beginning of the experiment, t0. The initial H_2O_2 concentrations produced by this supply ranged from 94.5 to 944.7 mg L^{-1}, i.e. from 20% to twice the H2O2 stoichiometric amount (S) for 100 mg L^{-1} paracetamol (from 0.2S to 2S).

2. **Transition stage (close-loop):** Continuous automatic addition of H_2O_2 (a peristaltic pump controlled by a SCADA keeps a pre-fixed flow rate, 0.287 mL min^{-1}) until the set DO level is attained. The DO levels set range from 4 to 12.5.

3. **Final stage (closed-loop):** An on-off controller is employed to automatically add H_2O_2 depending on the DO slope. A fixed rate H_2O_2 flow (0.287 mL min^{-1}) is turned off when the DO slope exceeds a maximum threshold and it is turned on when the DO slope falls below a minimum threshold (different threshold values are tested as explained in section 3.3.2).

5.3 Results and discussion

The dosage strategy presented in this work consists in dividing the reaction span in three stages and addressing them separately, assuming their

different qualitative effects in the reaction outcome and the significant differences on the dissolved oxygen production rate along the treatment, which hinders the use of this parameter as control variable with a single set point.

5.3.1 Initial Stage: Hydrogen peroxide initial addition

The process is initially determined by the classical Fenton chain reaction, known also as thermal Fenton, meaning that it is driven by thermal energy from the surroundings rather than photochemical energy (Pignatello et al., 2006). This step is characterized by a high H_2O_2 consumption, which is immediately after reflected in a high $HO^{\bullet}$ production and fast mineralization rate, suggesting the necessity of a high single initial H_2O_2 dose for the reaction kick-off. Thus, to determine the most adequate conditions in this stage, the effect of the initial H_2O_2 addition on process performance was evaluated using different initial concentrations. Based on the theoretical stoichiometric H_2O_2 concentration needed to achieve the complete mineralization of the wastewater (noted as S), different concentrations in the range from 20% (94.5 mg L^{-1}) to 200% (944.7 mg L^{-1}) of this theoretical concentration were selected. This range was assumed to represent very different situations from exhaustive H_2O_2 limitation to significant H_2O_2 excess. By way of example, the notation used for the initial addition experiments is 0.2S for 20% and 2S for 200% stoichiometric concentrations. As depicted in **Figure 5.2**, the results showed a saturation effect of the mineralization rate (mg of TOC removed min^{-1}) above ≈0.4S. In spite of increasing the initial H_2O_2 concentration, the mineralization rate reached a maximum value equivalent to ≈0.025 mg TOC min^{-1} after 5 min of reaction time. Below 0.4S, there was a lack of H_2O_2 in the reaction bulk so that not enough $HO^{\bullet}$ were produced, limiting the decontamination process. In contrast, above 0.4S there was no improvement of process performance since side reactions were favored. H_2O_2 can be auto-decomposed to water and dissolved oxygen. Simplified photo-Fenton mechanisms have proposed that $HO^{\bullet}$ may recombine or react with H_2O_2 yielding also dissolved oxygen (Cabrera-Reina et al., 2015). Therefore, the high amount of radicals produced together with the high amount of H_2O_2 initially present in the reaction bulk, increased the occurrence of reactions that are not related to organic matter oxidation but to dissolved oxygen generation. This is also in accordance with the H_2O_2 consumptions obtained, which increased linearly with the initial

amount of H_2O_2 added to the photoreactor (**Figure 5.2**). Whilst only 139 mg L^{-1} of H_2O_2 were consumed after 5 min of reaction time when 0.4S were used for the initial addition, this value increased linearly up to 675 mg. L^{-1} for 2S. Thus, since above 0.4S H_2O_2 was unnecessarily consumed, this value was selected as the optimum initial addition for the rest of the study. **Figure 5.3** reinforces the conclusions withdrawn from **Figure 5.2**. Initial additions beyond 0.4S show a clear increase in the DO signal that reflects the H_2O_2 excess in the system. This indicates an inefficient use of the reagent, which is deemed to be partially spent in competitive reactions.

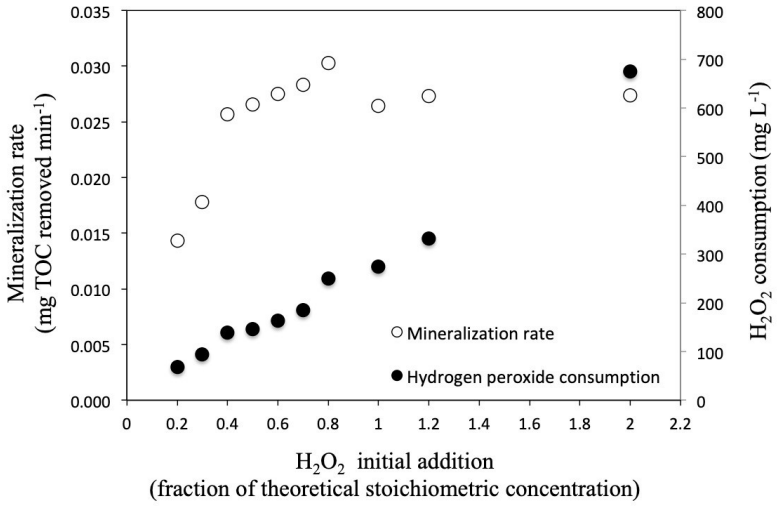

Figure 5.2. Effect of the H_2O_2 initial addition on mineralization rate and H_2O_2 consumption after 5 min of reaction time.

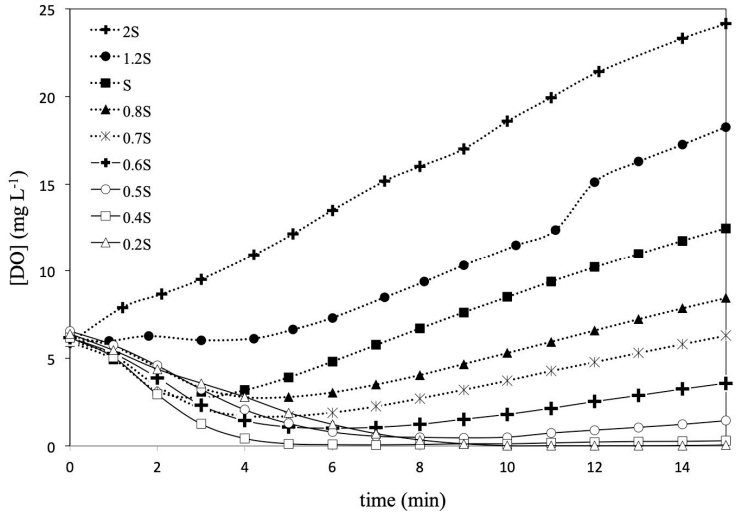

Figure 5.3. Effect of the H_2O_2 initial addition on DO evolution during the initial stage experiments.

5.3.2 Transition Stage: Continuous H_2O_2 addition

While the first addition is prefixed, the addition in the second stage is variable according to the time required to attain a convenient DO level with a constant predetermined flow. Despite the simplicity, this second stage is performed closed-loop and the control action (the end of the constant flow) depends on the measured response of the system. In this way, the transition stage considered a continuous H_2O_2 addition aimed at keeping the initially reached maximum mineralization without (significant) H_2O_2 accumulation using online DO signal as reference to stop the dosage once this accumulation starts to occur. Each assay of this experimental series followed the same procedure: (i) 0.4S H_2O_2 (188.9 mg L^{-1}) initial addition and (ii) fixed H_2O_2 continuous addition (0.287 mL·min^{-1} equivalent to 94.71 mg·min^{-1}) from the beginning of the experiment until reaching the corresponding DO set up.

During the initial min of the treatment, there was a decrease in the dissolved oxygen concentration due to Dorfman mechanism (Figure 5), which is characterized by carbon-centred free radicals (R·) reaction with dissolved oxygen (Dorfman et al., 1962; Kunai et al., 1986). Even though DO signal

diminished to concentrations close to zero after ≈3 min of reaction time; the mineralization rate was kept at maximum level. This was validated by an additional experiment at higher H_2O_2 addition rate (1.47 mL min^{-1} equivalent to 484 mg min^{-1}) from the beginning of the experiment until 16.5 min, when DO reached the highest concentration of the whole experimental series (12.5 mg L^{-1}). Although this change in the operating conditions allowed DO concentration not to decrease to zero, it did not improve the mineralization rate (data not shown). It is important to note that this is not in accordance with the results obtained by Santos-Juanes et al., (2011), who reported that such a low DO value indicates a lack of H_2O_2 in the reaction bulk. Probably, the higher wastewater TOC concentration selected for that work, the differences in the experimental set up (photo-reactor) and the different irradiance levels available during the experiments are responsible of the differences in the information provided by the DO signal. This points out the necessity of developing generalized H_2O_2 dosage strategies that must be afterwards locally optimized.

From ≈5 min, DO signal started to increase (**Figure 5.4**). The selected DO concentrations at which the H_2O_2 dosage pump was stopped were 4, 6, 8, 10 and 12.5 mg L^{-1} (noted in **Figure 5.4** as DO4, DO6, DO8, etc.), which corresponded to 22, 24, 29, 35 and 39 min of operation time, respectively. From this point on, experiments are codified as follows: "initial addition_DO set point selected for H_2O_2 dosage pump stop". By way of illustration, 0.4S_DO6 is the notation for the experiment with 0.4S initial addition and continuous H_2O_2 addition from the beginning of the experiment until DO signal reaching 6 mg L^{-1}.

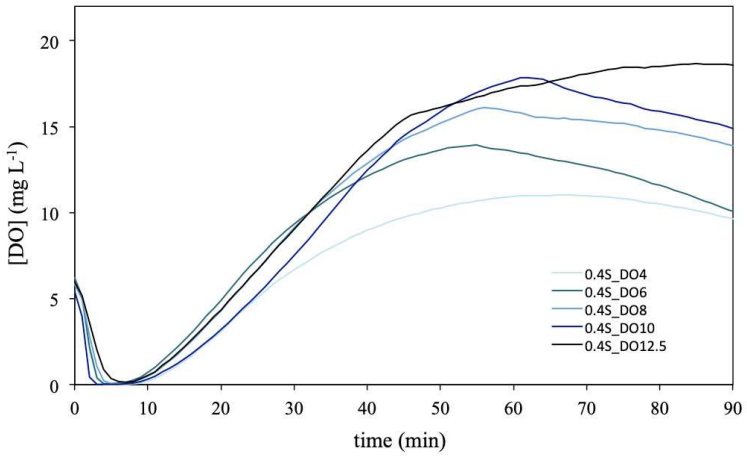

Figure 5.4. DO evolution profiles for the transition stage experiments in which different DO set points for H_2O_2 dosage pump stop were studied.

The results showed no significant differences in the mineralization rates up to 45 min, indeed, the average pseudo-first order kinetic constants related to TOC mineralization of this experimental series were in the range from $4.8 \cdot 10^{-3}$ to $5.6 \cdot 10^{-3}$ min^{-1} with no trend related to the DO signal. The ratios of TOC removed to H_2O_2 consumed (mg/mg) were obtained at 15, 30 and 45 min of reaction time for the different transition stage experiments (duplicate assays; the average value is shown in **Figure 5.5-A**). Indeed, they are extremely similar, independently of the DO set-point selected. The H_2O_2 concentration curves demonstrated that, between 15 and 25 min of reaction time, the H_2O_2 starts to accumulate in the system, which is detrimental for process performance due to side reactions proliferation (**Figure 5.5-B**). While the H_2O_2 concentration remained in the range from 90 to 100 mg L^{-1} between 5 and 15 min of operation time, this concentration increased up to 110 - 140 mg L^{-1} after 30 min depending on the experiment. In addition, to keep H_2O_2 dosage after DO concentration achieving 4 mg L^{-1} not only involved H_2O_2 accumulation, but also the unnecessary increase of H_2O_2 consumption. Consequently, 4 mg L^{-1} of DO (22 min) was selected as reference to stop the H_2O_2 dosage pump in the transition stage.

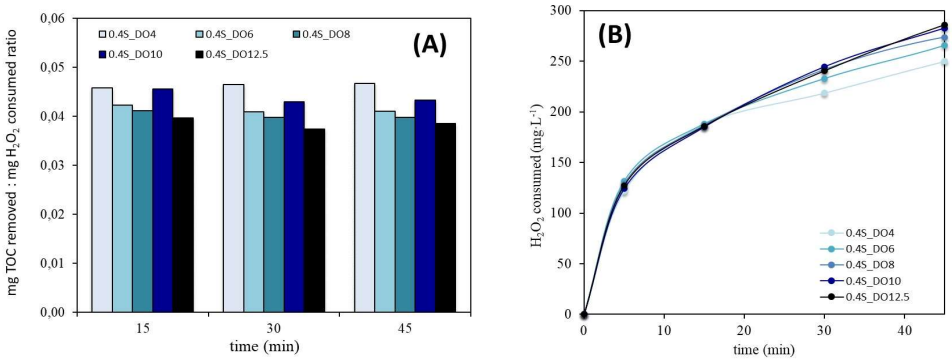

Figure 5.5. H_2O_2 concentration curves (A) and mg of TOC removed to mg of H_2O_2 consumed ratio calculated at different reaction times (B) obtained for the experiments of the transition stage.

5.3.3 Final Stage: Automatic H_2O_2 dosage

After the simple close-loop control performed during the transition stage, a more flexible close-loop strategy is adopted for the final stage. The final on-off automatic control next presented automatically cuts and restarts the H_2O_2 dosage pump (0.287 mL min^{-1}) depending on the value attained by the DO slope, which will be justified in the following subsections.

5.3.3.1 Drawbacks of DO as control variable

Based on previous experience, to maintain ≈100 mg L^{-1} of H_2O_2 in the reaction bulk is a suitable operational condition during industrial wastewater treatment by photo-Fenton not to limit mineralization with acceptable side reactions propagation. Several works based on sequential (manual) addition have used this reference value to decide when to carry out a new H_2O_2 addition as well as to choose the approximate amount to add (Cabrera-Reina et al., 2019; Ballesteros Martín et al., 2009; Cabrera-Reina et al., 2017). Thus, at the end of the transition stage, it can be assumed that the mineralization was at maximum rate and the H_2O_2 at optimum concentration. Accordingly, the objective of the final stage is to define an automatic dosage strategy aimed to maintain H_2O_2 ≈100 mg L^{-1} up to the end of the process. Although

DO concentration has been successfully used as control signal with this objective (Ortega-Gómez et al., 2012; Prieto-Rodríguez et al., 2011); the DO concentration value obtained at the end of the transition stage (4 mg L^{-1}) does not allow this possibility in this particular case. Oxygen saturation concentration in water at 25°C is 8.3 mg L^{-1}; this means that dissolved oxygen will automatically increase to this value as the final stage progresses even without dissolved oxygen generation reactions. Furthermore, since Dorfman mechanism is not relevant anymore after the initial reaction min, dissolved oxygen will never decrease again to 4 mg L^{-1} independently of H_2O_2 addition. Therefore, control systems like the one proposed by Ortega-Gómez et al., (2012) based on a single DO signal set point cannot be adopted as a generalized solution because control set up cannot be selected at 4 mg L^{-1} (≈50% saturation concentration). It is fair to comment that the amount of H_2O_2 needed will increase when treating waters with a higher initial pollution load leading to higher DO values that would allow the use of a control systems based on DO. However, this is not the only disadvantage of using DO concentration as a reference variable to obtain information about H_2O_2 concentration variation in the reaction bulk. This parameter presents an important delay in its response to H_2O_2 changes in the reaction system, as depicted in **Figure 5.6**, which corresponds to a preliminary experiment of the final stage. This assay followed the above-proposed strategies for the initial and transition stages (0.4S_DO4, i.e. 0.4S H_2O_2 initial addition and continuous H_2O_2 addition until DO signal reaching 4 mg L^{-1}) and, during the final stage, alternated H_2O_2 dosage and no dosage periods each 10 min. From the start of the final stage (22 min) DO signal always increased, even when H_2O_2 concentration in the system diminished due to no dosage periods. This means that DO signal provided misinformation about process performance. After 85 min, when the dosage was definitively stopped until the end of the experiment, 16 min were needed to observe a decrease in the DO signal, which is indeed a very high response time. Since DO seems to be useful only under certain conditions, efforts were focused on finding new options to select a new control variable.

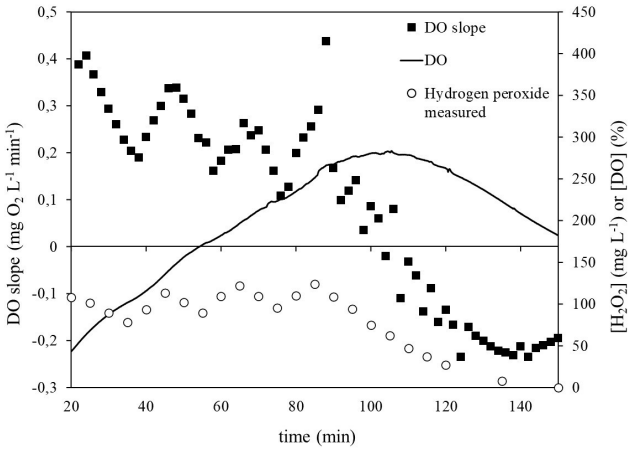

Figure 5.6. Comparison between DO and DO slope (Δt=2 min) responses to changes in H_2O_2 concentration in the reaction bulk during the final stage.

Despite the drawbacks commented, slight variations in the DO curve trend could be observed each time the H_2O_2 dosage pump was switched on/off. This suggests the significance of the information that the DO slope may bring. Consequently, the DO slope evolution is also provided in **Figure 5.6**. DO slope of the already available experiments was calculated by means of **Eq. 5.4** to delve in the information provided by this parameter.

$$DO\ slope = \frac{\Delta DO}{\Delta t} = \frac{\overline{DO_1} - \overline{DO_2}}{\Delta t} \qquad \textit{Eq. 5.4}$$

Where $\overline{DO_1}$ is the average DO corresponding to the time period from "t-Δt" to "t" and $\overline{DO_2}$ is the average DO corresponding to the time period from "t-2·Δt" to "t-Δt", being Δt a certain period of time that can be selected by the user. By way of illustration, the DO slope calculated on a 2 min basis (Δt) corresponding to minute 8 can be obtained as the difference between the average DO from minute 6 to minute 8 and the average DO from minute 4 to minute 6, divided by 2 min.

Different values of Δt from 1s to 3 min were used to compare the different DO slope responses. The results showed that the response of this variable starts to be representative of the H_2O_2 concentration behaviour when Δt is

in the range from 1 to 2 min. For instance, during the H_2O_2 concentration decrease observed from minute 22 to 35 in the above-mentioned preliminary experiment of the final stage (**Figure 5.6**), DO always tended to increase, however, DO slope (Δt = 2 min) decreased accordingly with a slight delay. Lower values of Δt based on a few seconds showed almost constant responses because the changes in DO signal were zero or extremely low, while calculations based on Δt of around half a minute were in general representative but presented an important dispersion, as occurs with DO signal.

5.3.3.2 New control strategy based on DO slope

The control strategy presented is based and tuned according to these observations. Given that the DO slope presents a faster and more representative response to H_2O_2 concentration changes than DO and, additionally, that any value can be selected as set-point independently of the DO level, a control system to tune DO slope (Δt = 2 min) and consequently H_2O_2 concentration during the final stage of the photo-Fenton process is proposed. Notation for these experiments follows the one selected for previous stages and adds the specific code for this step, which gives practical information about H_2O_2 dosage pump automatic control. By way of illustration, 0.4S_DO4_L0.2_H0.35 means 0.4S H_2O_2 initial addition, continuous H_2O_2 addition until DO reaching 4 mg L^{-1} and H_2O_2 automatic dosage with H_2O_2 dosage pump stop when DO slope reaches 0.35 mg L^{-1}·min^{-1} and H_2O_2 dosage pump re-start when DO slope reaches 0.20 mg L^{-1}·min^{-1}.

According to **Figure 5.6**, DO slope values of ≈0.2–0.3 mg L^{-1} min^{-1} can be associated to H_2O_2 concentrations of ≈100 mg L^{-1} in the reaction bulk. In this way, a first experiment was carried out using an on-off control system tuned to control DO slope values between 0.20 mg L^{-1} min^{-1} (low limit, H_2O_2 dosage pump switch on) and 0.35 mg $L^{-1}min^{-1}$ (high limit, H_2O_2 dosage pump switch off). The results showed slight H_2O_2 accumulation from 70 min so that the H_2O_2 concentration in the system almost reached 140 mg L^{-1} at the end of the experiment, indicating that the selected control range could be improved. The average H_2O_2 concentration during the final stage of this experiment was 113±18 mg L^{-1}. Therefore, the control limits were diminished to 0.15 and 0.25 mg·L^{-1}·min^{-1}, which allowed a more precise control of the H_2O_2 concentration resulting in an average value of 102±8 mg L^{-1}. Thus, the proposed strategy

was validated since, with a very simple control system, the H_2O_2 concentration could be controlled with an acceptable accuracy. As can be seen in **Figure 5.7**, no difference was found in the mineralization profiles obtained between both control strategies, therefore, the DO slope limits were again decreased to 0.10 and 0.20 mg L^{-1}·min^{-1} in order to maintain a lower H_2O_2 concentration in the reaction bulk during the experiment. Again, an equivalent mineralization profile with respect to the previous experiments was obtained. The average H_2O_2 concentration of this assay during the final stage was 81 mg L^{-1}, however, two different zones can be observed after the initial addition period (**Figure 5.7**). From ≈60 min up to the end of the experiment, the H_2O_2 concentration rounded 70 mg L^{-1}, which was the primary objective of reducing the DO slope. In contrast, from ≈25 min to ≈60 min, the H_2O_2 concentration decreased from ≈100 mg L^{-1} to 70 mg L^{-1}. Based on the obtained results, which indicate that 70-80 mg L^{-1} of H_2O_2 concentration is a better option than 100 mg L^{-1}, the DO set-point of the transition stage could also probably be diminished without any significant decontamination efficiency lose.

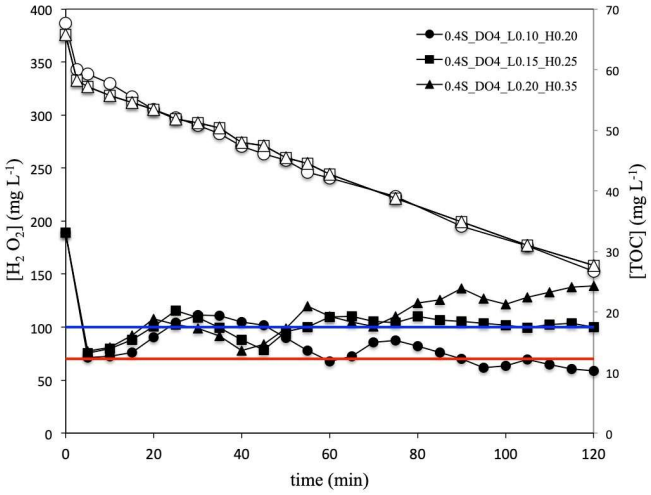

Figure 5.7. Comparison of H_2O_2 concentration curves (full symbols) and TOC mineralization profiles (empty symbols) using different DO slope set-points during final stage experiments. The red and blue lines represent different H_2O_2 concentration objectives to maintain during the final stage experiments.

5.3.4 H_2O_2 dosage validation

It is important to note that the objective of this work was not to optimize the H_2O_2 dosage, but to develop a methodology to do it. No additional experiments using lower DO slope set-points or diminishing the DO set-point of the transition stage were carried out because it makes no sense to optimize the treatment of a simple synthetic wastewater. Real wastewaters will for sure lead to higher H_2O_2 consumption due to the presence of radical scavengers in the water matrix and to longer treatment times. In contrast, to validate the developed H_2O_2 dosage methodology, four additional assays using different H_2O_2 single one-shot additions in the range from S to 2S were done.

The amount of TOC removed was significantly lower for all the experiments in which H_2O_2 was completely added from the beginning of the assays due to side reactions proliferation as a consequence of H_2O_2 excess.

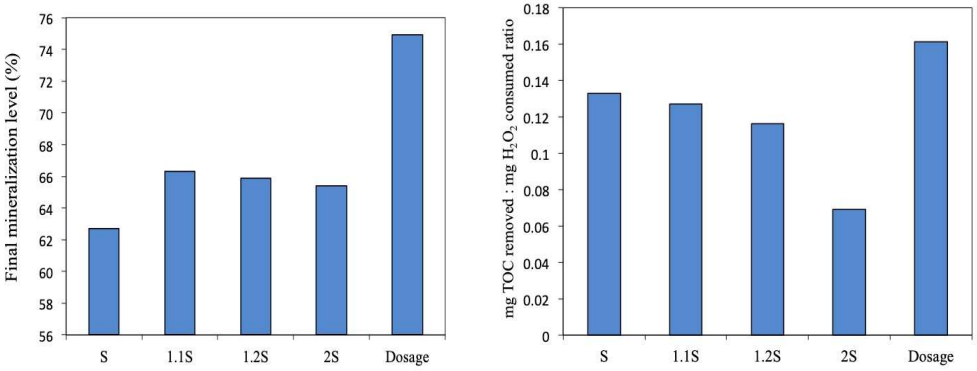

Figure 5.8. Comparison of the % TOC removed (left) and the TOC removed:H_2O_2 consumed ratio obtained for the single addition experiments and the assay in which the developed H_2O_2 dosage strategy was used.

While 63, 66, 66 and 65 mg L^{-1} of TOC were removed for the S, 1.1S, 1.2S and 2S single one-shot addition experiments, respectively, the TOC removed with the 0.4S_DO4_L0.10_H0.20 experiment increased up to 75 mg L^{-1} (**Figure 5.8-left**). Furthermore, the H_2O_2 consumption of the latter experiment was only

464 mg L^{-1}, i.e. 98% of the theoretical stoichiometric concentration needed to achieve the wastewater complete mineralization, i.e. almost equivalent to the one of the S experiment. Thus, the TOC removed:H_2O_2 consumed ratio (**Figure 5.8-right**), which varied between 0.13 and 0.07 mg of TOC mg of $H_2O_2^{-1}$ in the single addition experiments, was meaningfully higher for the 0.4S_DO4_L0.10_H0.20 experiment (0.16 mg of TOC mg of $H_2O_2^{-1}$) validating the utility of the developed dosage strategy.

5.4 Conclusions

This work contributes a new insight towards improving photo-Fenton process by designing efficient hydrogen peroxide dosage strategies. In order to address the limitations of current approaches, a flexible hybrid method combining both open and closed loop dosage approaches is formalized and discussed. The novel dosage scheme is based on three different stages: the initial stage, the subsequent continuous H_2O_2 feed (transition stage), and the final on-off control stage.

The scheme results in five decision variables to be adjusted: the initial concentration of H_2O_2, the ramp of the continuous H_2O_2 feed in the transition stage (the flowrate and the DO set-point serving as the termination criterion), and the upper and lower limits of the slope of monitored DO that trigger the on-off control of such a H_2O_2 feed.

Results show that there exists a set of values for the decision variables that can be determined and that leads to enhancing the efficiency of the photo-Fenton operations. In the case studied, the experimental results showed that, for the same Paracetamol sample, the best settings for the flexible scheme proposed increased the process performance (the ratio TOC removed to H_2O_2 consumed) by ~ 15% with respect to the single initial addition option. Compared with other works reporting a value of 100 mg L^{-1} as a convenient set-point to be kept for the H_2O_2 concentration during the dosage, this work shows that it can be decreased to 70-80 mg L^{-1}, which means increased H_2O_2 savings.

Thus, this work shows quantitative and qualitative enhancements of the photo-Fenton process performance through more flexible H_2O_2 dosage

strategies and indicates that designing and tuning more efficient dosage strategies is still an open issue.

Further improvements of this methodology should focus on the treatment of more complex wastewaters (water matrix effect, different TOC concentrations and pollutants, etc.), the possibility of using variable DO slope set-points during the final stage, and the use of more complex control systems such as PI or PID.

5.5 References

Almeida, C.V.D.S., Macedo, M.S., Eguiluz, K.I.B., Salazar-Banda, G.R., Queissada, D.D., 2015. Indanthrene Blue Dye Degradation by UV/H_2O_2 Process: H_2O_2 as a Single or Fractioned Aliquot? Environ. Eng. Sci. 32, 930–937. https://doi.org/10.1089/ees.2015.0171

Ballesteros Martín, M.M., Sánchez Pérez, J.A., Casas López, J.L., Oller, I., Malato Rodríguez, S., 2009. Degradation of a four-pesticide mixture by combined photo-Fenton and biological oxidation. Water Res. 43, 653–660. https://doi.org/10.1016/j.watres.2008.11.020

Cabrera Reina, A., Santos-Juanes, L., García Sánchez, J.L., Casas López, J.L., Maldonado Rubio, M.I., Li Puma, G., Sánchez Pérez, J.A., 2015. Modelling the photo-Fenton oxidation of the pharmaceutical paracetamol in water including the effect of photon absorption (VRPA). Appl. Catal. B Environ. 166-167, 295–301. https://doi.org/10.1016/j.apcatb.2014.11.023

Cabrera Reina, A., Miralles-Cuevas, S., Casas López, J.L., Sánchez Pérez, J.A., 2017. Pyrimethanil degradation by photo-Fenton process: Influence of iron and irradiance level on treatment cost. Sci. Total Environ. 605, 230–237. https://doi.org/10.1016/j.scitotenv.2017.06.217

Cabrera Reina, A., Miralles-Cuevas, S., Rivas, G., Sánchez Pérez, J.A., 2019. Comparison of different detoxification pilot plants for the treatment of industrial wastewater by solar photo-Fenton: Are raceway pond reactors a feasible option? Sci. Total Environ. 648, 601–608. https://doi.org/10.1016/j.scitotenv.2018.08.143

Chu, W., Chan, K.H., Kwan, C.Y., Choi, K.Y., 2007. Degradation of atrazine by modified stepwise-Fenton's processes. Chemosphere 67, 755–761. https://doi.org/10.1016/j.chemosphere.2006.10.039

Dorfman, L.M., Taub, I.A., Bühler, R.E., 1962. Pulse radiolysis studies. I. Transient spectra and reaction-rate constants in irradiated aqueous solutions of benzene. J. Chem. Phys. 36, 3051–3061. https://doi.org/10.1063/1.1732425

Esteves, B.M., Rodrigues, C.S.D., Madeira, L.M., 2018. Synthetic olive mill wastewater treatment by Fenton's process in batch and continuous reactors operation. Environ. Sci. Pollut. Res. 25, 34826–34838. https://doi.org/10.1007/s11356-017-0532-y

ISO 6332:1988, Water quality – Determination of iron – Spectrometric method using 1,10-phenanthroline

Kunai, A., Hata, S., Ito, S., Sasaki, K., 1986. The Role of Oxygen in the Hydroxylation Reaction of Benzene with Fenton's Reagent. Oxygen 18 Tracer Study. J. Am. Chem. Soc. 108, 6012-6016. https://doi.org/10.1021/ja00279a057

Martínez, E., 2007. Extremum-seeking control of redox processes in wastewater chemical treatment plants, in: Comput. Aided Chem. Eng. Elsevier, pp. 865–870. https://doi.org/10.1016/S1570-7946(07)80167-2

Monteagudo, J.M., Durán, A., San Martín, I., Aguirre, M., 2009. Effect of continuous addition of H2O2 and air injection on ferrioxalate-assisted solar photo-Fenton degradation of Orange II. Appl. Catal. B Environ. 89, 510–518. https://doi.org/10.1016/j.apcatb.2009.01.008

Nogueira, R.F.P., Oliveira, M.C., Paterlini, W.C., 2005. Simple and fast spectrophotometric determination of H2O2 in photo-Fenton reactions using metavanadate. Talanta 66, 86–91. https://doi.org/10.1016/j.talanta.2004.10.001

Ortega-Gómez, E., Moreno Úbeda, J.C., Álvarez Hervás, J.D., Casas López, J.L., Santos-Juanes Jordá, L., Sánchez Pérez, J.A., 2012. Automatic dosage of hydrogen peroxide in solar photo-Fenton plants: Development of a control strategy for efficiency enhancement. J. Hazard. Mater. 237–238, 223–230. https://doi.org/10.1016/j.jhazmat.2012.08.031

Pignatello, J.J., Oliveros, E., MacKay, A., 2006. Advanced oxidation processes for organic contaminant destruction based on the fenton reaction and related chemistry. Crit. Rev. Environ. Sci. Technol. https://doi.org/10.1080/10643380500326564

Prato-Garcia, D., Buitrón, G., 2012. Evaluation of three reagent dosing strategies in a photo-Fenton process for the decolorization of azo dye mixtures. J. Hazard. Mater. 217, 293–300. https://doi.org/10.1016/j.jhazmat.2012.03.036

Prieto-Rodríguez, L., Oller, I., Zapata, A., Agüera, A., Malato, S., 2011. Hydrogen peroxide automatic dosing based on dissolved oxygen concentration during solar photo-Fenton. Catal. Today 161, 247–254. https://doi.org/10.1016/j.cattod.2010.11.017

Sannino, D., Vaiano, V., Ciambelli, P., Isupova, L.A., 2013. Mathematical modelling of the heterogeneous photo-Fenton oxidation of acetic acid on structured

catalysts, Chemical Engineering Journal, 224, 53-58, https://doi.org/10.1016/j.cej.2013.01.078

Santos-Juanes, L., Sánchez, J.L.G., López, J.L.C., Oller, I., Malato, S., Sánchez Pérez, J.A., 2011. Dissolved oxygen concentration: A key parameter in monitoring the photo-Fenton process. Appl. Catal. B Environ. 104, 316–323. https://doi.org/10.1016/j.apcatb.2011.03.013

Tokumura, M., Morito, R., Hatayama, R., Kawase, Y., 2011. Iron redox cycling in hydroxyl radical generation during the photo-Fenton oxidative degradation: dynamic change of hydroxyl radical concentration. Appl. Catal. B Environ. 106, 565–576. https://doi.org/10.1016/j.apcatb.2011.06.017

Wang, N., Zheng, T., Zhang, G., Wang, P., 2016. A review on Fenton-like processes for organic wastewater treatment. J. Environ. Chem. Eng. 4, 762–787. https://doi.org/10.1016/j.jece.2015.12.016

Yamal-Turbay, E., Graells, M., Pérez-Moya, M., 2012. Systematic assessment of the influence of hydrogen peroxide dosage on caffeine degradation by the photo-Fenton process. Ind. Eng. Chem. Res. 51, 4770–4778. https://doi.org/10.1021/ie202256k

Xiangwei, Y., Somoza-Tornos, A., Graells, M., Pérez-Moya, M., 2020. An experimental approach to the optimization of the dosage of hydrogen peroxide for Fenton and photo-Fenton processes. Sci. Total Environ. 743. https://doi.org/10.1016/j.scitotenv.2020.140402

6. Towards an efficient generalization of the online dosage of hydrogen peroxide in photo-Fenton process

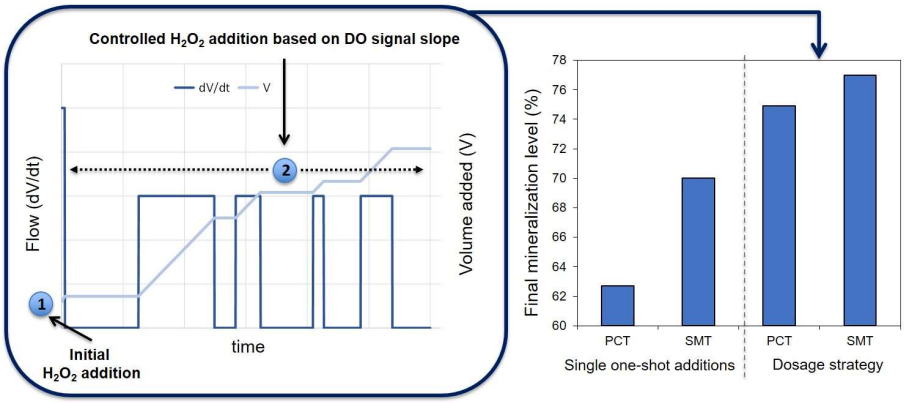

6.1 Introduction

The study of the application of Fenton and photo-Fenton processes to the degradation of refractory organic substance has been developing since the early work by Henry Fenton in the 1890s, increasing attention over the last decades. Particularly, the Fenton process is an effective method that takes place on the presence of Fenton reagents hydrogen peroxide (H_2O_2) and Fe^{2+} as catalyst (**Eq. 6.1**) yielding hydroxyl radical ($HO^{\bullet}$). Fenton reaction is enhanced with UV radiation (**Eq. 6.2**), improving the production of the highly reactive hydroxyl radicals ($HO^{\bullet}$), which in turn, unselectively react with organic matter (M) to yield organic intermediates and, eventually, its complete mineralization (**Eq. 6.3**).

$$Fe^{2+} + H_2O_2 \rightarrow Fe^{3+} + HO^- + HO^{\bullet} \qquad \textit{Eq. 6.1}$$

$$Fe^{3+} + H_2O + h\nu \rightarrow Fe^{2+} + HO^{\bullet} + H^+ \qquad \textit{Eq. 6.2}$$

$$M + HO^{\bullet} \rightarrow M_1 + HO^{\bullet} \rightarrow M_2 + HO^{\bullet} \rightarrow \cdots \rightarrow CO_2 + H_2O \qquad \textit{Eq. 6.3}$$

At the same time, $HO^{\bullet}$ suffer parallel reactions:

$$HO^{\bullet} + HO^{\bullet} \rightarrow H_2O_2 \qquad \textit{Eq. 6.4}$$

$$H_2O_2 + HO^{\bullet} \rightarrow HO_2^{\bullet} + H_2O \qquad \textit{Eq. 6.5}$$

$$2HO_2^{\bullet} \rightarrow H_2O_2 + O_2 \qquad \textit{Eq. 6.6}$$

Equations from 4 to 6 are considered unproductive and can consume the $HO^{\bullet}$. at a rate higher than that of the oxidation of organic matter. Mostly because of the second-order nature of (**Eq. 6.4**), an unnecessarily high concentration of $HO^{\bullet}$ (i.e. an excess of H_2O_2) may be counterproductive and may cause the process performance to drop (Tokumura et al., 2011). This poses a trade-off and conveniently dosing H_2O_2 along the reaction span arises as a difficult optimization problem (Xiangwei et al., 2020; Yamal-Turbay et al., 2012).

For batch operation (the research mainstream) a single load of H_2O_2 at the reaction start was soon revealed inefficient (Ince, 1999; Mirzaei et al., 2017). The ratio between the Fenton reagents (Fe^{2+}/H_2O_2) and the contaminant was

later acknowledged as a significant factor (Gulkaya et al., 2006) and was widely studied in the literature for decades (Pignatello et al., 2006). However, the search of a convenient ratio is limiting when assuming a constant value (Ortega-Gómez et al., 2012), since such a value should be adapted to the changing concentrations of a dynamic process (Audino et al., 2019a; Xiangwei et al., 2020). Thus, the sequential addition of load portions along the reaction time has been reported to improve mineralization (Chu et al., 2007; Monteagudo et al., 2009) and continuous automatic dosage has been investigated (Prieto-Rodríguez et al., 2011). However, the determination of a convenient dosage profile should not be limited to a pre-fixed recipe (open-loop control), but it should incorporate process feed-back (closed-loop control) to adapt to process disturbances and or model mismatch in a robust way (Xiangwei et al., 2021). Moreover, H_2O_2 dosage strategy is extremely important since the H_2O_2 is the most expensive reagent, being its consumption the key reagent to save in operation cost (Cabrera Reina et al., 2017).

Providing the necessary feedback requires selecting a practical and informative on-line measurement. Different measurements have been proposed, such as Redox potential (Martínez, 2007), but dissolved oxygen (DO) has proved to be efficient and useful, as well as conceptually consistent with the kinetic model (**Eq. 6.6**) (Santos-Juanes et al., 2011).

A recent work explored the idea of exploiting the derivative of the online DO measurement and revealed that a significant improvement in process performance can be achieved (Xiangwei et al., 2021). The proposed hybrid strategy for H_2O_2 dosage consists in an initial single addition of H_2O_2 plus a continuous feeding of H_2O_2 until an appropriate DO level is attained, while on-off control on H_2O_2 inflow is applied from this point on to keep the DO slope between convenient upper and lower bounds. Despite proving the concept, the evidence and the assessment were limited to samples of synthetic water of a single compound (Paracetamol, PCT, 100 mg L^{-1}). Hence, this work addresses the generalization and improvement of such H_2O_2 dosage methodology by extending its validation and assessment to more complex wastewaters: water matrix effect, different initial TOC concentrations and pollutants. The practicality and efficiency of more simplified and robust dosage approach is finally discussed in the light of the results. These findings are extremely relevant for improving photo-Fenton

treatment competitiveness in the context of industrial wastewater treatment.

6.2 Materials and methods

6.2.1 Reagents

Paracetamol (PCT, 98% purity) and Sulfamethazine (SMT, 99% purity) were supplied by Sigma-Aldrich. Hydrogen peroxide (reagent-grade, 33% w/v) was provided by Panreac. Heptahydrate ferrous sulphate ($FeSO_4 \cdot 7H_2O$) used as ferrous ion source was purchased from Merck. Sulfuric acid (H_2SO_4, 95%) was acquired from Fisher. Ammonium metavanadate (NH_4VO_3 98.5%) used for H_2O_2 measurements was from Fisher. Distilled water (DW) was used as water matrix in the main experiments. Assays designed for assessing water matrix effect were using natural water (NW).

6.2.2 Pilot plant

The pilot plant scale photo-reactor used consisted of a glass reservoir tank (13.5 L) and a glass tubular photo-reactor (1.5 L), total reaction volume of 15-L. The centrifugal pump (Iwaki Magnet Pump, MD-30RZ-220, 1-16HP-220V), operated at a flow rate of 12 L min-1 to ensure complete mixing of the solution. The radiation source is a Philips Actinic BL TL 36 W/10 1SL lamp (UVA-UVB), the incident photon power, $E = 3.36 \times 10^{-4}$ Einstein min^{-1} (300 and 420 nm) was measured using potassium ferrioxalate actinometry. On-line measurement sensors are equipped for pH (Hamilton Polilyte HTVP 120), temperature and DO/DO slope (Hamilton Oxysens) monitoring. H_2O_2 is automatically dosed through a peristaltic pump (Watson Marlow, OEM 313 24V), this pump is controlled by a PLC program (Siemens SIMATIC S7-1200) that is managed by the plant SCADA system (InTouchR® software). More details of pilot plant are shown in (Xiangwei et al., 2021).

6.2.3 Analytical methods

Total organic carbon (TOC) concentration was measured by a TOC (TOC-VCSH/CSN Shimadzu; Kyoto, Japan) analyzer. H_2O_2 concentration was determined by means of the spectrophotometric method developed by (Nogueira et al., 2005). The absorption at 450 nm was detected via a Lambda 365 UV/Vis spectrophotometer (Perkin Elmer, United States).

6.2.4 Experimental procedure

The conditions of all the photo-Fenton experiments are described as follows: the pilot plant was filled with 15 L of distilled water or natural water depending on assay. Then, the corresponding pollutant concentration was added. Four different options have been studied in this work: (i) 100 mg L^{-1} of PCT (63 mg TOC L^{-1}), (ii) 200 mg L^{-1} of PCT (126 mg L^{-1} of TOC), (iii) 50 mg L^{-1} of PCT and 61.5 mg L^{-1} of SMT (63 mg L^{-1} of TOC, where each pollutant provided half of the total TOC concentration) and (iv) 123 mg L^{-1} of SMT (63 mg L^{-1} of TOC). Then, the pH was adjusted to 2.8 with H_2SO_4 followed by the addition of the corresponding amount of pre-dissolved Fe^{2+} (in form of $FeSO_4 \cdot 7H_2O$). After 10 min of robust homogenization, first sample was taken for initial iron and TOC measurements. H_2O_2 was added and the UV lamp switched on simultaneously in order to trigger the photo-Fenton process. Duplicate TOC measurements were always performed.

Experiments were mostly performed following the proposed hybrid H_2O_2 dosing strategies by Xiangwei et al., 2021:

1. **Initial stage (open-loop):** Single initial addition at the beginning of the experiment to activate the photo-Fenton process and fast boost the mineralization rate. The initial H_2O_2 concentrations were based on the H_2O_2 stoichiometric amount, S (i.e. for 100 mg L-1 of PCT the stoichiometric concentration S is 472 mg L^{-1}; for 123 mg L^{-1} of SMT it is 631 mg L^{-1}), and they were coded accordingly (e.g. 40% of the stoichiometric amount was named 0.4S).

2. **Transition stage (close-loop):** Continuous automatic addition of H_2O_2 from the beginning of the assays (a peristaltic pump controlled

by a SCADA maintained a pre-fixed flow rate, 0.287 mL min^{-1}) until the set DO level is attained. The previously proposed DO set point was 4 mg L^{-1} so that the feasibility of this value for the new conditions studied in this work was validated. The DO set point was added to the experiment code (e.g. 4 mg L^{-1} of DO as set point was codified as 0.4S_DO4).

3. **Final stage (closed-loop):** Once the continuous addition is stopped, an on-off controller is employed to automatically add H_2O_2 depending on the DO slope value. The controller was used to add a suitable amount of H_2O_2 in the system. A fixed rate H_2O_2 flow (0.287 mL min^{-1}) was turned off when the DO slope reached a maximum threshold, 0.2 mg L^{-1} min^{-1}, and it was turned on when the DO slope fell below a minimum threshold, 0.1 mg L^{-1} min^{-1}.

6.3 Results and discussion

Different assays were planned to assess the performance of the dosage strategy under different adjustments and for different conditions, substances and mixtures. The assays are summarized in **Table 1**. The dosage set up is given in terms of the initial H_2O_2 addition and the initial H_2O_2 concentration it causes, and the application or not of the three dosage stages (Initial, Transition, and Final). The initial conditions are given by the initial concentration of PCT and SMT, and the corresponding TOC. This information is arranged in a code for each assay that will be explained in the corresponding sections.

Assays would be discussed in terms of various outcomes such as the evolution of the concentration of the different species and will be quantitatively assessed in terms of the efficiency in which the reactants are used to achieve the mineralization of the organic load (mg TOC removed / mg H_2O_2 used). Another performance indicator considered is the H_2O_2 concentration in solution during the experiments, which should be ideally kept within the 50 – 100 mg L^{-1} range to minimize side reactions.

Table 1. Experimental plan

Assay code	PCT	SMT	TOC	Iron	Initial H_2O_2	Dosage stage		
	mg L^{-1}	mg L^{-1}	mg L^{-1}	mg L^{-1}	mg L^{-1}	Initial	Transition	Final
PCT_0.4S_DO4_L0.15_H0.25_DW	100	0	63	20	189	YES	YES	YES
PCT_0.4S_DO4_L0.15_H0.25_NW	100	0	63	20	189	YES	YES	YES
2PCT_0.25S_DO4	200	0	126	20	236	YES	YES	NO
2PCT_0.3S_DO4	200	0	126	20	283	YES	YES	NO
2PCT_0.4S_DO4	200	0	126	20	378	YES	YES	NO
2PCT_0.4S_DO4_2Fe	200	0	126	40	378	YES	YES	NO
2PCT_0.3S_DO4_L0.1_H0.2	200	0	126	20	283	YES	YES	YES
2PCT_0.4S_DO4_L0.1_H0.2	200	0	126	20	378	YES	YES	YES
2PCT_0.4S_DO4_2Fe_L0.1_H0.2	200	0	126	40	378	YES	YES	YES
PCT_0.4S_DO4	100	0	63	20	189	YES	YES	NO
SMT_0.4S_DO4	0	123	63	20	252	YES	YES	NO
0.5PCT_0.5SMT_0.4S_DO4	50	61.5	63	20	221	YES	YES	NO
SMT_0.2S	0	123	63	20	126	YES	NO	NO
SMT_0.3S_CA	0	123	63	20	189	YES	YES	NO
SMT_0.4S	0	123	63	20	252	YES	NO	NO
SMT_0.4S_CA	0	123	63	20	252	YES	YES	NO
SMT_0.6S	0	123	63	20	379	YES	NO	NO
SMT_0.8S	0	123	63	20	505	YES	NO	NO
SMT_S	0	123	63	20	631	YES	NO	NO
SMT_0.4S_CA_L0.1_H0.2	0	123	63	20	252	YES	NO	YES
SMT_0.3S_CA_L0.1_H0.2	0	123	63	20	189	YES	NO	YES
SMT_0.4S_L0.1_H0.2	0	123	63	20	252	YES	NO	YES

6.3.1 Water matrix effect on dosage strategy: distilled water vs natural water

Water matrix constituents present a significant impact, in general, on advanced oxidation processes (Lado Ribeiro et al., 2019) and, particularly, on photo-Fenton process (Malato et al., 2009). As first approach to evaluate the previously proposed H_2O_2 dosage strategy under conditions closer to the treatment of actual industrial wastewaters, the water matrix was changed from DW to NW. Consequently, conductivity, which is a good indicator of the water matrix inorganic content, increased from 1.5 µS cm^{-2} to 1,010 µS cm^{-2}. This is significant, since the presence of inorganic ions in solution has a negative effect on the mineralization rate, mainly due to the complexation of the inorganic ions with iron species in solution and the scavenging of $HO^{\bullet}$, generating other less reactive inorganic ions (Zapata et al., 2009).

The experiments related to the initial stage (single one-shot addition of H_2O_2) showed almost negligible differences between NW and DW experiments. The most adequate initial addition was the same in both cases: 40% of the theoretical stoichiometric concentration (denoted as 0.4S), with a slightly higher H_2O_2 consumption in the former. Regarding the transition stage (continuous H_2O_2 addition until DO the achievement of the set-up value –4 mg L^{-1} according to previous studies (Xiangwei et al., 2021), the results showed that the presence of a higher inorganic load in the water matrix accelerated oxygen production. The DO set point was reached after 20.5 min in NW, which is 5 min earlier than in DW. Initially, oxygen is consumed in the Dorfman reaction to generate less reactive oxygen species (ROS) (Gernjak et al., 2006; Santos-Juanes et al., 2011). Probably, the Dorfman mechanism is accelerated due to the higher amount of ROS participating in the reaction mechanisms as a consequence of the higher inorganic load so that oxygen is earlier recovered. Immediately after the transition stage, the H_2O_2 continuous addition was stopped and the automatic addition (on-off control system based on the DO slope signal) was started. Based on previous results (Xiangwei et al., 2021), 0.15 mg O_2 L^{-1} min^{-1} and 0.25 mg O_2 L^{-1} min^{-1} were used as low and high set points for H_2O_2 addition re-start and stop, respectively. The resulting average H_2O_2 concentrations in the reaction bulk during this last stage were 79.8 ± 17 mg L^{-1} in DW and 76.8 ± 12 mg L^{-1} in NW. Both values, which are practically equivalent, are in the desired range (50 – 100 mg L^{-1}) that allows minimizing side reactions favoring organic

matter mineralization. The H_2O_2 consumptions were 464 mg L^{-1} and 482 mg L^{-1} for DW and NW, respectively, showing again that the inorganic components of the water matrix slightly increase the oxidant agent consumption. The comparison between DW and NW complete experiments is presented in **Figure 6.1**. These results show that the proposed dosage strategy perfectly suits the new water matrix characteristics, which means a step forward in the look for a generalized H_2O_2 dosage solution. Obviously, further actions are still needed, and future studies should consider the treatment of simulated and/or actual industrial wastewaters.

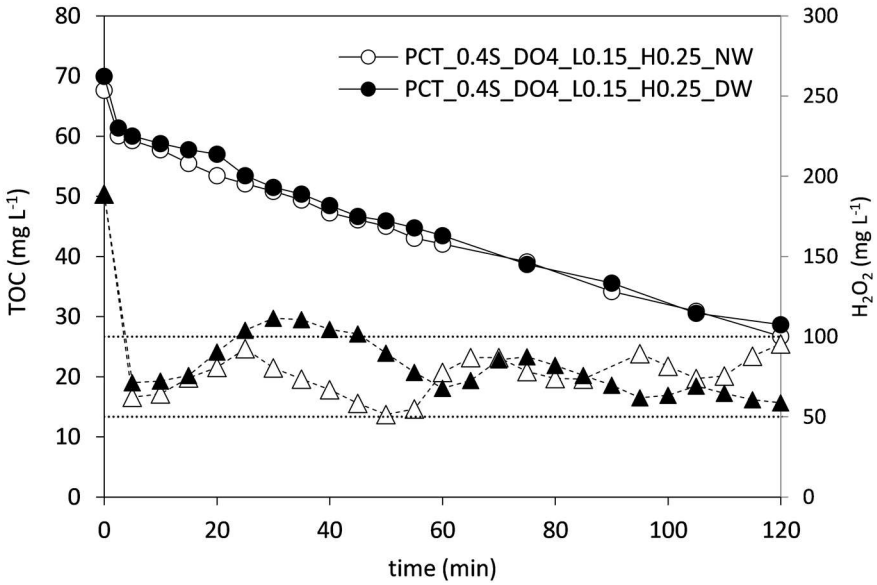

Figure 6.1. Comparison of TOC and H_2O_2 concentration profiles when the 0.4S_DO4_L0.15_H0.25 dosage strategy is applied for the treatment of PCT contaminated wastewater (63 mg L-1 TOC) in NW and DW by photo-Fenton process.

6.3.2 Validating dosage strategy against changes in initial pollutant concentration

Industrial wastewater characteristics are highly dependent on the type of industry; indeed, within the same type of activity, the organic load depends on the source and time. Hence, to validate the dosage strategy in front of these changes, the PCT initial concentration was increased from 100 mg L^{-1} to 200 mg L^{-1}, which corresponds to a TOC increase from 63 mg L^{-1} to 126 mg L^{-1}.

Using double PCT initial concentration, the H_2O_2 concentration decreased from 378 mg L^{-1} (0.4S, 40% of the stoichiometric concentration) to a minimum value of 118 mg L^{-1} after 15 min (**Figure 6.2A**). Then, the oxidant agent slowly accumulated in the reactor up to 180 mg L^{-1} after 39 min of reaction time, when DO reached 4 mg L^{-1}. These values are above the desired concentration range, which has been ideally set between 50 mg L^{-1} and 100 mg L^{-1}.

In any case, the H_2O_2 concentration was beyond the 100 mg L^{-1}, the value accepted in this work and the literature (Ballesteros Martín et al., 2009; Cabrera Reina et al., 2017), during the whole assay. This suggests that the continuous addition of H_2O_2 could be stopped earlier, ideally from the beginning. It is significant that this option would involve reducing the time of the transition stage to zero, which may indicate that the transition stage could be bypassed or removed.

The problems found with the H_2O_2 dosage strategy came from a too high initial addition and/or the subsequent continuous addition. This causes H_2O_2 concentration to fall short to reach the desired concentration range. The organic load is obviously the most important factor affecting the final consumption of H_2O_2; however, it has a low impact on the initial consumption. The main factor determining the initial consumption is the Fenton reaction. Since this step consists of the reaction between iron and H_2O_2, as far as H_2O_2 is not the limiting reagent, it will be iron concentration the key factor. In this context, two new alternatives were evaluated: (i) to diminish the initial one-shot addition of H_2O_2 and (ii) to increase the iron concentration.

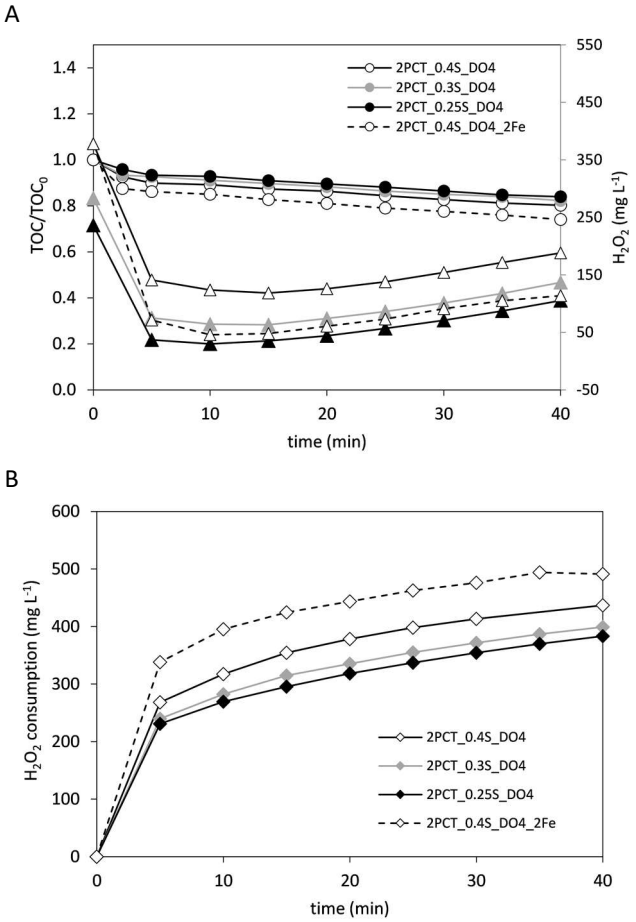

Figure 6.2. TOC and H_2O_2 concentration profiles -round and triangular symbols, respectively- (A) and H_2O_2 consumption curves (B) obtained using 0.25S_DO4, 0.3S_DO4, and 0.4S_DO4 dosage strategies, including an additional assay doubling the iron concentration (0.4S_DO4_2Fe), when PCT concentration was doubled up to 126 mg L-1 TOC.

Regarding the initial one-shot addition modification, 2PCT_0.3S_DO4 and 2PCT_0.25S_DO4 dosage strategies were evaluated. As can be seen in Figure 2, mineralization slightly increased with the amount of the initial addition and H_2O_2 consumption followed the same trend. Probably, the 2PCT_0.3S_DO4 strategy was the most adequate option because it balances the mineralization rate with respect to the total H_2O_2 addition. As previously

stated, the H_2O_2 concentration is always above 100 mg L^{-1} when selecting the 0.4S_DO4 strategy and, the more the H_2O_2 concentration deviates above the proposed concentration range (50 – 100 mg L^{-1}) the more the inefficient consumption of H_2O_2 is favored. The opposite situation is found for the 2PCT_0.25S_DO4 alternative. H_2O_2 concentration (30 mg L^{-1}) falls below the lower limit of this range, which agrees with a reduction of the mineralization rate. In any case, all three experiments presented similar efficiencies (mg of TOC removed mg of H_2O_2 consumed^{-1}) despite the differences found in the H_2O_2 concentration evolution during the experiments (**Table 6.2**).

These four assays (**Table 6.2**) reveal that the DO slope can be used also at the transition stage. In such a case, the dosage can be stopped earlier and attain the same outcome (**Table 6.2**). For instance, using DO slope (0.2 mg L^{-1} min^{-1}) in the transition stage of assay 2PCT_0.4S_DO4_Fe would allow stopping dosage after 31 minutes, about 8 minutes earlier. The same efficiency would be obtained (0.06 mg TOC mg $H_2O_2^{-1}$) with less time (20% approx.) and less H_2O_2 (8% approx.).

Consequently, small deviations during a short time (few minutes) can be assumed not to significantly impact the process efficiency. It is also worth noting that adopting the DO slope signal (0.2 mg L^{-1} min^{-1}) instead of DO as control variable allows improving the process performance, even though selecting 4 mg L^{-1} of DO still provides an acceptable response.

The equivalent concentration is defined as the one that would result from the addition of the same amount of H_2O_2 to a non-reacting system and is used as a reference for the measured concentration (actual).

Regarding the other alternative, the iron concentration was increased proportionally to the H_2O_2 initial one-shot addition increases i.e., it was doubled from 20 mg L^{-1} to 40 mg L^{-1} (2PCT_0.4S_DO4_2Fe). Increasing iron concentration allows increasing H_2O_2 consumption, which results in a higher production of radicals. However, increasing iron concentration should be carefully balanced against the possibility that radiation could become limiting. In this particular case, the limit for the iron concentration in the photo-reactor is 40 mg·L^{-1} (Audino et al., 2019) and higher concentrations would have no further effect on the process outcome during the illuminated phase of the treatment.

Table 6.2. Information for each dosage strategy studied about H_2O_2 addition/evolution, reaction time and efficiency needed to reach the proposed set points when PCT concentration was doubled up to 126 mg L-1 TOC.

		Dosage strategy			
		2PCT_0.25S_DO4	2PCT_0.3S_DO4	2PCT_0.4S_DO4	2PCT_0.4S_DO4_2Fe
Initial H_2O_2 concentration (mg L^{-1})		236	283	377	377
Minimum H_2O_2 concentration in reaction bulk (mg L^{-1})		30	63	118	46
DO set point (4 mg L^{-1})	time (min)	55	47	39	36
	Equivalent* H_2O_2 concentration (mg L^{-1})	583	580	623	604
	Actual H_2O_2 concentration (mg L^{-1})	169	159	184	106
	Efficiency (mg TOC mg $H_2O_2^{-1}$)	0.06	0.06	0.06	0.06
DO slope set point (0.2 mg L^{-1} min^{-1})	time (min)	47	34	31	26
	Equivalent* H_2O_2 concentration (mg L^{-1})	533	498	573	541
	Actual H_2O_2 concentration (mg L^{-1})	125	114	157	75
	Efficiency (mg TOC mg $H_2O_2^{-1}$)	0.06	0.05	0.06	0.06

The key point is to find out if this theoretical higher availability of radicals is translated into organic matter oxidation reactions. As depicted in **Figure 6.2,** mineralization was improved with respect to the previously described experiments. The H_2O_2 concentration in the reaction bulk could be kept within the 50-100 mg L^{-1} range from 5 min of reaction time up to the moment in which the set point was reached. Indeed, the results showed that the use of both the 4 mg L^{-1} DO and the 0.2 mg L^{-1} min^{-1} DO slope set points could be selected as control signals for the transition stage. In terms of efficiency, this strategy presented equivalent values to the ones obtained for the initial dosage modification alternative (**Table 6.3**).

These results have shown that the initial H_2O_2 concentration is a particularly important factor for the dosage strategy. Furthermore, 40% of the H_2O_2 stoichiometric amount seems a good initial guess, although the value is subject to tuning, especially for highly contaminated wastewaters. Adjusting this value should consider that the H_2O_2 concentration in the reaction bulk should be within the 50-100 mg L^{-1} range. The results obtained for the iron modification are also interesting. A simple solution when the TOC initial concentration is increased with respect to the reference value could be to proportionally increase the H_2O_2 initial one-shot addition according to the new stoichiometric concentration as well as and the iron concentration in the same proportion. This option was also validated with an intermediate concentration of PCT (150 mg L^{-1} of the compound equivalent to 95 mg L^{-1} of TOC) with identical results to the ones described in this section for the assays having double PCT initial concentration (data not shown).

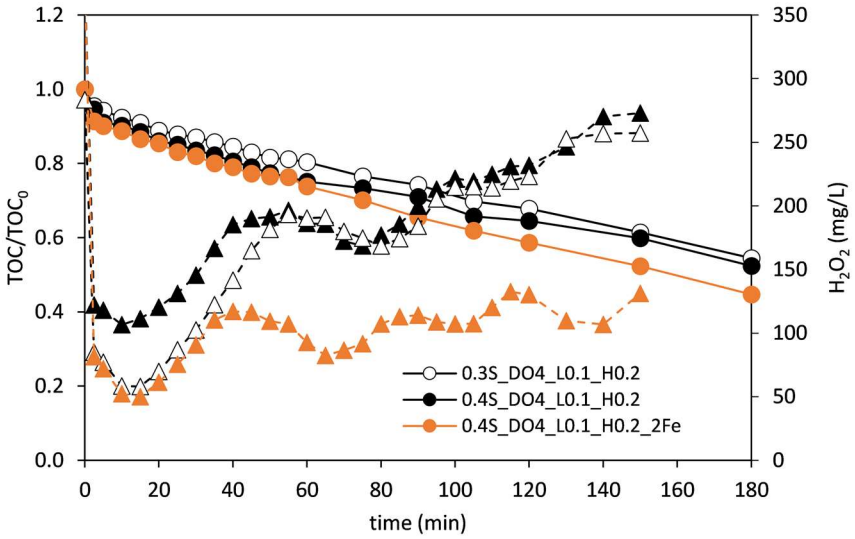

Figure 6.3. TOC and H_2O_2 concentration profiles -round and triangular symbols, respectively- for the treatment of 2PCT contaminated wastewater (126 mg L^{-1} TOC) by photo-Fenton process.

Finally, three particular assays are analyzed: 2PCT_0.3S_DO4_L0.1_H0.2, 2PCT_0.4S_DO4_L0.1_H0.2, and 2PCT_0.4S_DO4_2Fe_L0.1_H0.2. These assays were performed in order to assess the complete dosage strategy (all

three steps) with double concentration of Paracetamol (2PCT). **Figure 6.3** reveals a different behavior for assay 2PCT_0.4S_DO4_2Fe_L0.1_H0.2, the one having double iron concentration. The same dosage strategy produces a similar reduction of TOC in all cases but preserving the ratio iron to contaminant allows keeping H_2O_2 concentration closer to the desired range 50-100 mg L^{-1}. The effect of the concentration of the catalyst arisen by this observation deserves further research, which is out of the scope of this study.

6.3.3 Modifying the wastewater organic matter nature

6.3.3.1 Paracetamol and sulfamethazine mixtures

The PCT_0.4S_DO4 strategy tested in 100 mg L^{-1} of PCT (63 mg of TOC L^{-1}) was also tested in a mixture containing both PCT and SMT. The new solution was prepared so that each species contributed one half (31.5 mg L^{-1}) of the TOC concentration (i.e. 50 mg L^{-1} of PCT and 61.5 mg L^{-1} of SMT). The corresponding assay is coded 0.5PCT_0.5SMT_0.4S_DO4 and it is compared with assay PCT_0.4S_DO4 and SMT_0.4_DO4 (**Table 6.1**).

The results for this new assay showed that H_2O_2 concentration decreased from 220 mg L^{-1} to 88 mg L^{-1} in 10 min. Then, it increased up to ≈100 mg L^{-1} until DO reached 4 mg L^{-1} after 19 min (**Figure 6.4**). Therefore, the 0.4S_DO4 strategy was once again validated. Due to the interesting results regarding the use of DO slope as set point for the transition stage obtained in previous sections, the evolution of H_2O_2 concentration with respect to this variable was also monitored. When the DO slope reached 0.2 mg L^{-1} min^{-1} (11 min), the H_2O_2 concentration was 90 mg L^{-1}, highlighting once again that this variable could be an interesting alternative to DO also for the transition stage.

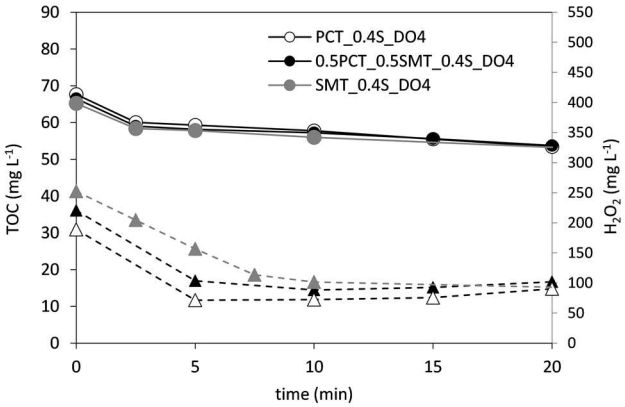

Figure 6.4. TOC and H_2O_2 concentration curves obtained with the 0.4S_DO4 dosage strategy when treating a PCT_SMT mixture (63 mg of TOC L^{-1}).

6.3.3.2 Sulfamethazine contaminated wastewater

The next set of assays was performed using only SMT (63 mg of TOC L^{-1}), for which the three stages of the H_2O_2 dosage strategy were completely re-evaluated.

The process performance under different one-shot initial additions from 0.2S to 1S (126 mg L^{-1} – 631 mg L^{-1}) was first evaluated (**Figure 6.5**). Only the 0.2S experiment presented a lower TOC reduction rate (mg L^{-1} min^{-1}) than the rest of assays, which showed equivalent values. With respect to the H_2O_2 consumption, it increased with the amount of the initial addition. While 176 mg L^{-1} were consumed in the 0.4S assay after 10 min, this value increased up to 208 mg L^{-1} for the 1S assay. In addition, the H_2O_2 concentration in the reaction bulk after 10 min for the 0.4S assay was 71 mg L^{-1}, in the middle of the desired range to minimize side reactions, whilst the H_2O_2 concentration after 10 min for the rest of the experiments was above 250 mg L^{-1}. Thus, the 0.4S (252 mg L^{-1}) option resulted in the best alternative. Since the transition stage involves the continuous addition of H_2O_2 from the beginning of the treatment and this somehow also influences the initial stage, the 0.4S approach was then compared to 0.4S and 0.3S one-shot initial additions followed by continuous addition from the beginning of the assay (SMT_0.4S_CA and SMT_0.3S_CA, respectively). There were no significant

differences between the different strategies up to 10 min of reaction time, hence, all three options were evaluated for the transition stage, including the 0.4S one-shot initial addition without further continuous addition.

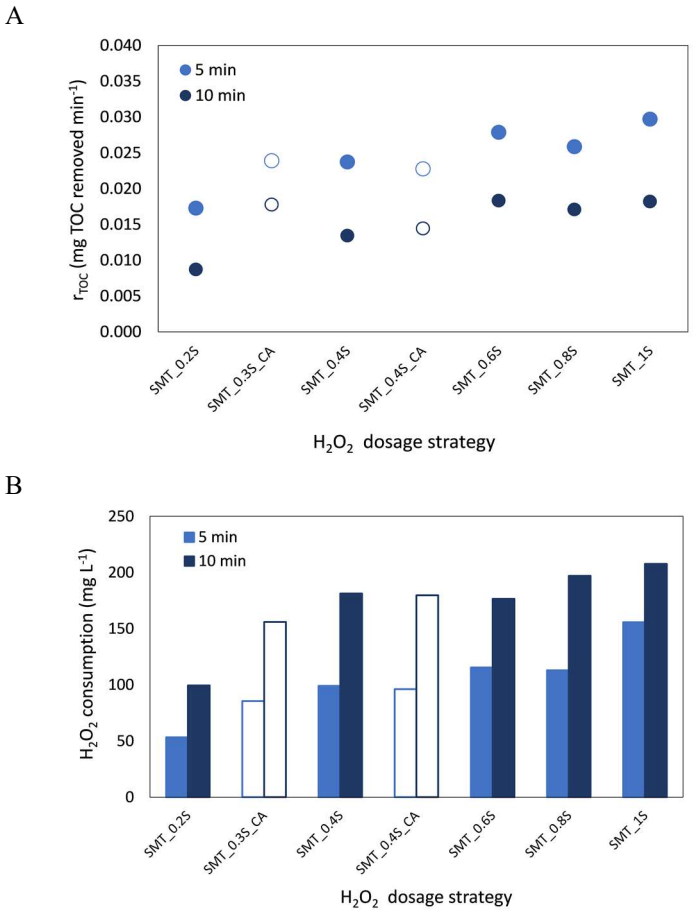

Figure 6.5. Mineralization rates (left) and H_2O_2 consumption (right) after 5 and 10 min of reaction time obtained for the treatment of SMT contaminated water under different initial H_2O_2 addition profiles (closed symbols: one-shot additions, open symbols: one-shot addition + continuous addition).

During the transition stage, the mineralization rates up to the moment in which each assay reached the DO set point (4 mg L^{-1}) were the same

independently of the selected strategy. In this way, the H_2O_2 evolution and consumption were the variables compared to determine the feasibility of the different alternatives. **Figure 6.6** shows that the H_2O_2 consumption was equivalent up to 20 min for the SMT_0.4S and SMT_0.3S_CA strategies. Moreover, the H_2O_2 concentration in the reaction bulk after 10 min was quite similar and within the objective range in both cases, 71 and 86 mg L^{-1}, respectively. Regarding the SMT_0.4S_CA strategy, there was a moderate increase of H_2O_2 consumption with respect to the other two options after 10 min. This is in accordance with its H_2O_2 evolution profile because the concentration of this reagent in the system remained above 135 mg L^{-1} from 10 to 20 min favoring the proliferation of side reactions. Consequently, the SMT_0.4S and the SMT_0.3S_CA dosage strategies presented a more adequate performance than the SMT_0.4S_CA strategy.

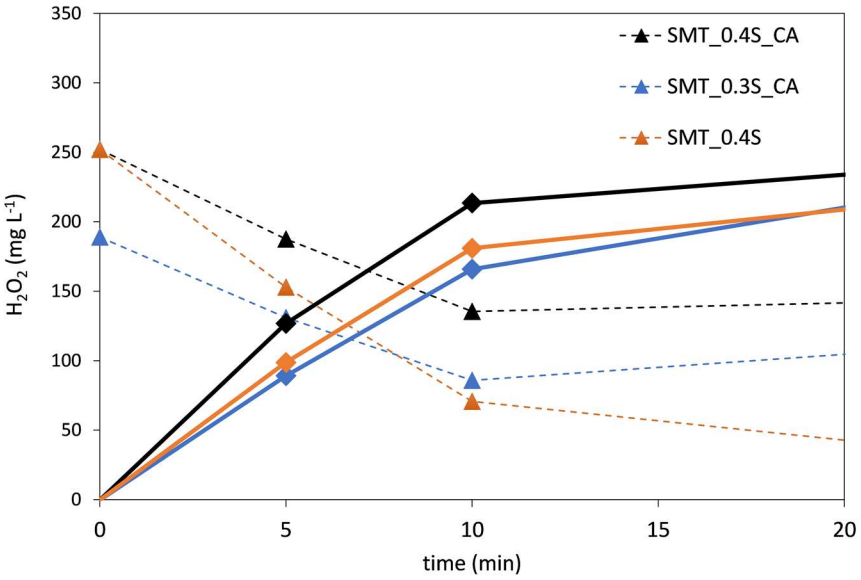

Figure 6.6. Comparison of H_2O_2 consumptions (continuous lines) and concentration (doted lines) profiles obtained with the SMT_0.4S_CA, SMT_0.3S_CA and SMT_0.4S dosage strategies during the transition stage of SMT contaminated water treatment.

The information provided by the DO and DO slope signals was suitable in both cases but again more precise for the latter (**Figure 6.7**). In the SMT_0.3S_CA experiment, the DO set point was reached in 19 min while the DO slope

reached 0.2 mg L^{-1} min^{-1} in 12 min. Since the H_2O_2 concentration started to accumulate in the system from 86 mg L^{-1} at min 10 to >100 mg L^{-1} at min 20, to stop the continuous addition at min 12 is a more adequate response, even though 19 min is a perfectly acceptable stop time. In the SMT_0.4S_CA experiment there was an excess of H_2O_2 so that the faster the control variable achieving the set point the better. In this sense, the DO reached the set point in 14 min and the DO slope in 9 min. Considering that H_2O_2 consumption in this assay was higher with respect to the 0.4S and SMT_0.3S_CA experiments only from 10 min, probably the process efficiency could be similar to these assays if the dosage is stopped at minute 9. On the other hand, it is important to note that there was no continuous addition for the 0.4S experiment, and no set point has been previously proposed with this type of strategy for the transition stage. The H_2O_2 concentration decreased from 71 mg L^{-1} at minute 10 to 53 mg L^{-1} at minute 15, therefore, the H_2O_2 addition should ideally start within this time range. The DO did not reach 4 mg L^{-1} after 30 min of reaction time while the DO slope reached 0.1 mg L^{-1} in 10 min. This last value, which has been already used in previous sections during the final automatic dosage stage to re-start the H_2O_2 addition, could be also used in this case to start H_2O_2 addition pump and to move to the automatic dosage stage.

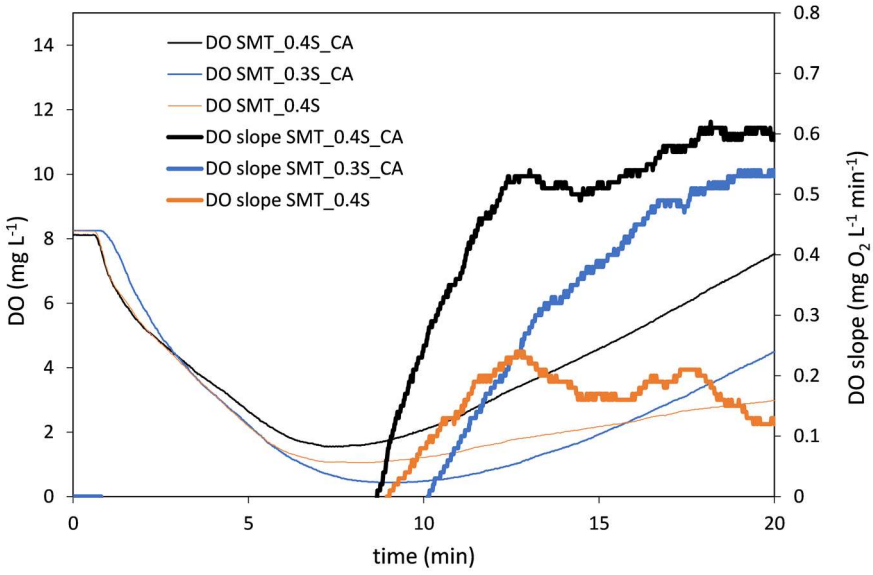

Figure 6.7. DO and DO slope evolution profiles during the transition stage of SMT contaminated water treatment using SMT_0.4S_CA, SMT_0.3S_CA and SMT_0.4S dosage strategies.

All the data obtained in this work suggest that DO slope provides more accurate information about H_2O_2 evolution than DO during the transition stage. Furthermore, the same values that have been previously used as set points for the on-off control system during the final automatic dosage stage have been probed to give the right information to stop/start the continuous addition and to mark the automatic dosage kick off. Consequently, to integrate the transition stage and the automatic stage seems the logical step because both phases can be based on the same control variable and set points. This means a new step forward in the look for a simple and generalized H_2O_2 dosage strategy.

In this context, the last set of experiments was focused on the direct coupling of the selected initial dosage strategies (SMT_0.4S, SMT_0.3S_CA and SMT_0.4S_CA) with the on-off control system using 0.1 mg L^{-1} min^{-1} and 0.2 mg L^{-1} min^{-1} DO slope values as set points, as explained in previous sections (SMT_0.4S_L0.1_H0.2, SMT_0.3S_CA_L0.1_H0.2 and SMT_0.4S_CA_L0.1_H0.2). Although some small differences between the assays can be observed (**Figure 6.8**), the results of all three options were suitable with nearly equivalent efficiencies. The 0.4S_L0.1_H0.2 strategy showed a slightly lower mineralization rate (0.25 mg of TOC removed min^{-1}) than the other two experiments but also a lower H_2O_2 consumption (416 mg L^{-1}). The opposite situation was found in the 0.3S_CA_L0.1_H0.2 and 0.4S_CA_L0.1_H0.2 assays, the mineralization rates were slightly higher (0.27 and 0.26 mg of TOC removed min^{-1}, respectively) but the H_2O_2 consumptions were also higher (458 and 480 mg L^{-1}, respectively). The average H_2O_2 concentrations in the system from 15 min to 120 min were 52±8 mg L^{-1}, 58±9 mg L^{-1} and 66±15 mg L^{-1} for the SMT_0.4S_L0.1_H0.2, SMT_0.3S_CA_L0.1_H0.2 and SMT_0.4S_CA_L0.1_H0.2 assays, respectively. This indicates the ability of the control system for maintaining the H_2O_2 concentration within the desired range using only the DO slope as control variable and under different dosage strategies.

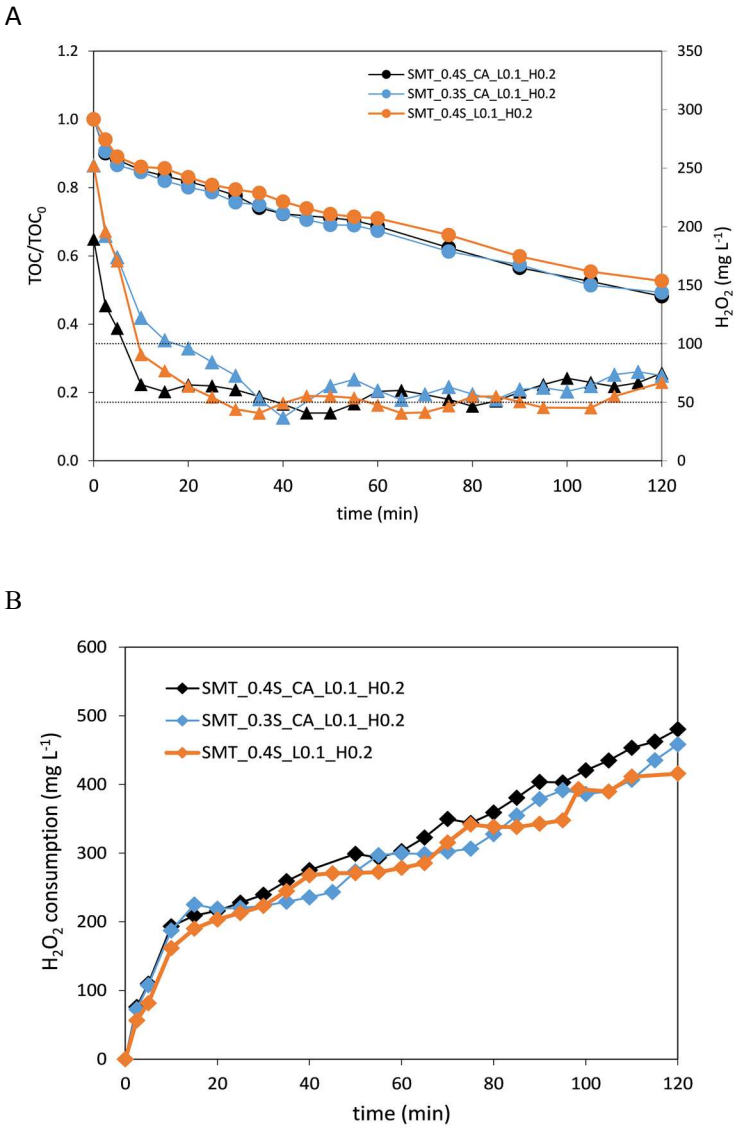

Figure 6.8. Mineralization and H_2O_2 evolution (left) and H_2O_2 consumption profiles (right) obtained with the SMT_0.4S_L0.1_H0.2, SMT_0.3S_CA_L0.1_H0.2 and SMT_0.4S_CA_L0.1_H0.2 strategies.

If these results are translated into efficiencies, the SMT_0.4S_L0.1_H0.2 and SMT_0.3S_CA_L0.1_H0.2 dosage strategies are the assays that presented the

highest values, 0.72 and 0.71 mg of TOC removed per mg of H_2O_2 consumed, respectively, followed closely by the SMT_0.4S_CA_L0.1_H0.2 assay that exhibited 0.67 mg of TOC removed per mg of H_2O_2 consumed. In any case, as shown in **Figure 6.9**, these values represent 25-35% improvement with respect to the efficiency obtained in the 1S assay (one-shot initial addition of the theoretical stoichiometric concentration) validating the proposed dosage strategies.

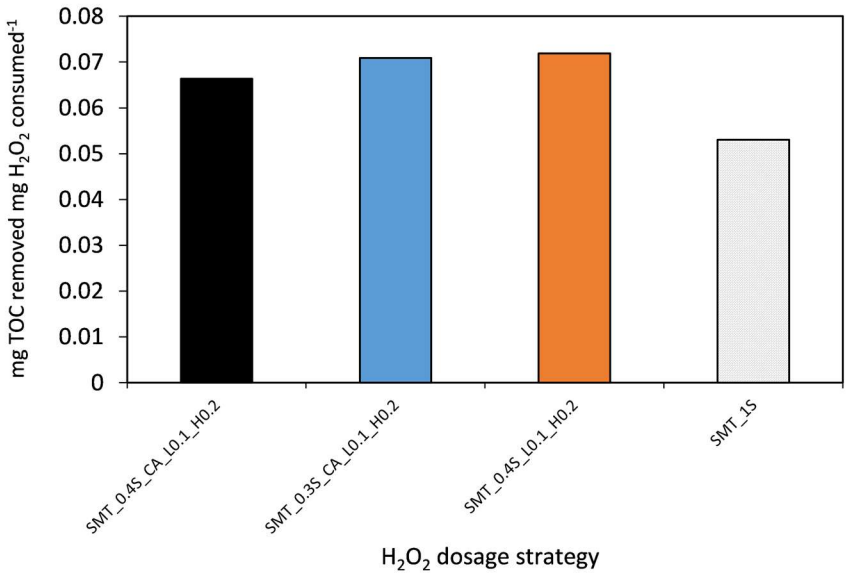

Figure 6.9. Comparison of the photo-Fenton process efficiency in terms of mg of TOC removed per mg of H_2O_2 consumed for each dosage strategy, including the one-shot initial addition of the theoretical stoichiometric concentration.

6.4 Conclusions

This work expands recent ideas on H_2O_2 dosage to the treatment of different compounds and mixtures. It also provides a new insight into this dosage strategy based on the monitoring of DO that enables redesigning it into a simpler and more robust scheme.

Results obtained for PCT, SMT and their mixtures have proved the dosage strategy to be general enough to produce similar degradation rates for the same organic load (TOC) despite the species involved in the sample solutions addressed. Results also have proved that the dosage strategy could be easily adjusted to address different organic loads for instance, while addressing double concentration of PCT or while having only half the PCT concertation in a mixture with SMT. The practical findings can be summarized in the improvement of the reaction efficiency (mg TOC removed / mg H_2O_2 used), which ranges from 8 to 15%.

A particular set of assays revealed that the DO slope used for driving the control of the last dosage stage can be used also at the transition stage. For these cases, the transition stage could be reduced while achieving the same outcome. Hence, the original conception combining open-loop and closed-loop dosage control was tested against only using the closed-loop dosage control after the initial addition of H_2O_2 and similar results were obtained for both contaminants, PCT and SMT.

Further research is underway in regard of exploring the tuning of this new dosage scheme beyond the current limiting assumptions. The on-off control has been tuned according to the range of H_2O_2 concentration values recommended in the literature (50-100 mg L^{-1}). However, this recommendation does not contemplate the feedback that the DO slope can provide, and this range could be also tuned for further increasing the efficiency of the dosage. Finally, more insight is required to fully comprehend the role of the DO slope beyond its practical use and in relation to the indirect measurement of the ratio of each species at each time, which should allow envisaging improved dosage schemes.

6.5 References

Audino, F., Campanyà, G., Pérez-Moya, M., Espuña, A., Graells, M., 2019a. Systematic optimization approach for the efficient management of the photo-Fenton treatment process. Science of the Total Environment 646, 902–913. https://doi.org/10.1016/j.scitotenv.2018.07.057

Audino, F., Conte, L.O., Schenone, A.V., Pérez-Moya, M., Graells, M., Alfano, O.M., 2019b. A kinetic study for the Fenton and photo-Fenton paracetamol degradation in an annular photoreactor. Environmental Science and Pollution Research 26, 4312–4323. https://doi.org/10.1007/s11356-018-3098-4

Ballesteros Martín, M.M., Sánchez Pérez, J.A., Casas López, J.L., Oller, I., Malato Rodríguez, S., 2009. Degradation of a four-pesticide mixture by combined photo-Fenton and biological oxidation. Water Research 43, 653–660. https://doi.org/10.1016/j.watres.2008.11.020

Cabrera Reina, A., Miralles-Cuevas, S., Casas López, J.L., Sánchez Pérez, J.A., 2017. Pyrimethanil degradation by photo-Fenton process: Influence of iron and irradiance level on treatment cost. Science of the Total Environment 605–606, 230–237. https://doi.org/10.1016/j.scitotenv.2017.06.217

Chu, W., Chan, K.H., Kwan, C.Y., Choi, K.Y., 2007. Degradation of atrazine by modified stepwise-Fenton's processes. Chemosphere 67, 755–761. https://doi.org/10.1016/j.chemosphere.2006.10.039

Gernjak, W., Fuerhacker, M., Fernández-Ibañez, P., Blanco, J., Malato, S., 2006. Solar photo-Fenton treatment - Process parameters and process control. Applied Catalysis B: Environmental 64, 121–130. https://doi.org/10.1016/j.apcatb.2005.12.002

Gulkaya, I., Surucu, G.A., Dilek, F.B., 2006. Importance of H2O2/Fe2+ ratio in Fenton's treatment of a carpet dyeing wastewater. Journal of Hazardous Materials 136, 763–769. https://doi.org/10.1016/j.jhazmat.2006.01.006

Ince, N.H., 1999. "Critical" effect of hydrogen peroxide in photochemical dye degradation. Water Research 33, 1080–1084. https://doi.org/10.1016/S0043-1354(98)00295-4

Lado Ribeiro, A.R., Moreira, N.F.F., Li Puma, G., Silva, A.M.T., 2019. Impact of water matrix on the removal of micropollutants by advanced oxidation

technologies. Chemical Engineering Journal 363, 155–173. https://doi.org/10.1016/j.cej.2019.01.080

Malato, S., Fernández-Ibáñez, P., Maldonado, M.I., Blanco, J., Gernjak, W., 2009. Decontamination and disinfection of water by solar photocatalysis: Recent overview and trends. Catalysis Today 147, 1–59. https://doi.org/10.1016/j.cattod.2009.06.018

Martinez, E., 2007. Extremum-seeking control of redox processes in wastewater chemical treatment plants. Computer Aided Chemical Engineering 24, 865–870. https://doi.org/10.1016/S1570-7946(07)80167-2.

Mirzaei, A., Chen, Z., Haghighat, F., Yerushalmi, L., 2017. Removal of pharmaceuticals from water by homo/heterogonous Fenton-type processes – A review. Chemosphere 174, 665–688. https://doi.org/10.1016/j.chemosphere.2017.02.019

Monteagudo, J.M., Durán, A., San Martín, I., Aguirre, M., 2009. Effect of continuous addition of H2O2 and air injection on ferrioxalate-assisted solar photo-Fenton degradation of Orange II. Applied Catalysis B: Environmental 89, 510–518. https://doi.org/10.1016/j.apcatb.2009.01.008

Nogueira, R.F.P., Oliveira, M.C., Paterlini, W.C., 2005. Simple and fast spectrophotometric determination of H2O2 in photo-Fenton reactions using metavanadate. Talanta 66, 86–91. https://doi.org/10.1016/j.talanta.2004.10.001

Ortega-Gómez, E., Moreno úbeda, J.C., Álvarez Hervás, J.D., Casas López, J.L., Santos-Juanes Jordá, L., Sánchez Pérez, J.A., 2012. Automatic dosage of hydrogen peroxide in solar photo-Fenton plants: Development of a control strategy for efficiency enhancement. Journal of Hazardous Materials 237–238, 223–230. https://doi.org/10.1016/j.jhazmat.2012.08.031

Pignatello, J.J., Oliveros, E., MacKay, A., 2006. Advanced oxidation processes for organic contaminant destruction based on the Fenton reaction and related chemistry. Critical Reviews in Environmental Science and Technology 36, 1–84. https://doi.org/10.1080/10643380500326564

Prieto-Rodríguez, L., Oller, I., Zapata, A., Agüera, A., Malato, S., 2011. Hydrogen peroxide automatic dosing based on dissolved oxygen concentration during solar photo-Fenton. Catalysis Today 161, 247–254. https://doi.org/10.1016/j.cattod.2010.11.017

Santos-Juanes, L., Sánchez, J.L.G., López, J.L.C., Oller, I., Malato, S., Sánchez Pérez, J.A., 2011. Dissolved oxygen concentration: A key parameter in monitoring the photo-Fenton process. Applied Catalysis B: Environmental 104, 316–323. https://doi.org/10.1016/j.apcatb.2011.03.013

Tokumura, M., Morito, R., Hatayama, R., Kawase, Y., 2011. Iron redox cycling in hydroxyl radical generation during the photo-Fenton oxidative degradation: Dynamic change of hydroxyl radical concentration. Applied Catalysis B: Environmental 106, 565–576. https://doi.org/10.1016/j.apcatb.2011.06.017

Xiangwei, Y., Graells, M., Miralles-Cuevas, S., Cabrera-Reina, A., Pérez-Moya, M., 2021. An improved hybrid strategy for online dosage of hydrogen peroxide in photo-Fenton processes. Journal of Environmental Chemical Engineering 9. https://doi.org/10.1016/j.jece.2021.105235

Xiangwei, Y., Somoza-Tornos, A., Graells, M., Pérez-Moya, M., 2020. An experimental approach to the optimization of the dosage of hydrogen peroxide for Fenton and photo-Fenton processes. Science of the Total Environment 743. https://doi.org/10.1016/j.scitotenv.2020.140402

Yamal-Turbay, E., Graells, M., Pérez-Moya, M., 2012. Systematic assessment of the influence of hydrogen peroxide dosage on caffeine degradation by the photo-Fenton process. Industrial & engineering chemistry research 51, 4770–4778.

Zapata, A., Oller, I., Bizani, E., Sánchez-Pérez, J.A., Maldonado, M.I., Malato, S., 2009. Evaluation of operational parameters involved in solar photo-Fenton degradation of a commercial pesticide mixture. Catalysis Today 144, 94–99. https://doi.org/10.1016/j.cattod.2008.12.030

7. Final remarks and future work

The complete work is next summarized, including general conclusions and prospective research lines:

First, the dosage problem has been formulated and modeled and an experimental approach to dosage optimization has been planned and run. The general strategy proposed sets a single objective, dividing the total amount of reactant (H_2O_2) into several fractions, and adding the split reactant at each discretized total reaction time. Assuming the discretization of reaction time in several time slots, then the time duration is determined. Hence, the next issue is determining the dosage level for each time slot. To simplify the dosage level, a binary decision is chosen as the method.

The first objective is minimizing total organic carbon (TOC) concentration. Compared with adding the total amount of H_2O_2 at the beginning, the TOC conversion increases 4.75% following the best dosage profile at 120 min, 6% improvement was achieved at 240 min.

This methodology opens promising research lines for exploring different variations, such as different objective functions, initial H_2O_2 amount, and interval time slots.

For example, to reverse the objective, the earliest time required to meet a certain TOC mineralization value depends on different dosage protocols. An amount of initial H_2O_2 addition favors the mineralization of TOC. Finally, changing time discretization is a very influential variable deserving further studies.

Next, the limitations of this first rigorous approach have been addressed. A part of the impracticability of this approach while detailed dynamic models are unavailable, a major drawback is the lack of mechanisms for timely responding to deviations of the expected behavior of the process. Addressing the H_2O_2 dosage problem in an open-loop is not enough, closed-loop could describe the process response to the dosage behavior, and dosage output affects control action in closed-loop system.

Hence, DO slope has been found and used as a practical informative on-line measurement that provides the necessarily required feedback. Based on DO monitoring and the value of DO slope, a novel dosage scheme combining open-and closed-loop approaches has been proved to enhance the efficiency

of photo-Fenton operations. The flexible hybrid method composes three stages: (i) one-shot initial H_2O_2 addition, (ii) continuous H_2O_2 dosage until reaching a specific DO level, and (iii) on-off control of H_2O_2 dosage using DO slope as control variable.

The proposed dosage strategy is successfully validated in the remediation of a Paracetamol solution (100 mg L^{-1}). The final tuning of the proposed strategy consists of: (i) only 40% of the stoichiometric H_2O_2 concentration, (ii) continuous feeding of H_2O_2 until 4 mg L^{-1} DO concentration is attained, and (iii) on-off control dosage selecting DO slope set points in 0.1 and 0.2 mg L^{-1} min^{-1}. In this best scheme setting, the process performance (the ratio TOC removed to H_2O_2 consumed) increased ~15% compared with the single initial addition. Furthermore, H_2O_2 concentration keeps around 70-80 mg L^{-1} during the photo-Fenton process is a desired value.

Finally, the proposed hybrid dosage scheme has been extended, generalized and validated. This has been done using more complex wastewaters, for instance, water matrix effect, different initial TOC concentrations and different pollutants.

Meanwhile, the proposed scheme including five decision variables: the initial H_2O_2 amount, the slope of the continuous H_2O_2 feed in the transition stage (the flowrate and the DO set-point serving as the termination criterion), and the upper and lower limits of the slope of monitored DO concentration. In order to reduce the variables and simplify the dosage step, a practically and efficiency of more simplified dosage approach is proposed.

The proposed dosage strategy (40% of the stoichiometric H_2O_2 concentration as initial addition 0.4S, continuous feeding of H_2O_2 until 4 mg L^{-1} DO concentration, DO slope set points in 0.1 and 0.2 mg L^{-1} min^{-1}) perfectly suits the new water matrix characteristics, H_2O_2 concentrations kept in a desired range (50-100 mg L^{-1}). Doubling the initial PCT concentration, and applied the strategy in a PCT-SMT mixtures, DO = 4 mg L^{-1} was a reasonable choice but DO slope signal (0.2 mg L^{-1} min^{-1}) was a better stop addition level. To test the proposed dosage strategy in a different contaminant solution SMT, 0.4S without continuous dosage and 0.3S + continuous dosage were better than 0.4S + continuous dosage. The ability of the control system for maintaining H_2O_2 concentration within the desired range using only the DO slope as control variable has been successfully proved.

Future work includes experimentally extending and improving this on-line closed-loop approach to produce finer tuning of the operational parameters and controlling variables, while in parallel further effort should be dedicated to developing detailed kinetic models that could be used for solving the dynamic optimization problem that dosage poses. In the long term, both approaches should converge to the optimal dosage strategy, which will be completely supported from the experimental and theoretical perspectives.

Communications

- Y. Xiangwei., M. Pérez-Moya., M. Graells., S.Miralles-Cuevas., A. Cabrera-Reina., Improving photo-Fenton process through hydrogen peroxide dosage based on dissolved oxygen monitoring. CHISA, Prague, Czech Republic, 15-18th March 2021 (virtually).

- Oral presentation: Yu Xiangwei, Moisès Graells, Sara Miralles-Cuevas. Alejandro Cabrera-Reina, Montserrat Pérez-Moya, Improving photo-Fenton process by hydrogen peroxide dosage strategies. Dissolved oxygen performance indicator. MeCCE, Barcelona, Spain, 16-20th December 2020 (virtually). DOI: https://doi.org/10.48158/mecce-14.dg.09.15

- Flash presentation and poster presentation: Xiangwei Y., Graells M., Pérez-moya M., A practical time discretization methodology for adjusting the dosage profile in photo-Fenton processes. CEST, Rhodes, Greece, 4-7th September 2019.

- Oral presentation and poster presentation: Y. Xiangwei., A. Somoza-Tornos., M. Graells., M. Pérez-Moya., Systematic dosage protocol of H_2O_2 for photo-Fenton process: application to paracetamol degradation. EAAOP-6, Portoroz-Portorose, Slovenia, 26-30th June 2019.

- Poster presentation: Yu X., Audino F., Toro Santamaria J. M., Graells M., Pérez-Moya M., Performance of Caffeine removal by using different AOPs technologies. CHISA, Prague, Czech Republic , 25-29th August 2018.